2002

The structural performance of flexible pipes

Muhannad Taher Suleiman
Iowa State University

INFORMATION TO USERS

This manuscript has been reproduced from the microfilm master. UMI films the text directly from the original or copy submitted. Thus, some thesis and dissertation copies are in typewriter face, while others may be from any type of computer printer.

The quality of this reproduction is dependent upon the quality of the copy submitted. Broken or indistinct print, colored or poor quality illustrations and photographs, print bleedthrough, substandard margins, and improper alignment can adversely affect reproduction.

In the unlikely event that the author did not send UMI a complete manuscript and there are missing pages, these will be noted. Also, if unauthorized copyright material had to be removed, a note will indicate the deletion.

Oversize materials (e.g., maps, drawings, charts) are reproduced by sectioning the original, beginning at the upper left-hand corner and continuing from left to right in equal sections with small overlaps.

ProQuest Information and Learning
300 North Zeeb Road, Ann Arbor, MI 48106-1346 USA
800-521-0600

The structural performance of flexible pipes

by

Muhannad Taher Suleiman

A dissertation submitted to the graduate faculty

in partial fulfillment of the requirements for the degree of

DOCTOR OF PHILOSOPHY

Major: Civil Engineering (Geotechnical Engineering)

Program of Study Committee
Robert Lohnes, Co-major Professor
Terry Wipf, Co-major Professor
Wayne Klaiber
Brian Coree
Thomas Rudolphi

Iowa State University

Ames, Iowa

2002

UMI Number: 3061868

UMI Microform 3061868

ProQuest Information and Learning Company
300 North Zeeb Road
P.O. Box 1346
Ann Arbor, MI 48106-1346

Graduate College
Iowa State University

This is to certify that the doctorate dissertation of

Muhannad Taher Suleiman

has met the dissertation requirements of Iowa State University

Signature was redacted for privacy.

Co-major Professor

Signature was redacted for privacy.

Co-major Professor

Signature was redacted for privacy.

For the Major Program

This dissertation is dedicated to:

All my loved ones specially, my parents, brothers, and sisters.
To the new babies Quds / Jerusalem, Taher, and juman we had in the family.

TABLE OF CONTENTS

LIST OF FIGURES

LIST OF TABLES

ABSTRACT

High density polyethylene pipes have been used for over a decade but little information is available on the in-service behavior of these pipes. At the request of the Minnesota Concrete Pipe Association, an investigation to evaluate the field performance of HDPE was undertaken. The objective of the first part of this dissertation was to investigate the field performance of in-service HDPE pipes using visual information obtained from a remote, motorized video camera. Ten projects with a total length of 12,006 feet were investigated in Minnesota. The performance characteristics considered in this evaluation were cross sectional deformations, wall buckling, wall crushing, wall cracking, joint separation, and sediments. Few major structural problems were noticed due to the effect of granular material used as a backfill.

CANDE is one of the commonly used programs for buried pipe analysis; however, the limitations of CANDE include application only to small deflections, and neglect the time effects. The recent tendency of using thermoplastic pipes for deep applications, which increased the need for investigating the effect of large deflections, and the dependency of the properties of such pipes on strain rate and time led to the use of ANSYS. The main advantage of CANDE relative to ANSYS is the use of the nonlinear soil models while ANSYS has the advantage of modeling large deflections. A computer code using ANSYS programming language was written to model the soil behavior using hyperbolic tangent modulus with both power and hyperbolic bulk modulus models. CANDE and the small and large deflection theories of ANSYS were compared with Moser's (1994) results. This comparison showed that CANDE over-predicts the pipe deflections as the soil approaches the shear failure and that ANSYS better describes the pipe behavior. CANDE can be used as long as the shear

failure of the soil was not reached. Considering large deflections for flexible pipe analysis becomes significant for pipes deflections of 4% or more.

Since the parallel plate test deflection rate is not related to practical loading rates and the time effect is not considered, new mathematical constitutive models were developed for HDPE material using the compression tests results performed by Zhang and Moore (1997). These constitutive models consider the effect of strain rate and time on the HDPE modulus. These mathematical models were programmed in the code written in ANSYS. A finite element analysis was used to validate the use of the programmed equations and to compare the pipe deflection using small deflection theory with linear elastic HDPE modulus and large deflection using strain rate dependent HDPE modulus for the case of SM soil. This comparison showed differences up to 32% at a depth of burial of 15 m. This emphasizes the importance of considering large deflection and strain rate pipe modulus for deeply buried HDPE pipes.

I. GENERAL INTRODUCTION

1.1 Objectives and Scope

The broad objective of this research is to improve and expand knowledge of the geostatic load response of high-density polyethylene (HDPE) pipe. Although this relatively new construction material has been used for over a decade, few data are available on its field performance. Also, current numerical methods of analyses are limited to small deflections, and existing constitutive models for the plastic pipe assume elastic behavior and ignore time effects. To address these issues, this study includes three separate components, each with its own specific objective: 1) evaluation of the field performance of in-service HDPE pipe, 2) expansion of finite element method (FEM) analyses of soil-HDPE pipe system to include application of ANSYS with regard to large deflections and 3) improvement of HDPE pipe constitutive models to include strain rate and creep effects. This tripartite approach has resulted in a dissertation that is organized in three distinct and somewhat independent parts.

Part I of this the dissertation deals with the field performance of HDPE pipe. At the request of the Minnesota Concrete Pipe Association (MCPA) an investigation to evaluate the field performance of HDPE was undertaken. One objective of this study is to investigate the field performance of in-service HDPE pipes using visual information obtained from a remote, motorized video camera. Ten projects were surveyed in Minnesota between July, 2000 and March, 2001. The performance characteristics that were considered in this evaluation were cross section deformations, wall buckling, wall crushing, wall cracking, joint separation, and sediments. These characteristics and their locations along the length of the pipe were recorded.

The finite element analysis of buried flexible pipes is presented in Part II of this thesis. The recent trend of using the plastic pipes for deep applications increased the need for investigating the effect of neglecting large deflections. *Culvert ANalysis and DEsign* (CANDE) is one of the most commonly used programs for buried pipe analysis; however, the limitations of CANDE include neglecting the time effect and its applicability only to small deflections. These limitations lead to the consideration of another analysis tool. In this study ANSYS, a general finite element program, was used to model the soil-pipe system. The main advantage of CANDE relative to ANSYS is the use of hyperbolic and power soil models, while ANSYS has the advantage of modeling large deflections. One objective of the theoretical analyses is to compare the results of CANDE with small and large deflection theories of ANSYS for elastic soil case with geostatic applied loads. A second objective is to write a code using ANSYS programming language to model the soil behavior using hyperbolic tangent modulus with both power and hyperbolic bulk soil modulus models. Using this code, the effect of large deflections on the behavior of polyethylene (PE) and Polyvinyl Chloride (PVC) flexible pipes is investigated. The written code was also improved to accommodate the modeling of the construction process of buried pipes.

Part III of the dissertation addresses the constitutive models of HDPE material. The objective of Part III is to develop mathematical models to describe the tangent modulus of HDPE material considering the effect of strain rate and time. These mathematical models were also programmed and included in the code written in ANSYS. The mathematical models, their derivation, ANSYS programming, and a finite element case study on the effect of HDPE modulus on pipe behavior are discussed in Part III.

1.2 Literature Review

Nearly all pipes can be classified as either flexible or rigid, depending on how they perform when installed. Flexible pipes take advantage of their ability to move, or deflect, under loads without structural damage. Common types of flexible pipes are manufactured from polyethylene, polyvinyl chloride, steel, and aluminum. Rigid pipes are classified as pipes that can not deflect more than 2% without significant structural distress such as cracking.

Both flexible and rigid pipes require a proper backfill to allow the load transfer from the pipe to the soil, although the pipe backfill interaction differs. When a flexible pipe deflects against the backfill, the load is transferred to and carried by the backfill. When loads are applied to rigid pipes, on the other hand, the load is transferred through the pipe wall into the bedding material.

In this section, the soil structure interaction, pipe performance limits, pipe performance parameters, plastic pipe installation, and previous analytical and experimental studies will be discussed.

1.2.1 Soil Structure Interaction

1.2.1.1 Marston's load theory

Marston (1913) published his original theory (now known as Marston's load theory) about how to determine the vertical loads carried by a ditch conduit. According to this theory, the backfill material tends to consolidate and settle downward relative to the native soil around the ditch. This relative movement creates shear (friction) acting upward. Based on the free body diagram of a ditch conduit shown in Figure 1.1, considering a thin horizontal soil element of a thickness *dh* within the ditch, the forces acting on the soil

element are the vertical load at the upper boundary (V), the vertical load at the lower boundary (V+dV), and the side friction forces. Marston neglected the effect of cohesion between the backfill material and the native soil and assumed that the ratio of active earth pressure is applied to calculate the horizontal stresses. The frictional force is calculated using the coefficient of sliding friction between the fill and the native soil (μ).

The value of the vertical force V at any depth can be calculated by solving the equilibrium equation of vertical forces shown in Figure 1.1. This value of the vertical force V is given by Equation 1.1.

$$V = \gamma . B^2 \frac{1 - e^{-2K\mu h / B}}{2K\mu} \qquad (1.1)$$

Marston (1930) formulated the differential equations for other types of pipe installations. For shallow embankments, depending on the relative movement between the soil column above the pipe (interior prism) and the embankment material around it (exterior prism), the shear forces can act downward or upward. If the exterior prism settles relative to the interior prism, the frictional forces on the interior prism will act downward and the load on the conduit is greater than the prism load (projection condition). On the other hand, if the interior prism settles relative to the exterior one, the frictional forces will be directed upward and the load applied on the pipe is less than that of the prism load (ditch condition). A neutral condition can also be considered where the top of the conduit settles the same amount as the exterior prism. In this case the load applied on the conduit is the prism load. Considering the direction of the frictional forces, the derivation of the equation of loads due to embankment installations is the same as shown in Figure 1.1. The value of the vertical force V at any

depth in an embankment installation is given by Equation 1.2. The positive sign is used for projection conditions while the negative sign is used for ditch conditions.

$$V = \gamma . D^2 \frac{e^{\pm 2K\mu h/B} - 1}{\pm 2K\mu} \qquad (1.2)$$

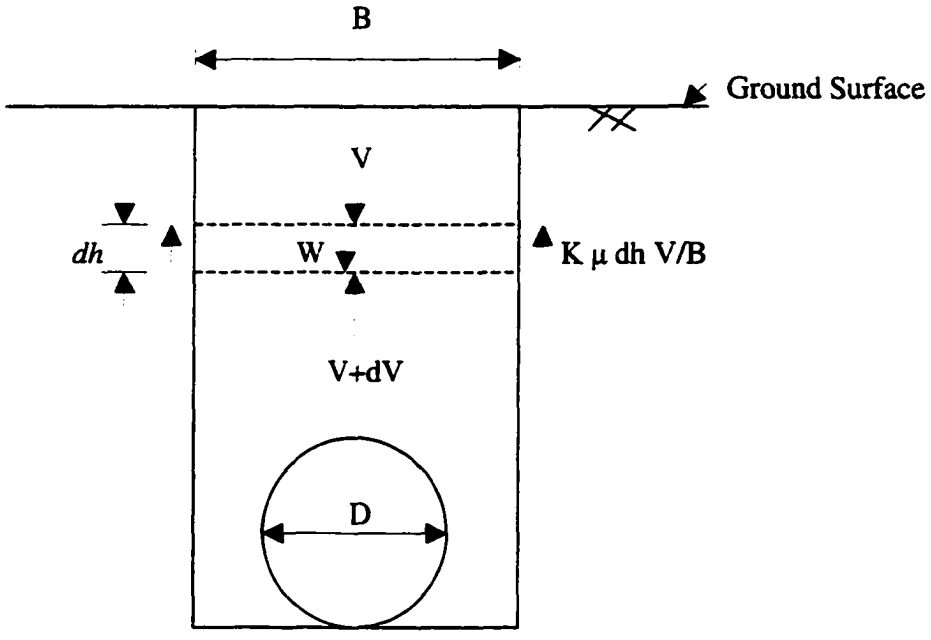

Notes:

B : Trench width.
D : Pipe Diameter.
W : Weight of soil element= $\gamma.dh$.
K : Ratio of active earth pressure.
The horizontal stress acting on the sides of the backfill is K V/B.
The horizontal force acting on a soil element with height dh is K Vdh/B.
The frictional vertical force acting on a soil element with height of dh is K μ dh V/B.
The weight of soil element with height of dh is γBdh.

Figure 1.1. Force diagram for a conduit in a ditch.

Equation 1.1 shows that as the trench width increases, the vertical load V increases. This is true as long as the calculated vertical load is less than that calculated by Equation 1.2

for the projecting conduit case. The width of the trench at which the calculated vertical loads using both equations, 1.1 and 1.2, are equal is called the transition width.

If the height of the fill is sufficiently increased, the shear stresses do not extend to the top of the embankment but cease at a horizontal plane within the fill. This plane is called the plane of equal settlement. In this case the load carried by the conduit depends on the prism load between the top of the conduit (pipe crown) and the plane of equal settlement. Equation 1.3 shows the value of the vertical force as a function of the height of the plane of equal settlement (H_e). The positive sign is used in case of projection condition, while the negative sign is used in case of ditch condition.

$$V = \gamma D^2 \{ \frac{e^{\pm 2K\mu h/B} - 1}{\pm 2K\mu} + (\frac{H}{D} - \frac{H_e}{D}) e^{\pm 2K\mu h/B} \} \qquad (1.3)$$

1.2.1.2 Iowa formula

Spangler (1941) proposed a hypothesis of the magnitude and distribution of various forces around a buried flexible pipe as shown in Figure 1.2. This hypothesis is based on the elastic ring theory and the experimental work performed on metal flexible pipes at Iowa Engineering Experimental station. Spangler's hypothesis considered, 1) Marston's load theory and assumed that the load is uniformly distributed over the bedding width of the pipe which is equal to the applied vertical load, and 2) the passive horizontal pressure on the pipe sides is distributed parabolically over 100° and the maximum value of pressure is equal to the modulus of passive resistance of the side-fill material (e) multiplied by half the horizontal deflection. This stress distribution was used to derive the original Iowa formula given in Equation 1.4.

$$\Delta X = \frac{K W_c r^3}{EI + 0.061 er^4} \tag{1.4}$$

where:

ΔX = Horizontal deflection or change in diameter, in.
D_L = Deflection lag factor.
K = Bedding constant.
W_c = Marston load per unit length of pipe, lb/in.
r = Mean radius of the pipe, in.
E = Modulus of elasticity of the pipe material, lb/in^2.
I = Moment of inertia of the pipe wall per unit length, in^4/in.
e = Modulus of passive resistance of the side fill, lb/(in^2)(in).

The modulus of passive resistance (e) was investigated by Watkins and Spangler (1958). They noticed that it does not have the dimension of a modulus and thus could not represent a soil property. The modulus of soil reaction (E') was derived as the product of the modulus of passive resistance and the mean radius of the pipe. Substituting the E' into Equation 1.4, a new formula called the "modified Iowa formula" was derived (Equation 1.5).

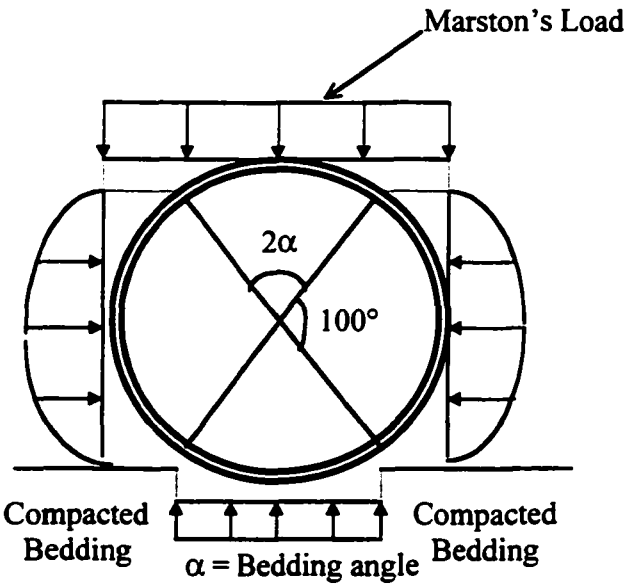

Figure 1.2. Assumed soil-stress distribution on pipe.

$$\Delta X = \frac{K W_C r^3}{EI + 0.061 E' r^3} \qquad (1.5)$$

where:

E' = Modulus of soil reaction, lb/in^2.

The fact that buried flexible pipes continue to deflect over time under a constant load, in the case of consolidated side-fills, led to the consideration of time dependent deflection. A deflection lag factor, D_L, was introduced to magnify the short term deflection as shown in Equation 1.6. The D_L value of 1.5 was found reasonable for long term deflection, but a value of 1.0 was to be used in case the prism load theory was used to calculate the applied loads. A more popular and practical form of this equation is shown in Equation 1.7 where the pipe stiffness, PS, can be measured using ASTM D-2412 parallel plate test.

$$\Delta X = \frac{D_L K W_C r^3}{EI + 0.061 E' r^3} \qquad (1.6)$$

$$\frac{\Delta X}{d} = \frac{100 D_L K}{0.149(PS) + 0.061 E'} \qquad (1.7)$$

where:

d = pipe diameter, in.

PS = pipe stiffness (lb./in./in.) = P/ΔY.

The problem with the soil stress distribution around flexible pipes is that the stiffness of the pipe was assumed equal to the stiffness of the surrounding soil. Sargand et al. (1998) stated that the stiffness of the profile wall plastic pipe is often (1/10) or less of the soil stiffness, specially when installed in a dense granular material. So the uniformly distributed vertical load along the horizontal surface passing through the pipe crown is questionable.

Moser (1990) indicated that the effective load on the flexible pipe lies somewhere between the load predicted by Marston's theory and the prism load.

Greenwood and Lang (1990) stated that the pressure distribution proposed by Spangler may not apply to all pipes but it is widely accepted together with the Iowa formula. Spangler and Handy (1982) noted that the Iowa formula has been derived for pipes made of elastic materials such as steel, so it may or may not apply to plastic pipes, especially those which experience creep and relaxation with time under constant loading.

Schluter and Caposselo (1999) compared the results of the modified Iowa formula with the actual field performance for both very stiff (semi-rigid) and very flexible pipes. It was shown that the modified Iowa formula excessively overestimates the deflection for very stiff pipes and underestimates the deflection for very flexible pipes.

Watkins (2001) stated that Spangler used the theory of elasticity to derive the Iowa Formula to *predict* ring deflections but it was not intended for *design*. Consequently, Iowa formula is limited to elastic behavior for both the pipe and the soil. Therefore, it is limited to the yield stress and small ring deflections. Watkins also stated that the performance limit of flexible pipes is not limited to the elastic range and the ring deflection at the performance limit is not small. Performance limit is in the plastic range and ring deflection based on the yield stress should not be the performance limit for buried flexible pipe. Nevertheless, ring deflection should be controlled because of its effect on the other performance limits.

Earth pressure exerted on a buried structure depends on the condition of the response of the structure to the earth pressure. There are three lateral earth pressure conditions: geostatic, active, and passive. Rankine's (1857) earth pressure coefficients can be used to calculate horizontal stresses. When the buried pipe is geostatic, with zero horizontal

deflection, the soil at the sides will be in a state of elastic equilibrium. The side fill will be in the active case when the horizontal diameter decreases and passive when the horizontal diameter increases.

1.2.2 Pipe Performance Limits

Moser (1990) stated that performance limits are usually established by the designer based upon the pipe material and the required performance. He also suggested that the performance limits could be divided into deflection, strain, stress, and buckling.

1.2.2.1 Deflection

According to Moser (1990) the performance limits of flexible pipes are usually deflection related. Excessive deflection reduces the flow capacity and causes joint leakage. Deflection can happen during transportation, construction, and due to imposed service loads. Flexible pipes can deflect (vertical diameter shortening) due to applied loads and can elongate (horizontal diameter shortening) as a result of the compaction process as shown in Figure 1.3. Deflections can be controlled by the method of installation and the backfill type. The buried pipe deflection should always be equal or less than the design deflection limit for a specific product. Deflection is usually expressed as a vertical deflection percent defined as the change in the vertical pipe diameter divided by the original pipe diameter. In a soil box, Spangler observed excessive steel pipe ring deflection up to 20%, so he recommended, with a factor of safety of 4, a maximum allowable ring deflection of 5%.

Spangler (1941) specified different stages of deflection for metal flexible pipes as shown in Figure 1.4. When the load applied on the metal pipe increases, the pipe deflects into the soil, and the passive soil pressure develops. If the load was increased and the soil was well compacted, the flexible pipe flatten at the pipe crown starts to develop. The shape of the

flexible pipe in this stage is described as heart shaped. The pipe crown forms an upward concave shape which result from increasing the load to greater levels.

Rogers et al. (1996) studied the influence of the installation procedure on pipe-soil structure interaction for PVC pipes using a visual method. Laboratory installations were used to model the field installation for two types of field practices which are called 'good site practice' and 'poor site practice'. The 'good site practice' was performed to model and study the effect of compaction on the pipe shape during construction. The 'poor site practice' was performed to model and study the effect of different haunch support conditions on the pipe deflection during construction. During the installation of PVC pipes, different cross-sectional configurations were observed. These configurations are elliptical, heart shaped, inverted heart shaped, square, and inverted Y deformations as shown in Figure 1.5.

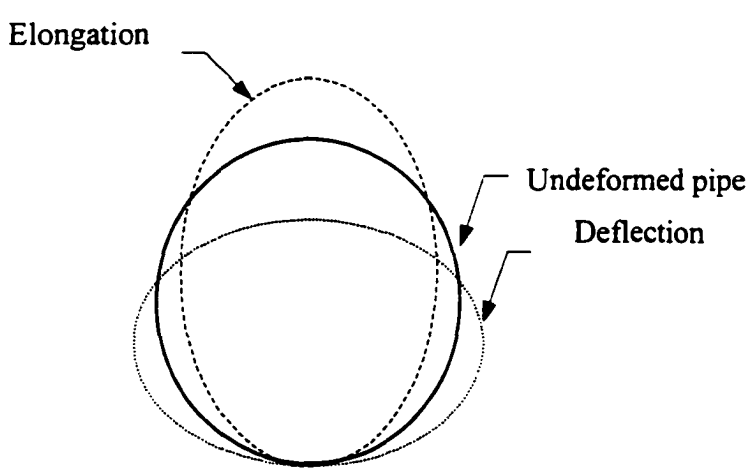

Figure 1.3. Flexible pipe deflection and elongation.

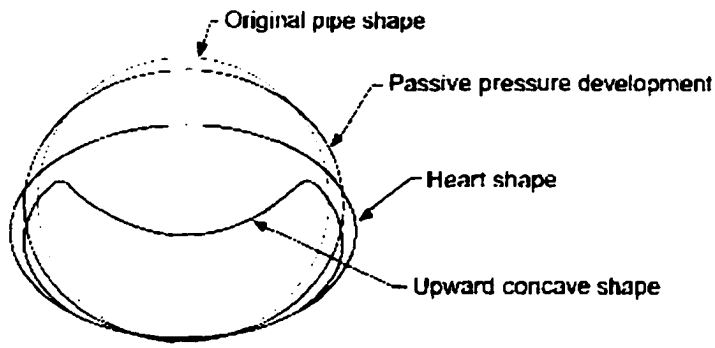

Figure 1.4. Stages of metal flexible pipes deflection (Spangler 1941).

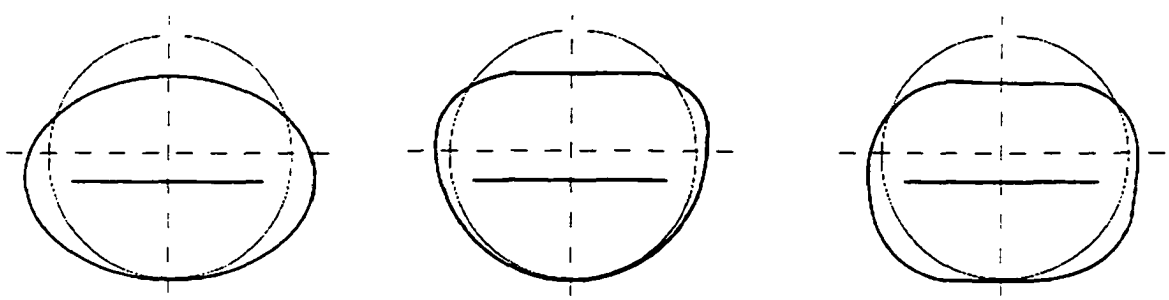

a. Elliptical deformation. b. Heart-shaped deformation. c. Square deformation.

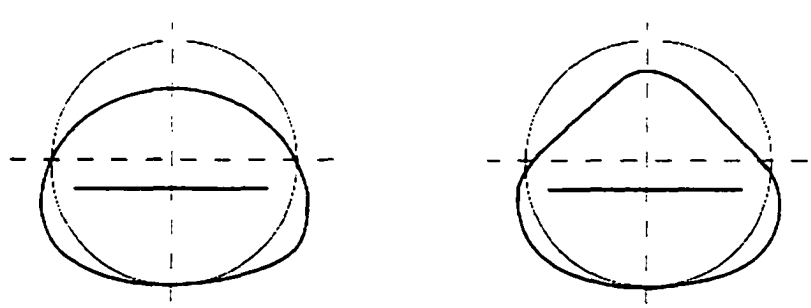

d. Inverted heart-shaped deformation. e. Inverted Y deformation.

Figure 1.5. Types of deformations in PVC flexible pipes (Rogers et al.1996).

1.2.2.2 Strain limit

Since strain is related to deflection, most manufacturers propose an installation technique to limit deflection and, thus, the strain. The strain limit is used to prevent strain corrosion which is defined as an environmental degradation of the pipe material after the pipe wall strain is greater than a threshold strain. Total circumferential strain consists of bending strain, ring strain, and strain due to Poisson's ratio as defined in Equations 1.10, 1.11, and 1.12.

$$\varepsilon_b = 6(\frac{t}{D})(\frac{\Delta y}{D}) \qquad (1.10)$$

$$\varepsilon_c = \frac{PD}{2tE} \qquad (1.11)$$

$$\varepsilon_v = -v.\varepsilon_l \qquad (1.12)$$

where:

ε_b = Bending strain.
ε_c = Compression strain.
ε_v = Poisson's circumferential strain.
ε_l = Longitudinal strain.
t = wall thickness, in.
D = Pipe diameter, in.
Δy = Vertical deflection, in.
P = Vertical soil pressure, psi.
E = Young's modulus of pipe material.
v = Poisson's ratio.

1.2.2.3 Buckling

Buckling phenomena may govern the design of the flexible pipes subjected to a high applied loads or soil pressure. The more flexible the pipe, the less is its buckling resistance. The buckling of flexible pipes does not only depend on the pipe material properties but also on the pipe geometrical properties and the surrounding soil stiffness. An exact solution for

the buckling of a pipe buried in soil is not warranted because soil behavior is not very predictable. The critical buckling pressure formula developed by Meyerhof and Baike (1963) for a buried circular pipe is given by Equation 1.13. Actual test showed that this equation works well for steel pipes (Moser 1990).

$$P_{cr} = 2\sqrt{\frac{E}{1-\nu^2}\left(\frac{EI}{R^3}\right)} \qquad (1.13)$$

where:

EI = Pipe stiffness.
R = Pipe radius.

Moser (1998) studied the performance characteristics of HDPE pipes as a function of the depth of soil cover using the Utah State University pipe-soil cell shown in Figure 1.6. Pipes were loaded until local and general buckling were noticed in full scale tests. Moser also described the difference between the classical buckling and the buried HDPE pipe buckling. The classical structural buckling is a catastrophic sudden failure once the critical load is applied. Increasing the load applied on HDPE pipe buried in soil results in the first stage of the wall local buckling which is called dimpling. The pipe then can sustain more load before the second stage of the local wall buckling, called waffling, takes place. If the load is increased, a general buckling will develop. These local buckling patterns are shown in Figures 1.7and 1.8, while in Figure 1.9 the general buckling of HDPE pipe illustrated. Table 1.1 presents a summary of the buckling results of the tests described in Moser (1998). The data in this table indicate that the dimpling pattern, which represents the beginning of the local buckling, was observed in most of the tests where local buckling was reported. These dimples were in the regions of "2 to 3 o'clock" and "9 to 10 o'clock".

(a) (b)

Figure 1.6. Soil-pipe cell of Utah State University.

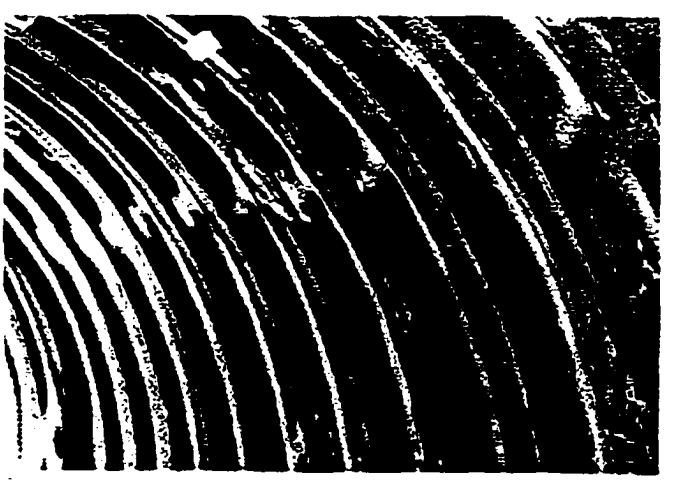

Figure 1.7. Dimpling local buckling pattern (Moser 1998).

Figure 1.8. Waffle local buckling pattern (Moser 1998).

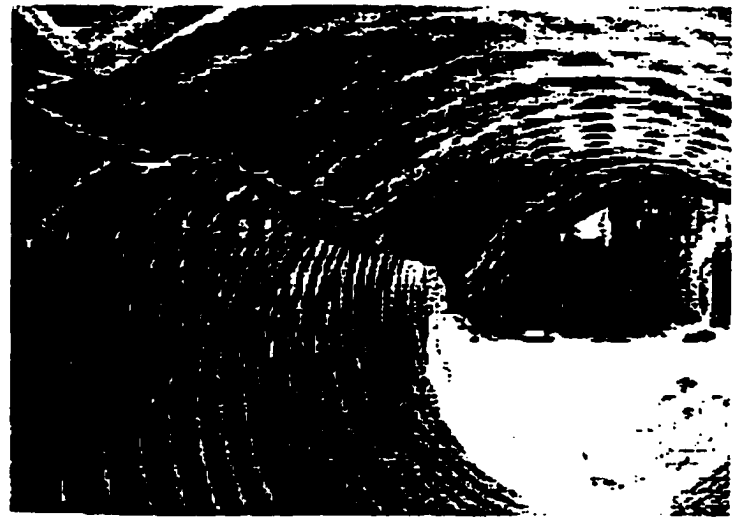

Figure 1.9. Global buckling pipe pattern (Moser 1998).

Table 1.1. Summary of the buckling results of the loading tests (Moser 1998).

Test No.	Diam.	Compaction (%)	Buckling
H-1	48 in.	95	Dimples at "2 & 10 o'clock"
H-2	48 in.	75	Dimples at "2 & 10 o'clock"
H-3	48 in.	85	Local buckling not reported General buckling at "3 & 9 o'clock"
H-4**	48 in.	85	Dimples at "2 & 10 o'clock"
H-5	60 in.	94	Dimples at "2 & 10 o'clock"
H-6	60 in.	85	Dimples start at "3 and extended to 2 o'clock"
A-1	48 in.	75	Hinge line at "3&9 o'clock"
A-2	48 in.	85	Dimples stars at "3 & 9 o'clock"
A-3	48 in.	96.5	General buckling "3 & 9 o'clock"
R-1	1900 mm *	87	Steel yield at "3 & 9 o'clock"
R-2	2000 mm*	86	Local buckling not reported
R-3	2000 mm*	91	Local buckling started at "5 & 7 o'clock" General started near "2, 3, 9, 10 o'clock"

*Steel ribbed HDPE
** Double thickness liner

1.2.2.4 Wall crushing

Wall crushing occurs if the compression stress reaches the pipe yield strength. Generally wall crushing is a primary performance limit for most rigid or brittle pipes (see Figure 1.10). This may also be reached for stiff flexible pipes. The ring compression stress is given by:

$$\sigma_c = \frac{PD}{2A} \tag{1.14}$$

where:

P = Prismatic soil load plus the effect of live load, psi.
D = Outside pipe diameter, in.
A = Pipe cross sectional area per unit length, in^2/in.

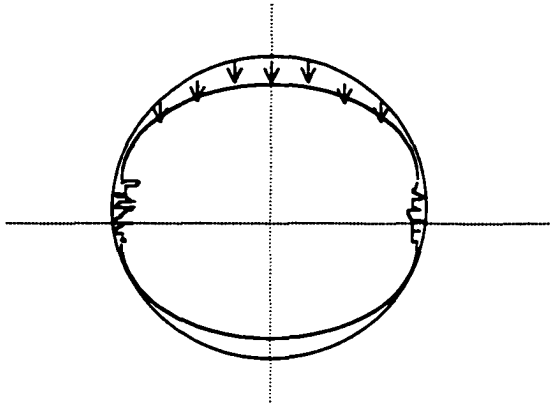

Figure 1.10. Wall crushing as a performance limit.

1.2.3 Pipe Performance Parameters

The behavior of buried flexible pipes is complicated by the soil-pipe interaction. Flexible buried pipe performance under applied loads is dependent on both the pipe and the surrounding soil strength.

1.2.3.1 Soil stiffness

Greenwood and Lang (1990) suggested that soil stiffness is the most important parameter that affects the flexible pipe performance. Soil stiffness is the ability of the soil to assist the pipe to withstand the applied loads, to retain the pipe's structural integrity, and to redistribute the stress around the pipe.

Watkins and Spangler (1958) introduced the empirical modulus of soil reaction, E′, to account for the restraint developed by the soil at the sides of the pipe. Hartley and Duncan (1988) mentioned that because of the empirical nature of the modulus of soil reaction (E'), it may introduce a large uncertainty in deflections calculated using the modified Iowa formula. Many researchers used Spangler's (1941) methodology of measuring the deflections of

installed pipes, and back-calculating the modulus of soil reaction using the modified Iowa formula to calculate the modulus of soil reaction values for pipe design. Howard (1977) collected deflection and installation data on over 100 buried pipelines. The modulus of soil reaction, E', was back-calculated and presented as a design recommendation for a variety of soil types and compacted densities as shown in Table 1.2. Table 1.3 shows the values of E' revised after considering the effect of burial depth published by Hartley and Duncan (1988).

The scatter of the available field data and the cost of carrying out field experiments led to the theoretical studies of modulus of soil reaction. Many studies have related E′ to constrained soil modulus (M_s) which was determined by performing one-dimensional tests on representative soil samples. The design values of E′ are found by multiplying M_s by a constant, k, whose value lies between 0.7 and 1.5 as found by elastic analysis (Chambers et al., 1980). Burns and Richard (1964) stated that the value of (k) depends only on the normalized pipe-soil stiffness, $(M_s R^3 / (EI)_{pipe})$, and the Poisson's ratio for the soil (ν_s). For most flexible pipe installations, they found that the value (k) is very close to unity. This means that the modulus of soil reaction, E′, is approximately equal to the constrained soil modulus, M_s, as shown in Equation 1.15. As a result of this conclusion, Chambers et al. (1980) and Krizek et al. (1971) suggested that M_s should be used in place of E′ in the modified Iowa formula.

$$E' = k M_s = \frac{k E_s (1 - \nu_s)}{(1 + \nu_s)(1 - 2\nu_s)} \qquad (1.15)$$

where:

k = Constant with a value between 0.75 and 1.5 (typically =1.0).
E_s = Young's modulus of the soil at the springline.
ν_s = Poisson's ratio of the soil at the springline.

Table.1.2. Design values of E' after Howard (1977).

Soil type-pipe bedding material (Unified Classification System).	E' for degree of compaction of bedding, psi			
	Dumped	Slight, <85% Prctor, <40% relative density	Moderate, 80%-95% Proctor, 40%-70% relative density	High, >95% Proctor, >70% relative density
Fine-grained Soils (LL<50) Soils with medium to no plasticity CL, ML, ML-CL, with less than 25% coarse-grained particles	50	200	400	1000
Fine-grained Soils (LL<50) Soils with medium to no plasticity CL, ML, ML-CL, with more than 25% coarse-grained particles, or Coarse-grained Soils with Fines GM, GC, SM, SC contains more than 12% fines	100	400	1000	2000
Coarse-grained Soils with Little or No Fines GW, GP, SW, SP contains less than 12% fines	200	1000	2000	3000
Crushed Rock	1000	3000	3000	3000

Table 1.3. Design values of E' (psi) after Hartley and Duncan (1988).

Soil Type	Depth of cover (feet)	Standard AASHTO relative compaction 85%	90%	95%	100%
Fine grained with less	0-5	500	700	1,000	1,500
Than 25% sand content	5-10	600	1,000	1,400	2,000
(CL, ML, CL-ML)	10-15	700	1,200	1,600	2,300
	15-20	800	1,300	1,800	2,600
Coarse grained with fines	0-5	600	1,000	1,200	1,900
(SM, SC)	5-10	900	1,400	1,800	2,700
	10-15	1,000	1,500	2,100	3,200
	15-20	1,100	1,600	2,400	3,700
Coarse grained with little	0-5	700	1,000	1,600	2,500
or no fines	5-10	1,000	1,500	2,200	3,300
(SP, SW, GP, GW)	10-15	1,050	1,600	2,400	3,600
	15-20	1,100	1,700	2,500	3,800

It is necessary to recognize that the soil modulus varies with stress or strain level and can be determined by various types of laboratory tests. Several types of soil moduli such as initial, tangent, and secant moduli determined from triaxial tests are applied to solve soil-structure interaction problems. Experimental studies by Janbu (1963) have shown that the initial tangent modulus can be expressed in terms of confining pressure as shown in Equation 1.16. Kondner (1963) proposed the use of a hyperbola to describe the soil stress strain relationship as shown in Equation 1.17.

$$E_i = K P_a \left(\frac{\sigma_3}{P_a} \right)^n \qquad (1.16)$$

where:

E_i = Initial tangent modulus.
K = A modulus number.
P_a = Atmospheric pressure.
σ_3 = Minor principal stress.
n = The exponent determining the rate of variation of E_i with σ_3.

$$\sigma_1 - \sigma_3 = \frac{\varepsilon}{\frac{1}{E_i} + \frac{\varepsilon}{(\sigma_1 - \sigma_3)_u}} \qquad (1.17)$$

where:

σ_1 = Major principal stress.
$(\sigma_1 - \sigma_3)_u$ = Ultimate deviator stress.

Duncan and Chang (1970) stated that soil behavior is nonlinear, inelastic, and dependent upon the magnitude of the confining pressures. Duncan and Chang (1970) combined Kondner and Janbu models to develop a soil tangent modulus model. This was done by linearizing the hyperbolic equation proposed by Kondner (1963) to find the values of the initial modulus and the ultimate deviator stress as a function of confining pressure. Then they suggested defining the ultimate deviator stress in terms of the soil strength parameters, and substituting the soil strength parameter for the ultimate deviator stress in the derivative of Equation 1.17 to get the tangent modulus shown in Equation 1.18, where E_i is defined by Equation 1.16.

$$E_t = \left[1 - \frac{R_f(1-\sin\phi)(\sigma_1 - \sigma_3)}{2c\cos\phi + 2\sigma_3\sin\phi}\right]^2 E_i \qquad (1.18)$$

where:

E_t = Tangent modulus.
E_i = Initial tangent modulus, referred to Equation 1.16.
R_f = Ratio between the asymptote to the hyperbolic curve and the maximum shear strength.
ϕ = Soil friction angle.
c = Soil cohesive strength.

σ_3 = Minor principal stress.
σ_1 = Major principal stress.

Duncan et al (1980) proposed a power model for the soil bulk modulus given in Equation 1.19. The limitations of this model are: 1) the use of only one point on the stress strain curve since the bulk modulus was assumed to be independent of the deviator stress (σ_1-σ_3) and only dependent on the confining stress (σ_3) which is constant for a given test; and 2) the bulk modulus is a secant , rather than tangent,

$$B_i = K_b P_a \left(\frac{\sigma_3}{P_a} \right)^m \qquad (1.19)$$

where:
K_b = A bulk modulus number.
m = The exponent determining the rate of variation of B_i with σ_3.

Selig (1988) suggested another mathematical model for the soil bulk modulus based on the hydrostatic compression test to be used for the design of buried pipes. The soil was compressed under an increasing confining pressure applied all around the soil sample. The curve relating the mean applied stress and the volumetric strain was found to be reasonably represented by a hyperbola as shown in Equation 1.20. The tangent bulk modulus equation and the parameters were determined using the same method Duncan and Chang (1970) used to define the tangent modulus. The bulk modulus equation is given in Equation 1.21.

$$\sigma_m = \frac{B_i \varepsilon_{vol}}{1 - (\frac{\varepsilon_{vol}}{\varepsilon_u})} \qquad (1.20)$$

$$B = B_i [1 + \frac{\sigma_m}{B_i \varepsilon_u}]^2 \qquad (1.21)$$

where:
B = Tangent bulk modulus.

B_i = Initial bulk modulus.
ε_{vol} = Volumetric strain.
ε_u = Ultimate strain.
σ_m = Mean stress.

Musser (1989) stated that using the hydrostatic soil parameters, B_i and ε_u, developed by Selig (1988) resulted in larger deflections than those based on field observations. Selig (1990) published soil stress strain parameters of hyperbolic tangent and bulk modulus models for plastic pipe installations at different compaction levels for different soils.

1.2.3.2 Pipe stiffness

Pipe stiffness can be determined using both the parallel plate test and the curved beam test while pipe material modulus can be determined using the compression test. Plastic pipe stiffness is strain rate and time dependent. In this section, different pipe tests and the dependency of the plastic pipe stiffness and modulus on loading rate and time will be discussed.

1.2.3.2.1 Parallel plate test

Plastic pipe stiffness is the measurement of the load capacity of the pipe itself subjected to loading conditions. Pipe stiffness is a function of the material type and the geometry of the pipe wall. Plastic pipe stiffness can be determined using the ASTM D-2412 parallel plate load test shown in Figure 1.11. A 6-inch long pipe specimen is loaded at a constant rate of 0.5 in./min at a constant temperature of 23^0 C. The pipe stiffness (PS) is defined as the ratio of the applied force (F) in pounds per linear inch over the measured change of pipe inside diameter (Δy). Pipe stiffness can also be defined as the slope of the load deflection diagram. The stiffness factor (SF), which is the value of pipe modulus multiplied by moment of inertia, is defined as shown in Equation 1.22. The pipe stiffness at

5% vertical deflection, i.e. the change in vertical pipe diameter divided by the original pipe diameter, is typically used as the design value of stiffness. This represents the secant pipe stiffness at 5% deflection. ASTM D-2412 stated that the stiffness of pipes with larger sizes made from relatively low modulus material may be affected by creep due to the time taken to reach the 5% deflection. Both pipe stiffness and stiffness factor are highly dependent on the degree of deflection. For a large magnitude of vertical deflection percent a correction factor C, $C= (1+ (\Delta y/2d))^3$, should be used to calculate the stiffness.

$$EI = 0.0186 \frac{F}{\Delta y} D^3 \qquad (1.22)$$

where:

E = Flexural modulus of elasticity.
I = Moment of inertia.
D = Mean diameter.
F = Load applied to the pipe ring.
Δy = Measured change in inside diameter in the direction of applied load.

1.2.3.2.2 Curved beam stiffness

Gabriel and Goddard (1999) stated that pipes in service are affected by the soil passive action at the pipe spring line. This reduces the pipe wall bending moment and increases the wall ring compression. In parallel plate laboratory tests, all lateral restraint is absent, which maximizes wall bending and minimizes ring compression. This is a significant departure from the anticipated field service conditions. Gabriel and Goddard (1999) proposed a curved beam test to measure the pipe stiffness. The curved beam responds to loads with less wall bending moment than that of full ring. Therefore, greater proportion of the wall compression dominates the response of the curved beam than that of a full ring. Hence, the curved beam more closely approximates the field conditions of a buried pipe, Gabriel and Goddard (1999).

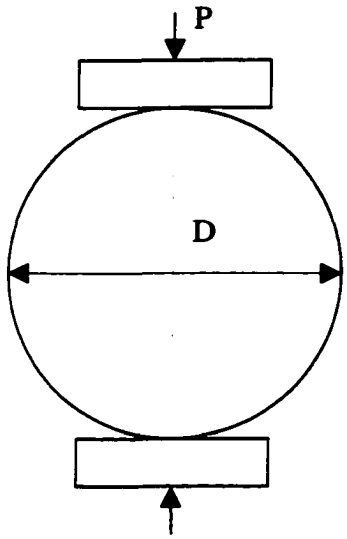

Figure 1.11. Parallel plate load test.

The curved beam test was performed by Gabriel and Goddard (1999) using 90^0 arcs cut from pipes of diameters ranging from 12 to 48 inches as shown in Figure 1.12. The pipe arcs were loaded in a short period of time and the stress relaxation of HDPE pipe material was investigated. Gabriel et al. (2002) proposed a time independent stiffness which was determined by back extrapolation of residual stiffness to zero time, using stiffness-displacement percent curve for a constant applied load.

1.2.3.2.3 Compression Test

Zhange and Moore (1997) studied the behavior of HDPE material using a compression test on cylindrical samples with a height of 1 inch and a diameter of 0.5 inches as shown in Figure 1.13. Tests were performed at different conditions including constant strain rates, abrupt strain rate, and creep. All of these tests were performed at a constant temperature of 23^0 C.

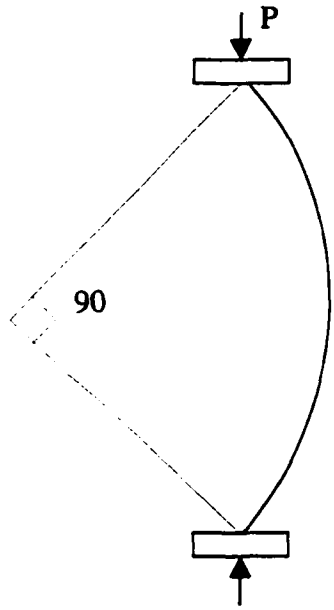

Figure 1.12. Flexible pipe curved beam test.

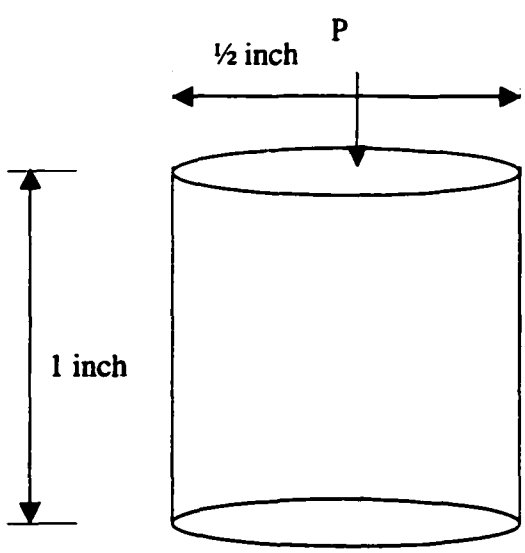

Figure 1.13. Compression test.

1.2.3.2.4 Loading rate effect on pipe stiffness

Schluter and Shade (1999) performed the parallel plate test at three different loading rates using PVC and HDPE pipes. These rates were 0.05 in./min, 0.5 in./min, and 5 in./min. Changing the loading rate by a factor of 100 resulted in a 6.5% stiffness change in PVC pipes and 56% of HDPE pipes. Schluter and Shade (1999) also stated that the ASTM D-2414 deflection rate of 0.5 in./min does not relate to the real world deflection rate and that a deflection rate of 0.05 in./min is more realistic. It was concluded that both laboratory measurements and theoretical calculations of ASTM D-2412 are too simplistic and that the deflection rate effect on PVC pipes is minor but has a great influence on HDPE stiffness. Sargand et al. (1998) stated that plastic pipes are rarely subjected to a deflection rate of 0.5 in./min which is specified in the parallel plate test and concluded, after a review of the field data, that plastic pipes generally have a deflection rate of 0.01 to 0.06 in./min. Sargand et al. (1998) also tested PVC and HDPE pipes using a variable rate parallel plate test at two different rates of 0.5 and 0.05 in./min. Figures 1.14 and 1.15 show the load per unit length (lb/in.) versus the vertical deflection percent results of variable loading rate parallel plate tests performed on 18 inch HDPE and PVC pipes respectively. The pipe stiffness calculated using Equation 1.22 is summarized in Table 1.4. These results showed that the loading rate has little effect on the PVC pipe stiffness, while HDPE material is more sensitive to the loading rate. The reduction of pipe stiffness was 3% to 6% for PVC and 25% for HDPE pipes. Figures 1.14 and 1.15 and Table 1.4 clearly show that special treatment needs to be considered when dealing with HDPE pipe properties.

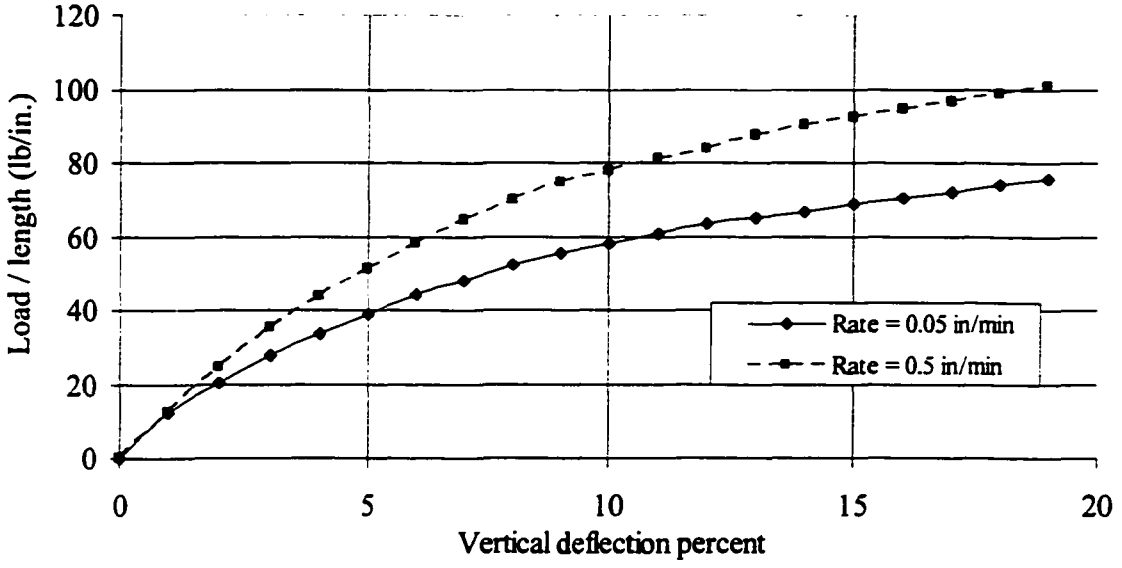

Figure 1.14. Parallel plate test for 450 mm HDPE pipe (Sargand et al. 1998).

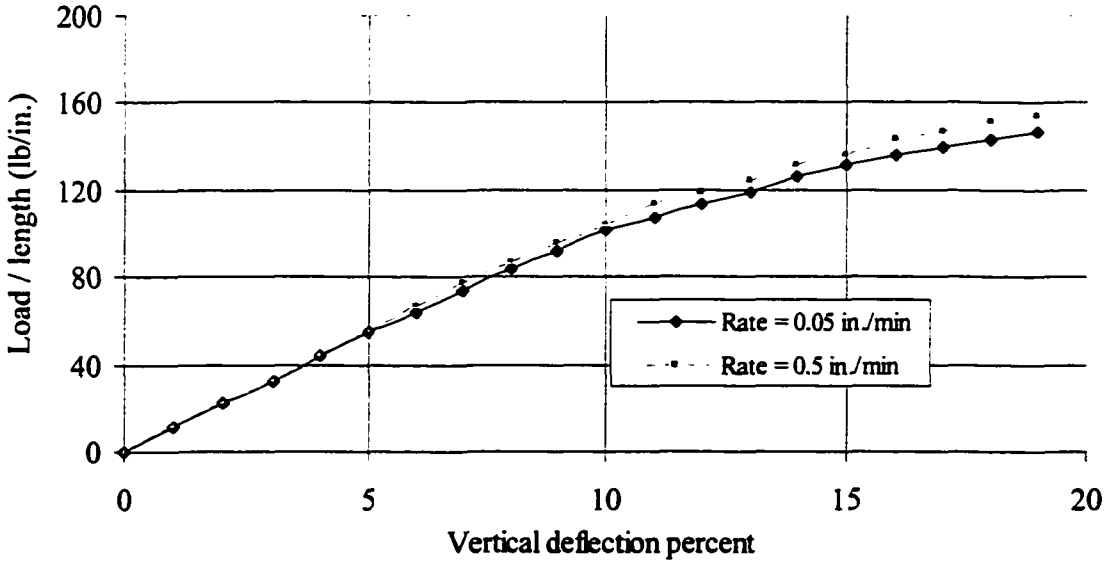

Figure 1.15. Parallel plate results for 450 mm PVC pipe (Sargand et al. 1998).

Table 1.4. Pipe stiffness of parallel plate test at two different loading rates.

	Loading rate	Pipe stiffness (lb/in.) at percent deflection of			
Pipe material	in/min	5%	10%	15%	19%
PVC	0.5	62	57.9	50.8	45
	0.05	60.5	55.6	48.4	42.5
HDPE	0.5	56.2	44.8	34.7	29.6
	0.05	42.5	33.2	25.9	22.3

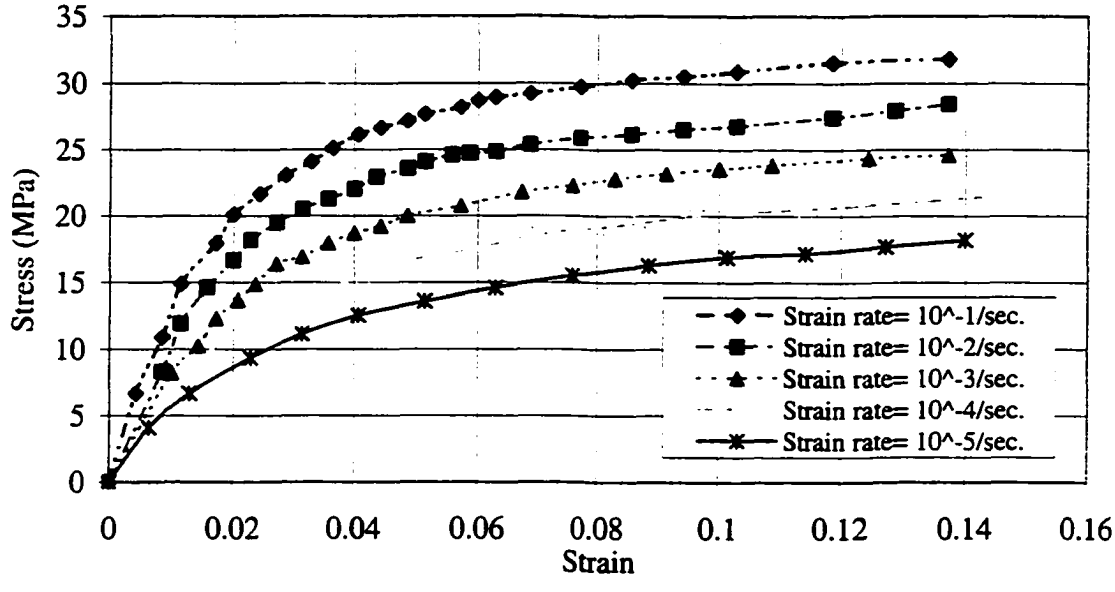

Figure 1.16. Stress-strain results of compression test (Zhange and Moore 1997).

Zhange and Moore (1997) performed various compression tests on HDPE pipe material. These tests were constant strain rate, abrupt strain rate, and creep. The constant rate tests were conducted at strain rates ranging from 10^{-5}/sec to 10^{-1}/sec. These results are shown in Figure 1.16. This Figure shows that for all strain rates the material is nonlinear with a modulus independent of strain rate at approximately 0.04 (or 4%) strain. For later reference

in this dissertation, the region with strains less than 4% is called region A while that with strains more than 4% is called region B. The strain abrupt test was performed by changing the strain rate from 10^{-3}/sec to 10^{-2}/sec; after a brief period of rapid stress increase, the stress attained the level it would have held if the new strain rate had been used from the beginning of the test. Zhang and Moore (1997) concluded that HDPE material does not have strain rate history dependency.

1.2.3.2.5 Time effect on pipe stiffness

Sargand et al. (1998) studied the stress relaxation of PVC and HDPE pipes using the parallel plate test. A variable load was applied over a period of one hour to maintain three different vertical deflection percentages of 5%, 10%, and 15%. Figure 1.17 shows the stress relaxation results for PVC pipes while Figure 1.18 shows the stress relaxation of HDPE pipes. The time was extrapolated to estimate the pipe stiffness at 50 years. Table 1.5 summarizes the results of both tests. The percent reduction in stiffness was dependent on the percent deflection for PVC pipes with a range of percent reduction between 12 and 32%. The percent reduction in pipe stiffness is greater for HDPE pipes but it is less dependent upon the vertical deflection percent. The percent reduction in stiffness for HDPE pipes was between 75 and 82%.

Goddard (1999) stated that parallel plate test results are not comparable from one diameter to another for plastic pipes because of the time effect of the test. The time required for a 12 inch pipe to reach the 5% deflection is 1.2 min, while it is 4.8 min for a 48 inch diameter pipe. Figures 1.17 and 1.18 show that PVC and HDPE stress relaxation starts upon the application of the load. Consequently, recorded loads of larger pipes are more heavily affected by rapid stress relaxation than smaller pipes. Gabriel et al. (2002) introduced the

idea of time-independent stiffness using curved beam tests. HDPE pipes of 12 to 48 inches in diameter were tested. A constant load was applied and the pipes deformed from 0% to 10% chord displacement in just over _ second. This near instantaneous displacement was

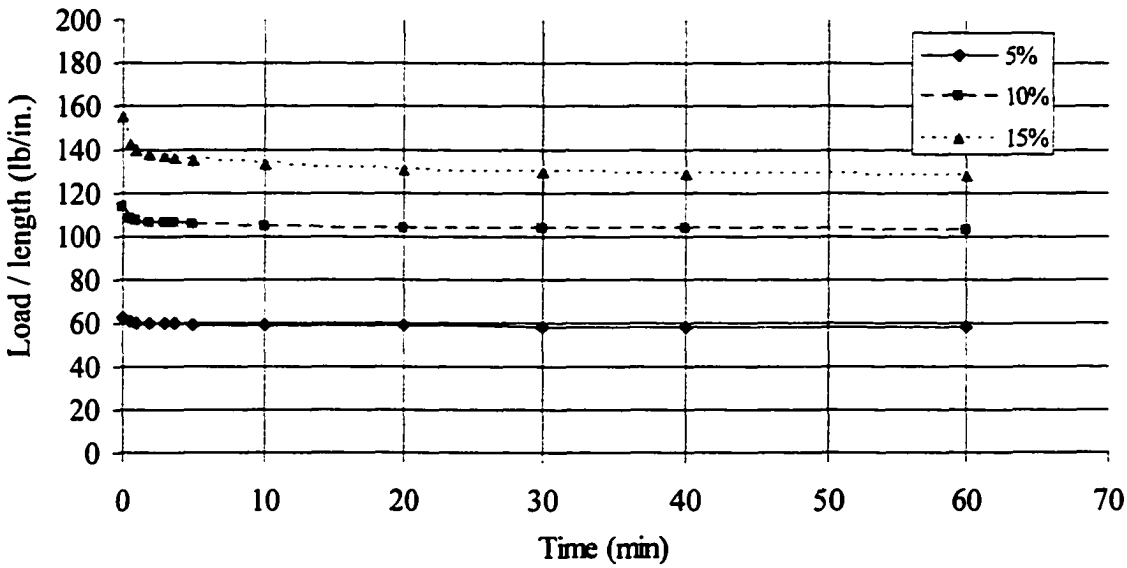

Figure 1.17. Results of stress relaxation test on PVC pipe (Sargand et al 1998).

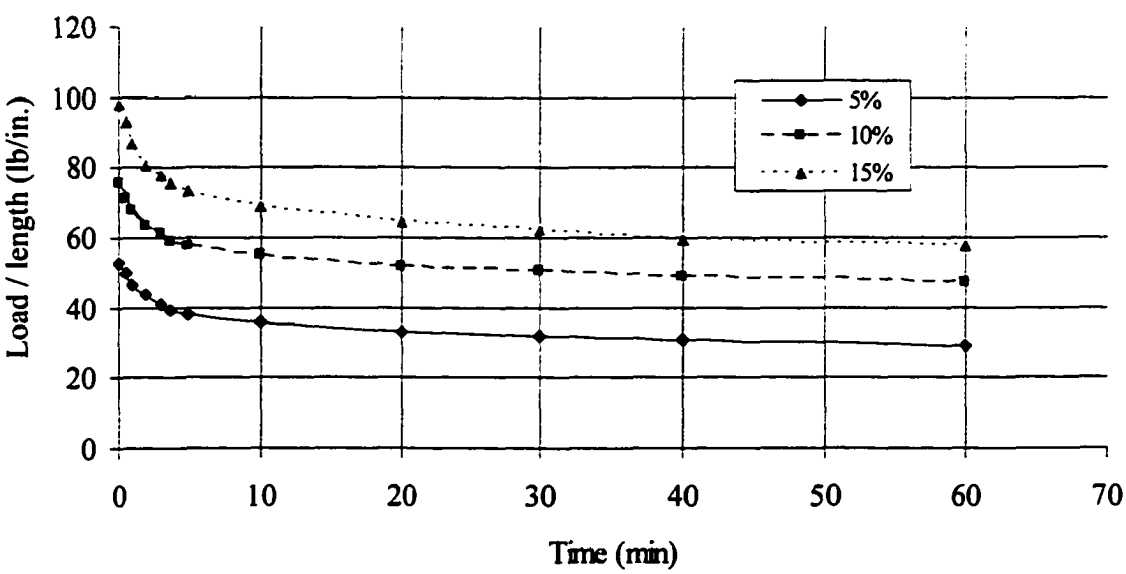

Figure 1.18. Results of stress relaxation test on HDPE pipe (Sargand et al1998).

Table 1.5. Pipe stiffness results of stress relaxation tests of parallel plate test.

Pipe material	Time	Pipe stiffness (lb/in.) at percent deflection		
		5%	10%	15%
PVC	1 min.	60.3	107.7	140.6
	50 years	52.6	88.7	95.7
HDPE	1 min.	46.8	67	88.1
	50 years	8.4	16.3	16.2

intended to decrease the stress relaxation. A regression line was fitted to the nearly linear portion of displacement-stiffness curve between 5% and 10%. The regression line was extrapolated backward to 0% displacement which represents the zero time. The value of stiffness at this point is called the time independent stiffness. The plastic pipe stiffness is time dependent, and back extrapolation to zero time does not yield a representative value of stiffness since the pipe stiffness at time "t" after installation is what controls the pipe behavior. The thermoplastic pipe stiffness is also depending on the loading rate which does not relate to the field condition in the tests described in Gabriel et al. (2002).

Zhange and Moore (1997) conducted creep tests at different stress levels using the compression test. It was noted that the secondary creep is almost constant and that the primary creep showed a rapid increase in creep strain. The results of creep tests at different stress levels are shown in Figure 1.19. The instantaneous strain was subtracted from these curves so the strain change could be modeled.

Greenwood and Lang (1990) suggested that the field measured deflections increase for a period of time and then stabilize to a constant level. By recognizing the long-term soil-

pipe behavior of creeping and relaxation, they expressed the pipe stiffness term as in Equation 1.23.

$$S_p = \frac{8C_{TP}EI}{D^3} \qquad (1.23)$$

where:

S_p = Pipe stiffness term.
C_{TP} = Pipe stiffness retention factor.
E = Pipe modulus of elasticity.
I = Moment of inertia.
D = Pipe diameter.

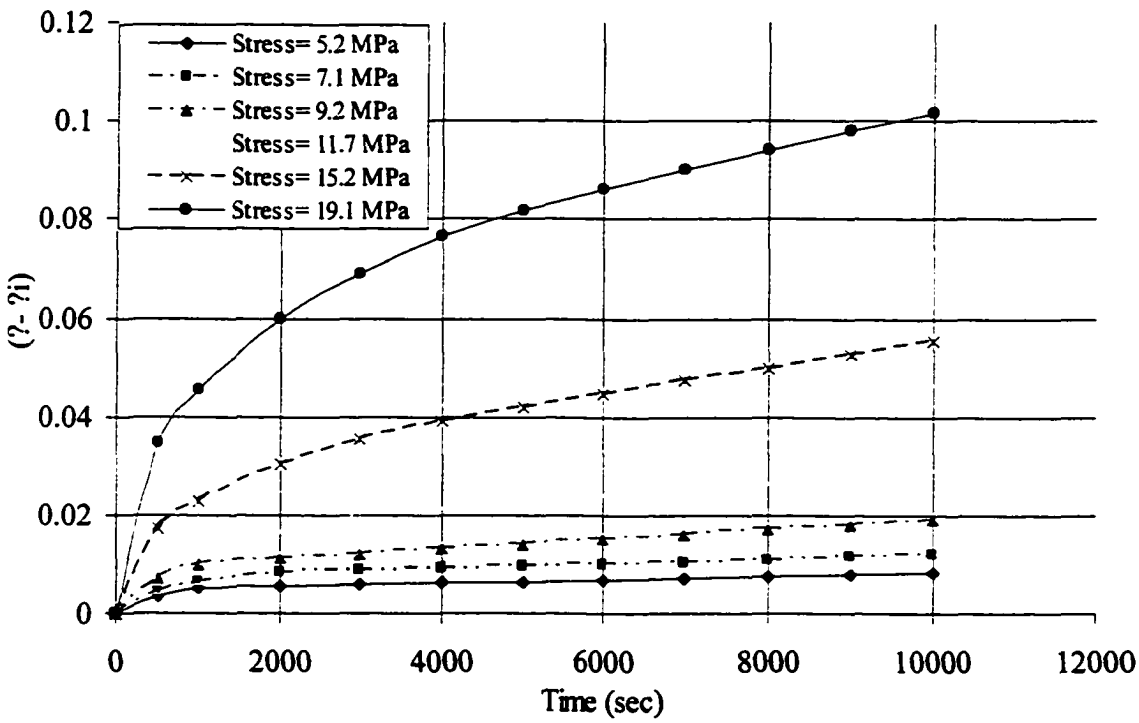

Figure 1.19. Creep test results subtracting the instantaneous strain (Zhange and Moore 1997).

Sargand et al. (2001) studied the time dependency of thermoplastic pipe deflection in the field using 12 HDPE and 6 PVC pipes with diameters between 30 and 60 inches buried under 20 and 40 feet embankments. These pipes were buried in two different backfills of

crushed limestone and river sand. The vertical and horizontal deflections and the circumferential shortenings were monitored for 8 months during and after construction. The vertical and horizontal deflections, and circumferential shortening stabilized within two months from the completion of the construction. Lars Janson (1996) reported that more than eight years of constant pipe deflection gave no reason from a practical point of view to change the long term pipe modulus that could be determined after only six weeks of testing. Trantina and Nimmer (1994) stated that the objective of the graphical curve fitting technique used to study the material time dependent properties was to obtain the most accurate fit while achieving reasonable extrapolation predictions with minimum complexity. Trantine and Nimmer (1994) also stated that engineering judgment should be used concerning the appropriate extrapolation in time and caution should be exercised when more than one order of magnitude of time extrapolation is used.

1.2.3.3 External loads

Buried pipes are subjected to dead loads and live loads. Dead loads are the weight of backfill materials carried by flexible pipes. For flexible pipes, the design dead load in the trench can be determined either using the Marston load or the prism load, whichever is larger.

Live loads are due to traffic, impact, construction, frost action, and expansive soil. The American Association of State Highway Transportation Officials (AASHTO) recommends pipe designers to use the wheel load of either H-20 or HS-20 as their design live load because highways and bridges are usually designed for "worst case" conditions.

Katona (1990) studied the minimum depth of soil cover for HDPE pipes under traffic

loading. Different cases of truck loading and pipe diameters were tested. The diameters investigated were 12, 15, 18, 24, 30, and 36 inches. Two different levels of compaction (85% and 100%) were used on the silty clayey sand. Minimum soil covers for the different diameters of pipe investigated are presented in Table 1.6. These results were calculated using the pipe short term properties for minimum and maximum moments of inertia in the case of 85% compaction and only minimum moment of inertia for the case of 100% compaction. Katona (1990) also noted that pipes with larger diameters require less depth of soil cover than small diameter pipes and suggested that manufacturers make larger diameters stronger. Klaiber et al. (1996) and Lohnes et al. (1997) studied the performance of HDPE pipes using laboratory and full scale tests on different pipe diameters. Laboratory parallel plate tests on different pipe diameters were completed to determine the pipe stiffness and the stiffness factor according to ASTM D-2412. Parallel plate tests revealed that pipes with smaller diameters have a greater pipe stiffness at 5% deflection than large diameter pipes. The stiffness factor (EI) that considers the effect of the pipe diameter showed that pipes with large diameters have greater stiffness factors than pipes with smaller diameters. Lohnes et al.' s full scale field tests on pipes from the same manufacturer showed that 48 inch diameter pipes, with the same backfill material, experienced less vertical deflection percent and less strains than 36 inch diameter pipes at the same loads. Comparing the vertical deflection percent does not necessarily imply that pipes with large diameters are stronger than pipes with smaller diameters. Two pipes with different diameters may deflect the same amount but this result in different values of vertical deflection percent where the effect of the pipe diameter is included.

Construction loads resulting from heavy equipment and installation may also be a concern when designing a pipe. Generally, construction equipment such as a hydraulic excavator is heavier than highway trucks, so the design load may be underestimated if a

Table 1.6. Minimum soil cover in inches (Katona 1990).

Pipe diameter	H-truck	85 % compaction		100% compaction
(inch)	H-x	I_{min}	I_{max}	I_{min}
12	H-10	12	12	12
	H-15	16	12	12
	H-20	19	15	12
	H-25	21	17	12
	H-30	23	19	12
15	H-10	12	12	12
	H-15	14	12	12
	H-20	18	14	12
	H-25	21	16	12
	H-30	23	18	12
18	H-10	12	12	12
	H-15	14	12	12
	H-20	18	13	12
	H-25	20	16	12
	H-30	23	18	12
24	H-10	12	12	12
	H-15	12	12	12
	H-20	15	12	12
	H-25	18	12	12
	H-30	20	14	12
30	H-10	12	12	12
	H-15	12	12	12
	H-20	12	12	12
	H-25	15	12	12
	H-30	18	12	12
36	H-10	12	12	12
	H-15	12	12	12
	H-20	12	12	12
	H-25	12	12	12
	H-30	15	12	12

traffic load is chosen for design. During pipe installation, McGrath and Selig (1994) observed that the impact resulting from compaction equipment on the pipe may lead to flexible pipe distortions, especially when the compaction is operated too close to the pipe. Therefore, it is necessary to design a pipe that can withstand not only the traffic load, but also the construction loads.

1.2.4 Plastic Pipe Installation

ASTM D-2321 provides recommendations for the installation of buried plastic pipes. These recommendations are intended to ensure a stable underground environment for thermoplastic pipes under a wide range of service conditions. Figure 1.20 shows different regions around an underground pipe as specified in ASTM D-2321. The space between the pipe and the trench wall must be wider than the compaction equipment used in the pipe zone. The trench width should be wider than the greater of pipe outside diameter plus 16 inches or pipe outside diameter times 1.26 plus 12 inches. Backfill material particle size is limited to material passing 1_ inch sieve. The recommendations for installation and use of different soils and aggregates for foundation, embedment, and backfill around the plastic pipes are shown in Table 1.7. The minimum soil densities were specified based on attaining an average modulus of soil reaction, E', of 1000 psi. The moisture content of embedment material must be within suitable limits to permit placement and compaction to the required levels with a reasonable effort. This moisture content limit is set in the pipe zone to control the pipe excessive deflection. A minimum depth of backfill above the pipe should be maintained before allowing vehicles or heavy construction equipment to transverse the pipe trench, which depends on the soil type. A key objective during installation of flexible plastic pipes is to compact embedment material under pipe haunches to ensure complete contact with the

pipe bottom and to fill voids below the pipe. The lack of adequate compaction of embedment material in the haunch zone can result in excessive deflection, since it is this material that supports vertical loads applied to the pipe.

Corrugated Polyethylene Pipe Association (CPPA) (1997) specified the minimum trench dimensions, the backfill envelop, and the minimum and maximum cover limitations. The typical trench width is twice the pipe nominal diameter but not more than the minimal diameter plus 2 feet. The height of the initial backfill shown in Figure 1.20 should be at least 6 inches above the pipe crown. The height of the initial and the final backfill should be at least 1 foot over the pipe crown. The height of the bedding material is typically between 2 and 6 inches.

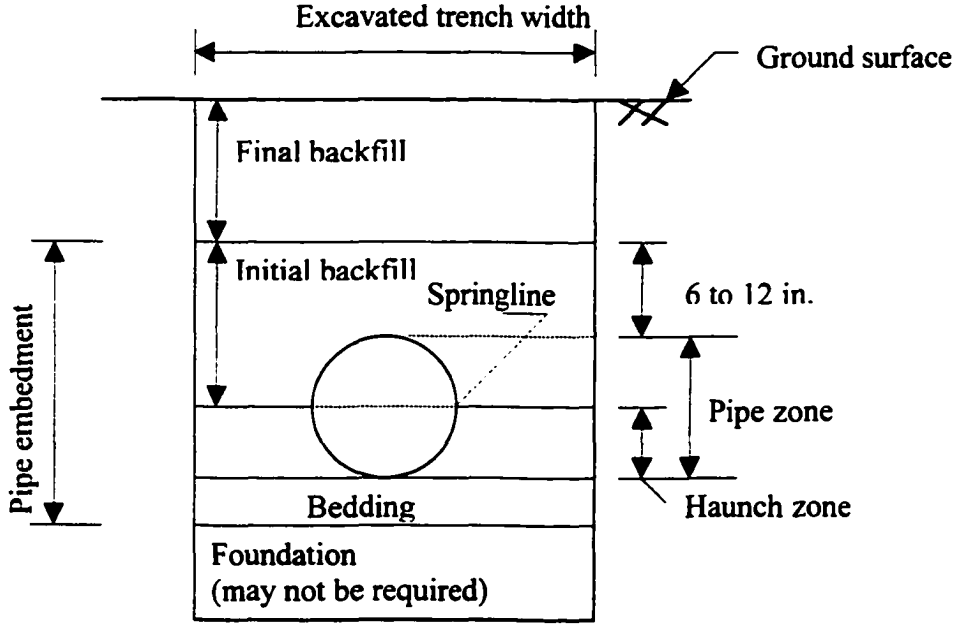

Figure 1.20. Trench cross section showing the terminology used by ASTM D2321.

Table 1.7. Recommendation for installation and use of soils and aggregate for pipe foundation embedment, and backfill (ASTM D2321).

	Soil class				
	Class IA	**Class IB**	**Class II**	**Class III**	**Class IV-A**
General Recommendation	do not use if migration of fines expected	process to obtain required gradation to minimize fines migration	check gradation in case of flow to minimize fines migration	do not use if water may cause instability	obtain geotechnical evaluation of oproposed material
Foundation	suitable	suitable	suitable	suitable	suitable if undisturbed
Bedding	suitable install in max. of 6" layer	suitable install in max. of 6" layer	suitable install inmax. of 6" layer	suitable only in dry trenches	suitable only in dry trenches
Haunching	suitable install in max. of 6" layer	suitable install in max. of 6" layer	suitable install in max. of 6" layer	suitable install in max. of 6" layer	suitable only in dry trenches
Initial Backfill	suitable install in min. of 6" layer	suitable install in min. of 6" layer	suitable install in min. of 6" layer	suitable install in min. of 6" layer	suitable install in min. of 6" layer
Embedment Compaction	use vibratory compactor	- min. density 85% Standard Proctor - use vibratory compactor or hand tampers	- min. density 85% Standard Proctor - use vibratory compactor or hand tampers	- min. density 90% Standard Proctor - use vibratory compactor or hand tampers	- min. density 95% Standard Proctor - use impact compactor or hand tampers
Final Backfill	compact as required by the engineer	compact as required by the engineer	compact as required by the engineer	compact as required by the engineer	compact as required by the engineer

1.2.5 Analytical and Experimental Studies

The first completely theoretical solution of flexible pipes was published by Burns and Richard (1964) for an elastic circular pipe deeply buried in an infinite elastic medium subjected to horizontal and vertical loading. Solutions for pipe deflection, thrust and moment were obtained for full bonding and free slip at the pipe-soil interface. Moser (1997) stated that the greatest shortcoming of Burns and Richard solution is that it assumes double symmetry. That is, it assumes the soil-pipe system is symmetric about horizontal and vertical axes. In the elastic solution, no assumption was made or needed for the pressure distribution around the pipe. On the other hand, Sargand et al. (1998) stated that the elastic solution can not account for different pipe installation modes and the results are not useful if the height of soil cover is a fraction of the pipe diameter.

Moore (1995) used a three-dimensional finite element analysis to model HDPE pipes subjected to various burial depths considering the pipe geometrical properties, corrugations, for various backfill materials using short and long term pipe material properties. The stresses were compared with a two-dimensional finite element analysis using a smooth, no corrugations, cross section of the HDPE pipe. His study showed that the two dimensional analysis can predict the compression and circumferential stresses of the pipe.

Taleb and Moore (1999) presented a two-dimensional finite element model to study the response of metal culverts to the compaction process. The culvert deformation and bending moment during the process of backfilling were predicted and compared with the experimental results. AFENA was used to perform the two-dimensional finite element analysis using elastic-plastic soil model with linear variation of soil modulus with depth. The plastic soil behavior was assumed as the behavior of the soil beyond shear failure. This

analysis showed a good agreement between the measured and analytical pipe deflections and bending moments.

Moore and Taleb (1999) used a three dimensional finite element analysis to study the metal culvert response to live loading and compared the results with the experimental results of Webb et al. (1998). Real truck load tests were performed by Webb et al. (1998) on metal pipes where the truck passed over metal pipes with two different depths of soil cover (1 and 2 feet) at two different soil condition (well and loose compacted). Moore and Taleb (1999) modeled the soil as a linear elastic material with a linear modulus variation with depth. The pipe performance properties studied were the distributions of deflection, thrust, and moment along the culvert axis. Culvert deflections show the correct pattern with a maximum magnitude difference of the pipe crown of 20%. The measured thrust exceeds the predicted values using a three-dimensional analysis with a maximum difference between measured and predicted values of about 50%. The bending moment pattern is successfully predicted with a magnitude of 50% to 70% difference from the measured values. Moore and Taleb (1999) suggested that this may be due to soil shear failure. They also performed a three-dimensional analysis using a reduced soil stiffness based on engineering judgment to take into consideration the shear soil failure. This approach affects the whole soil zone but gives more reasonable moment results. Their study showed that neglecting the shear failure of soil results in a greater difference between the measured and the analytical results.

Moser (1997) studied various methods of predicting the structural performance of flexible pipes. The theoretical methods were compared with full scale testing results. These theoretical methods were semi empirical equations (Iowa formula), closed form analytical solutions (Burns and Richard elastic solution), and the finite element method. Moser (1997)

stated that the finite element method most closely presents the full scale test results and that the assumption of elastic soil can lead to large errors.

Hashash and Selig (1990) studied the long-term performance by monitoring a 24 inch diameter and 576 feet long HDPE pipe under a soil fill up to 100 feet for 722 days. The bedding, haunch, and the initial backfill materials were well graded crushed stone with 100% compaction. A 77% of arching was determined from the measured field stresses, so the pipe is only carrying 23% of the prism load.

Sargand et al. (2001) measured the soil pressure at various heights above two 30 inch diameter pipes of PVC and HDPE pipes. The measured geostatic pressure reached the pipe crown was greater for the PVC pipe than the HDPE pipe. The soil pipe interaction zone extended only about one pipe diameter above the pipe for both HDPE and PVC pipes.

PART I. EVALUATION OF HIGH DENSITY POLYETHYLENE PIPE INSTALLATIONS

2. INTRODUCTION AND METHODOLOGY

2.1 Objective

Although high density polyethylene (HDPE) drainage pipes have been used for over a decade, little information is available on the in-service behavior of these pipes. At the request of the Minnesota Concrete Pipe Association (MCPA) an investigation to evaluate the field performance of HDPE pipes was undertaken.

A list of potential sites was provided by MCPA for investigation. Ten projects were selected from this list by the research team for evaluation based on a variety of variables including pipe diameter, age of installation, and native soil conditions.

The objective of this study was to evaluate the field performance of in-service HDPE pipes using visual information obtained from a remote, motorized video camera. The ten projects were surveyed in Minnesota between July, 2000 and March, 2001. These projects are located in the cities of Mankato, Blaine, Moundsview, Fairmont, Gaylord, Le Center, and Maple Grove as shown in Figure 2.1. The total pipe length surveyed in these projects was 12,006 feet; pipe diameters ranged between 12 and 48 inch.

2.2 Methodology

The surveys were conducted with a remote, motorized television camera that moved through the pipe. Figure 2.2 shows the type of camera used in the study. The interiors of the pipes were televised and recorded on videotape. The tapes were sent to Iowa State University where they were evaluated, and apparent structural and/or sediments problems were noted.

The performance characteristics that were considered in the evaluation were cross section deformations, wall buckling, wall crushing, wall cracking, joint separation, and

sediments. These characteristics and their locations along the length of the pipe were recorded. Data sheets for recording these characteristics are shown in Appendix A. The data for all the projects were collected and evaluated.

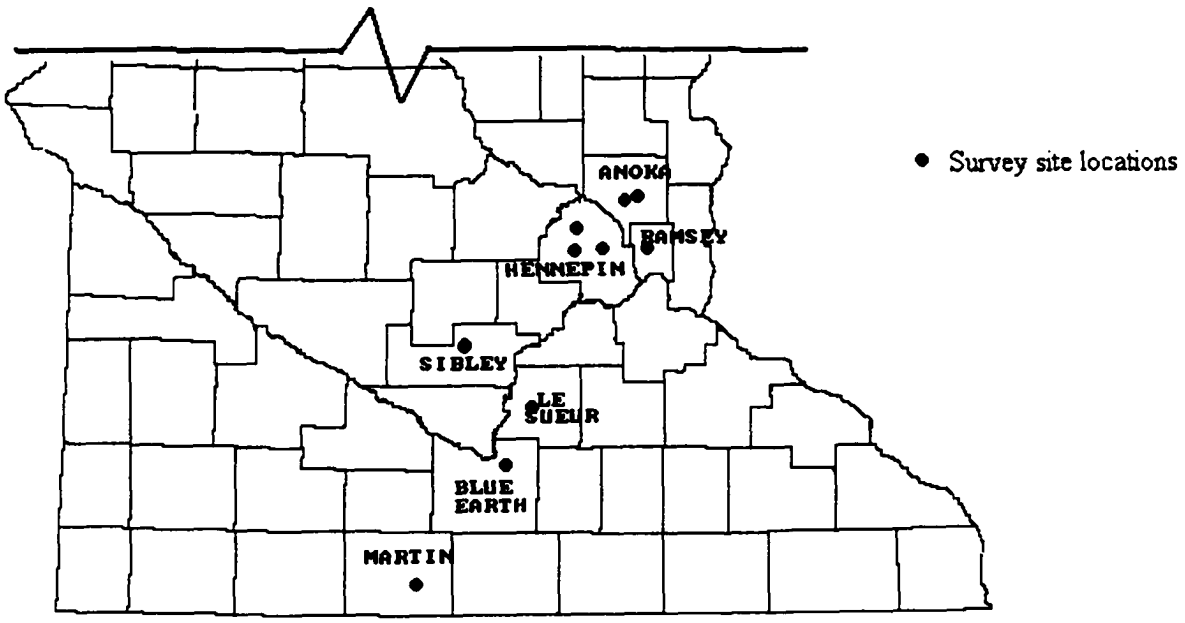

Figure 2.1. Partial Minnesota map with survey site locations.

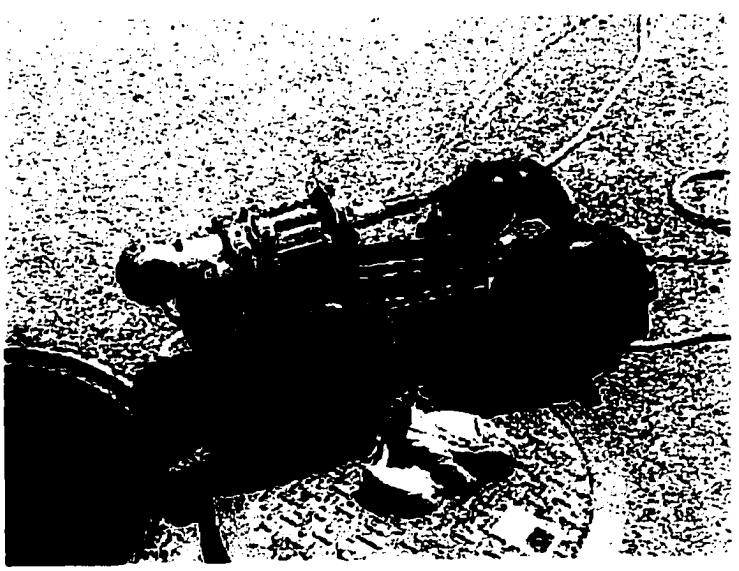

Figure 2.2. Remote, motorized camera used in this survey.

2.3 MN. DOT specifications for HDPE pipe installations

Minnesota Department of Transportation (MN. DOT) HDPE pipe specifications are presented in Figure 2.3. These specifications allow for a maximum pipe diameter of 36 inches and require well-graded granular backfill with 100% passing the 1 inch sieve. Well graded backfill material should extend at least 12 inches above the pipe crown. The total depth of soil cover above the pipe crown should be between 2 and 20 feet. The bedding immediately beneath the pipe is to be compacted sufficiently to provide a uniform support. The trench width should be the larger of 24 inches plus the inside pipe diameter or two pipe diameters.

Maple Grove uses the same specifications with a different type of required trench which is shown in Figure 2.4. The improved pipe foundation material, more than 6 inches in depth, is used in the case of poor native soil. The projects surveyed in this study were reported to have been installed according to MN. DOT specifications except for three installations where HDPE pipes with diameters larger than 36 inches were used and the sites in Maple Grove where a different type of trench is required.

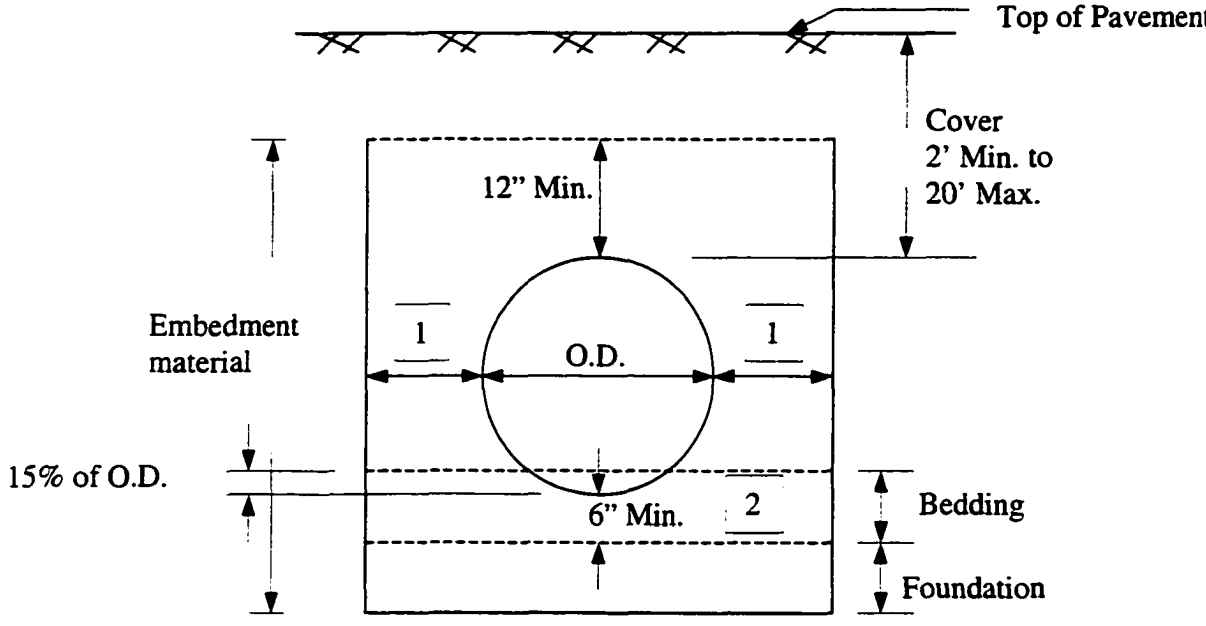

Notes:
Maximum nominal pipe diameter is 36 inches. Embedment material per Spec. 3149.20 modified to 100% passing the 1 inch sieve. Construction requirements per Spec. 2451 modified so that the embedment material is compacted in uniform layers 8 inches or less in thickness. Bedding shall be class B per. Spec. 2451.3.

1 Trench width per ASTM D2321 except as modified to provide ½ nominal inside pipe diameter or 12 inches (whichever is greater) on each side of the pipe, to allow for compaction.

2 The zone immediately beneath the pipe shall only be compacted sufficiently to provide uniform support.

Figure 2.3. MN. DOT specifications for plastic pipe storm sewer installations.

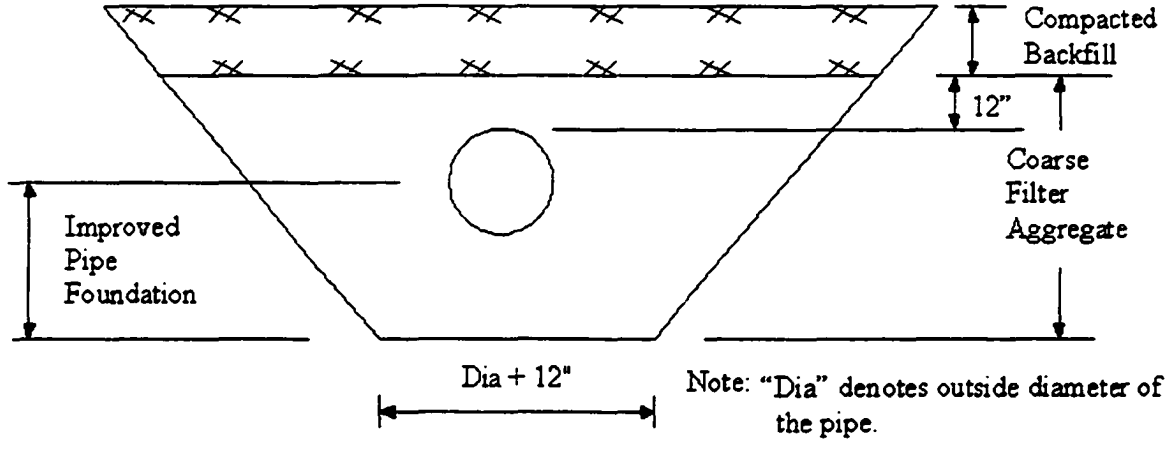

Figure 2.4. Maple Grove specifications for plastic pipe installations.

3. DATA EVALUATION AND INTERPRETATIONS

The observations and problems of the sites surveyed in this study are summarized in Appendix B. This chapter contains the evaluations of the surveyed projects and their interpretations.

3.1 Structural Problems

Table 3.1 presents a summary of the total lengths surveyed for each HDPE pipe diameter. The total length of the surveyed HDPE pipes was 12,006 feet. As may be seen, nine different diameters of the HDPE pipes were surveyed ranging from 12 to 48 inches. Over 56% of the HDPE pipes surveyed were 30 inches or more in diameter.

Table 3.1. Diameter and length of HDPE pipes surveyed.

Pipe Diameter (inch)	Total Length (feet)
12	347
15	1,590
18	397
24	2,807
27	61
30	2,027
36	1,962
42	342
48	2,473
Total length	12,006

It was observed that structural problems occurred in 19% of the length of the 48 inch diameter pipe, 8% of the 36 inch diameter pipe, 6% of the 30 inch diameter pipe, 6% of the 24 inch diameter pipe, 33% of the 18 inch diameter pipe, 2% of the 15 inch diameter pipe and 3% of the 12 inch diameter pipe. Figure 3.1 illustrates the weighted percent of structural problems observed for each pipe diameter. The weighted average of structural problems is defined as the ratio of the length with structural problems for each pipe diameter to the total

length surveyed for the same diameter all multiplied by the ratio of the length surveyed for the pipe diameter to the total pipe length surveyed. Structural problems are defined as the existence of local buckling dimpling pattern, cross sectional deformations, wall cracks, and/or pipe sags. Figure 3.1 shows a general trend of increasing structural problems as the diameter increases. Pipes with 27 and 42 inch diameters showed no cross sectional deformations. The percent of structural problems in the 48 inch diameter pipe was dramatic when compared with other pipe diameters. This indicates an increasing probability of problems with pipes whose diameters are greater than 36 inches, which is the largest HDPE pipe diameter allowed by the Minnesota DOT specifications.

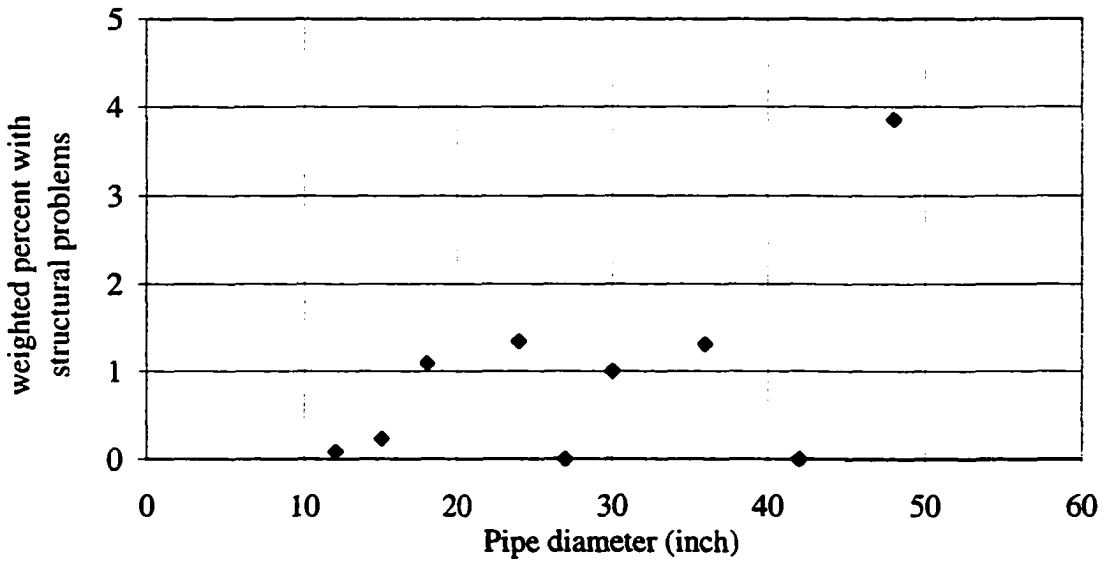

Figure 3.1. Weighted percent of pipe length having structural problems.

Elliptical cross sectional deformations with both horizontal and vertical shortenings were noticed at several locations during this study. Figure 3.2 is an example of the horizontal shortening of a pipe. An example of vertical shortening associated with significant increase in the horizontal diameter is illustrated in Figure 3.3. Figure 3.4 shows the relationship of

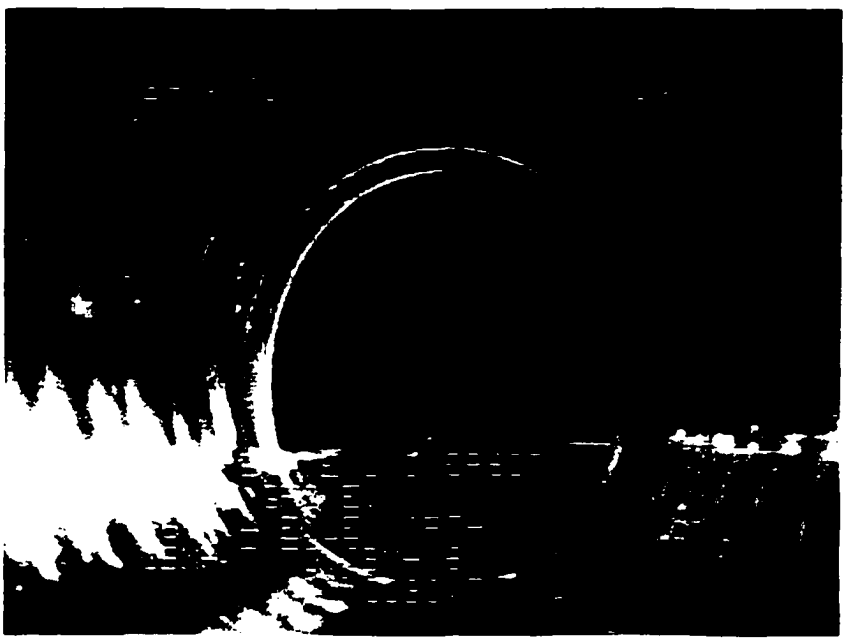

Figure 3.2. Cross sectional deformation with horizontal shortening associated with vertical joint offset in 15 inch pipe.

Figure 3.3. Cross sectional deformation with vertical shortening.

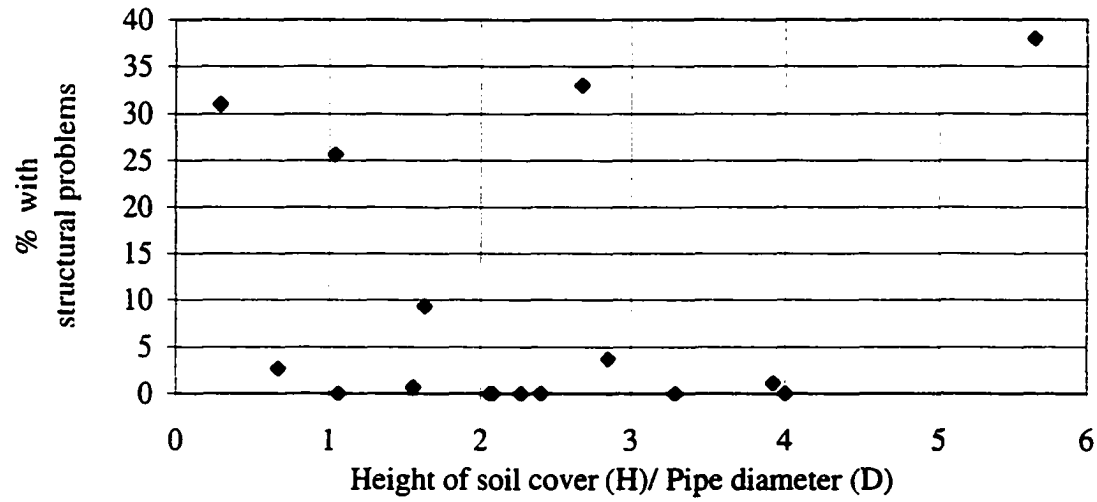

Figure 3.4. Percent of structural problems vs H/D ratio.

percent of structural problems with the ratio of the height of the soil cover (H) to the inside pipe diameter (D). This figure shows that pipes with small or large H/D ratios have a higher percent of structural problems. The largest value of H/D indicated the highest percent of structural problems (mainly cross sectional deformation with vertical shortening). This was interpreted as the effect of geostatic loads on the pipe crown. The smallest value of H/D also indicated a high percent of structural problems (mainly cross sectional deformations with horizontal shortening). This was interpreted as the effect of installation with a shallow soil cover and no surface loads to restore the pipe to 'round' again. Dimpling at small H/D ratios was also observed at two locations. This was interpreted as the effect of traffic loads. Except for one case (H/D= 2.7), all pipes with H/D ratios between 2 and 4 did not show any structural problems.

The 24 inch diameter pipe cross-section shown in Figure 3.3 has 10 to 12 inches of elliptical cross sectional deformations (vertical shortening) that extended for 10 feet. This represents an average of 46% deflection of pipe diameter. Associated with the vertical

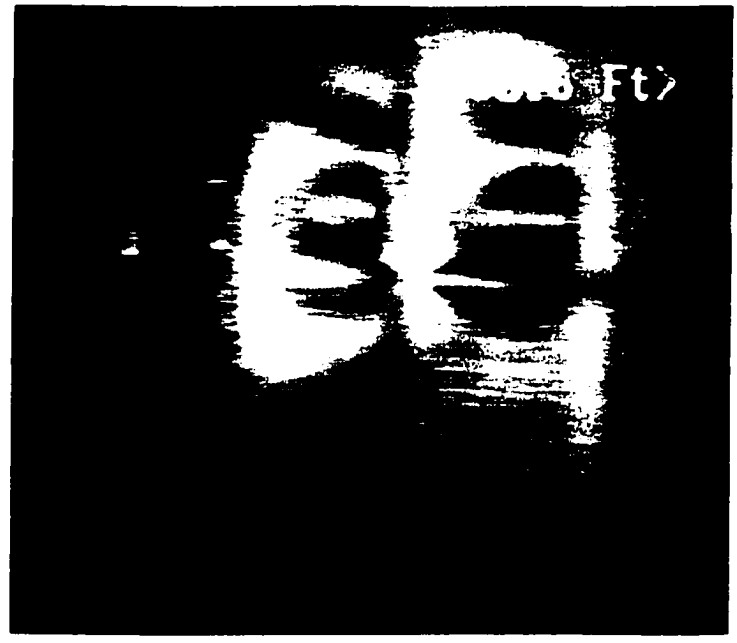

Figure 3.5. One inch dimples in 24 inch diameter pipe.

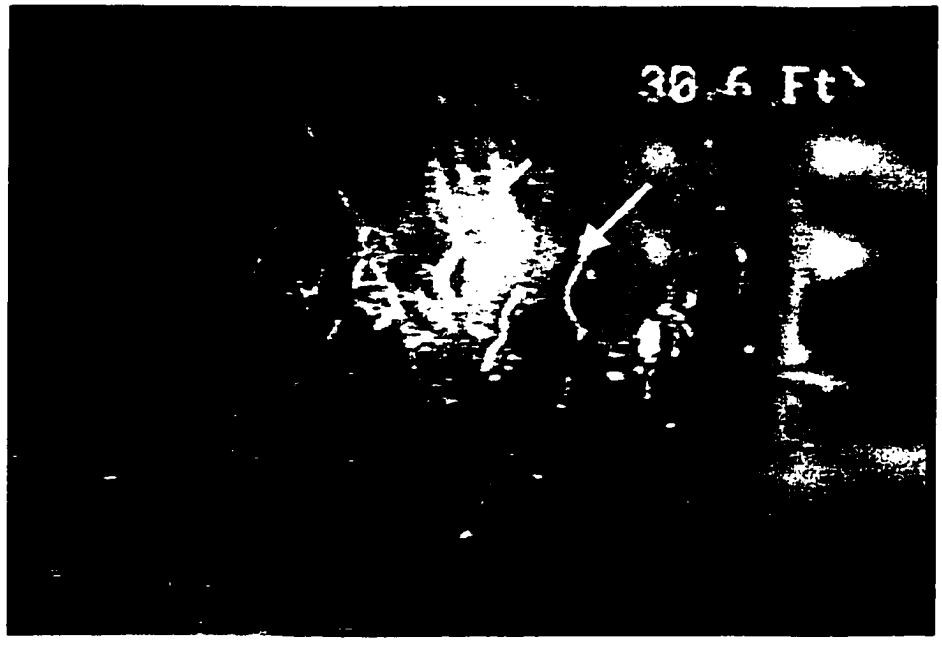

Figure 3.6. Cracks and dimples in 24 inch diameter pipe.

deformation were 1 to 2 inch dimples and pipe wall cracks at "2 o'clock"; these are shown in Figures 3.5 and 3.6. A Pipe sag of 8 to 10 inches in a 24 inch diameter pipe that extended for 6 feet was also noticed in the pipe shown in Figure 3.3; no plans were available for this site. The horizontal increase in the pipe diameter suggested that the soil around the pipe was not compacted properly.

Dimpling patterns, pipe wall deflections, and wall cracks were noticed nine times in the regions of "1 to 3 o'clock" and "9 to 11 o'clock" - four cases with cracks, three with wall deformations, and two with dimpling. Figure 3.7 shows a 3 inch wall deformation between "1 and 3 o'clock" in the 15 inch diameter pipe which represents 20% of the pipe diameter. These match Moser's (1998) results that were shown in Table 1.1, where six out of nine local buckling cases reported had dimpling between "2 to 3 o'clock".

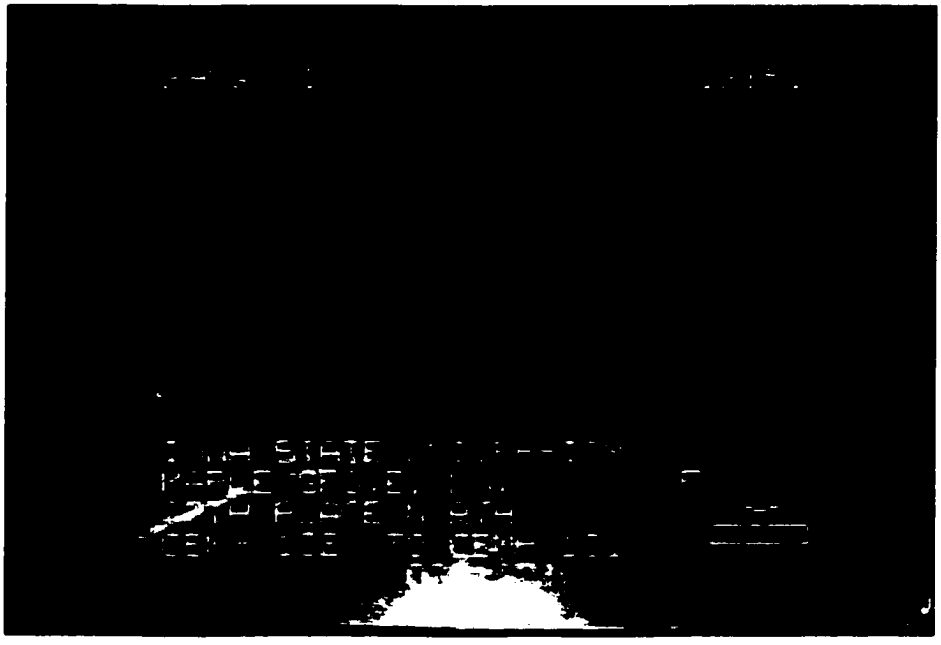

Figure 3.7. Pipe wall deflection between "1 and 3 o'clock" in a 15 inch diameter pipe.

Dimpling was observed at four different sites in this survey. It was in pipes with 15, 24, 30, and 36 inch diameters. One example of the dimpling in a 24 inch diameter pipe is shown in Figure 3.5. The dimples occur over 152 feet of the pipe length surveyed, which represents 1.25% of the total pipe length. In two of the cases that showed dimpling, the pipes were buried at a relatively shallow depth of 1 to 2 feet under surface traffic loads. The minimum specified soil cover by the MN. DOT is 2 feet, as was shown in Figure 2.3. Table 1.4 showed that the minimum soil cover calculated by Katona (1990) is even less than 2 feet. One of the two cases that showed dimpling with shallow soil covers has a 2 foot depth of soil cover which satisfies the Minnesota DOT specifications, while the other has a 1.2 feet of soil cover which satisfies the soil cover calculated by Katona (1990).

Pipe wall tearing was noticed twice in this survey. Figure 3.8 shows an example of a wall tearing (pointed by the arrow) in a 15 inch diameter pipe. This wall tearing is expected to be caused by or during the construction process.

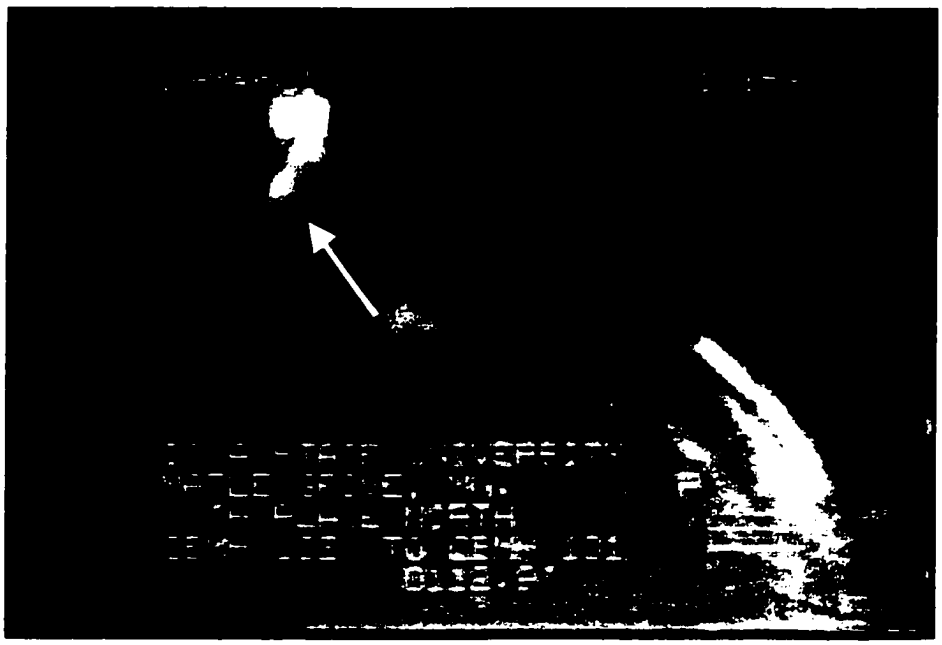

Figure 3.8. Pipe wall tearing in a 15 inch diameter pipe.

A summary of the structural performance for the pipe diameters that showed structural defects is presented in Table 3.2. The overall length percent of dimpling for the 15 inch diameter is 0.25%, 0.37% for the 24 inch diameter, 5.8% for the 30 inch diameter, and 1% for the 36 inch diameter. The 36 inch diameter pipe that showed dimpling is buried at a depth of 2 feet, while the 30 inch diameter pipe with dimpling was buried at a depth of 2.6 feet; both of these pipes were under road surface.

At one site, a 48 inch diameter pipe with 1.7 feet of average soil cover heaved to above the ground surface. Associated with the heave was a joint separation and a circumferential crack 75 inches long and about 0.04 inches (1 mm) wide as shown in Figures 3.9, 3.10, and 3.11. The location of the heave, about 30 feet from the outlet into a marsh, suggests that buoyancy from a high water table combined with the shallow depth of cover may have caused the heave.

Pipes buried in sandy native soils with diameters 36 and 48 inches show cross sectional deformations. The 48 inch diameter pipe, buried at a depth of 1.2 feet, showed cross sectional deformations with horizontal shortening. The 48 inch diameter pipe buried at 6.5 feet of soil cover showed 1 inch elliptical cross sectional deformation over 22 feet, which represents 0.9% of the 48 inch diameter pipe surveyed. Pipes buried in regions with a native soil of till and lake sediments with 12, 15, 18, 24, 36, and 48 inch diameters showed cross sectional deformations.

Pipes surveyed are buried in two different types of trenches. Pipes buried in a trench like that shown in Figure 2.3 experienced a slightly higher percentage of structural problems (9%) than pipes buried in a trench like that shown in Figure 2.4 which had 7% structural problems.

Table 3.2. The structural performance of each pipe diameter.

Project	Diameter (inch)	Deformed percent length (%)	Dimpling percent of length (%)	* Structural problems percent length (%)	**Joints w. problem/ total joint number	Ave. depth/Ave. depth at deformation (feet/feet)	Native soil
Fairmont	12	2.88	0.00	2.88	0/17	N/A	*** till
Maple Grove	15	1.38	0.25	1.76	6/72	4/4.9	*** till
Maple Grove	18	33.00	0.00	33.00	3/18	4.5/4	*** till
Mankato Thompson	24	0	0.00	0.68	3/14	3.1	peat
Mankato Woodland	24	37.99	0.00	37.99	2/16	11.3/11.3	limestone
Moundesview	24	0.00	0.00	0.00	0/24	8	fine sand
Blaine	24	0.00	0.00	0.00	0/43	4.8	sand
Fairmont	24	0.00	0.00	0.00	0/16	2.12	*** till & lake sediments
Gaylord	24	25.0	25.00	40.00	0/1	N/A	*** till
Maple grove	24	0.66	0.00	3.96	2/22	4/4	*** till
Fairmont	27	0.00	0.00	0.00	0/3	5.1	*** till & lake sediments
Blaine	30	0.00	25.65	25.65	0/22	3.6/2.6	sand
LeCenter	30	0.00	0.00	0.28	5/34	N/A	*** till & lake sediments

Table 3.2. (continued)

Project	Diameter (inch)	Deformed percent length (%)	Dimpling percent of length (%)	* Structural problems percent length (%)	**Joints w. problem/ total joint number	Ave. depth/Ave. depth at deformation (feet/feet)	Native soil
Fairmont	30	0.00	0.00	0.00	0/18	5.15	***till & lake sediments
Gaylord	30	0.00	0.00	0.00	0/24	5.2	*** till
Lecenter	36	15.51	0.00	15.51	11/39	N/A	*** till & lake sediments
Fairmont	36	0.00	1.80	2.69	3/42	6.37/2.0	*** till & lake sediments
Moundsview	42	0.00	0.00	0.00	0/18	11.5	fine sand
Moundsview	48	31.00	0.00	31.00	2/61	2.8/1.2	fine sand
Gaylord	48	1.57	0.00	9.34	0/67	5/6.5	*** till

* structural problems noticed include, dimpling, deformation, sag, and cracks.

** joints with separation, deflection at joint, roots, infiltration.

*** native soil determined from surface geology map.

Figure 3.9. Circumferential crack 75 inch in length in 48 inch diameter pipe.

Figure 3.10. Heaving of 48 inch diameter pipe to above the ground surface.

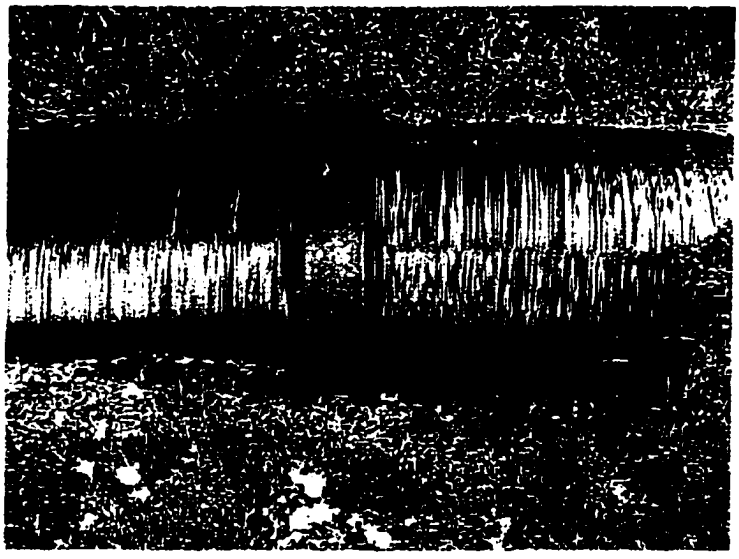

Figure 3.11. Joint separation in the 48 inch diameter pipe.

Pipes with diameters 12, 24, 30, 36, and 48 inches showed pipe sags. No information was available on the foundation material. All of these cases occurred where the native soil is till or lake sediments. This suggests that care should be exercised when using HDPE pipes in regions where till or lake sediments may be the foundation material. Pipes buried in sandy native soils showed no pipe sag. One of the cities specified that the sand native soil can be used as a foundation material after dewatering.

Joint separations, deformations, or deformations of the piece connecting two pipes were noticed at 37 locations which is 6.5% of the total number of joints surveyed. Joint separations with root penetration were noticed at three locations where the pipe was buried in a native peat soil (see Figure 3.12). Deformation of the connection between two adjoining pipes was noticed at 10 locations. Cracks were noticed at five different sites with 27 total cracks. Examples of these cracks are shown in Figures 3.6 and 3.13.

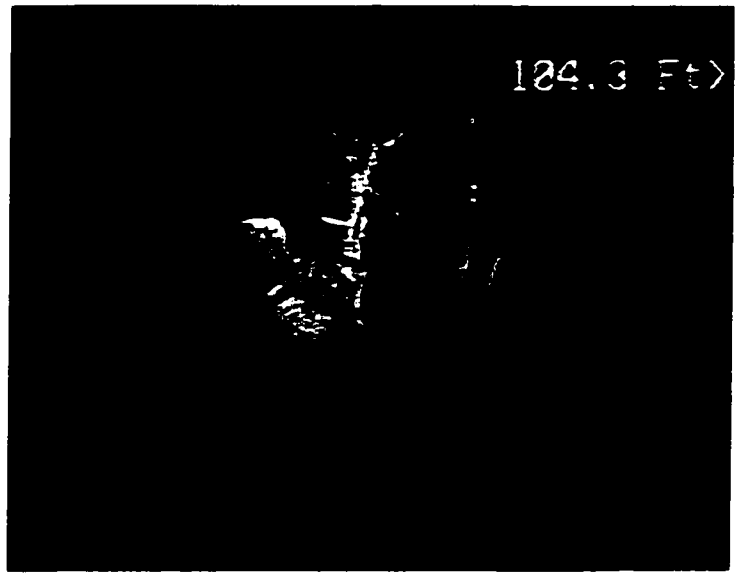

Figure 3.12. Joint separation with roots penetrating through.

Figure 3.13. Twelve inch crack between "9 and 12 o'clock".

The relationship between the year of installation for a given project and the percent of structural problems is shown in Figure 3.14. This figure shows that pipes recently installed have more structural problems than pipes that have been in service for a longer period of time. HDPE material elastic modulus decreases with time, so pipes with a short in-service time period should have more stiffness to resist the applied load than old pipes (i.e. those in service for several years). This was not observed in the locations surveyed in this study.

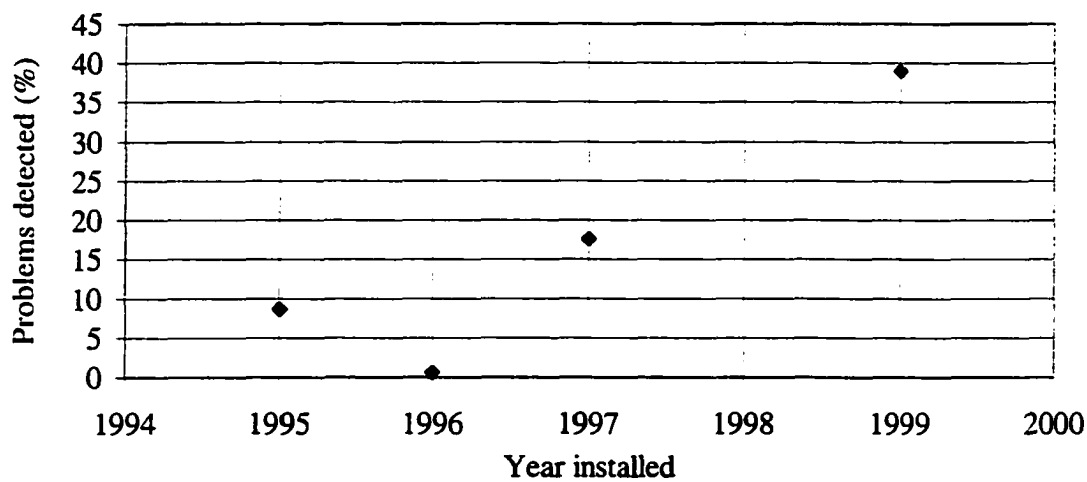

Figure 3.14. Percent of structural problems vs installation year.

3.2 Sediments

Sediments and water were observed in many of the pipes surveyed. The percentage of sediments in the pipes was plotted versus pipe slope in Figure 3.15. Though there is a wide scatter, a general trend could be observed in the decreasing percentage of sediments with the increasing pipe grade, especially when the grade is more than 0.4%. Locations with pipe sags had no significant relation with the scatter of the data shown in Figure 3.15. This suggests that the sediments observed in these pipes are caused by hydraulic factors and not by structural deformations.

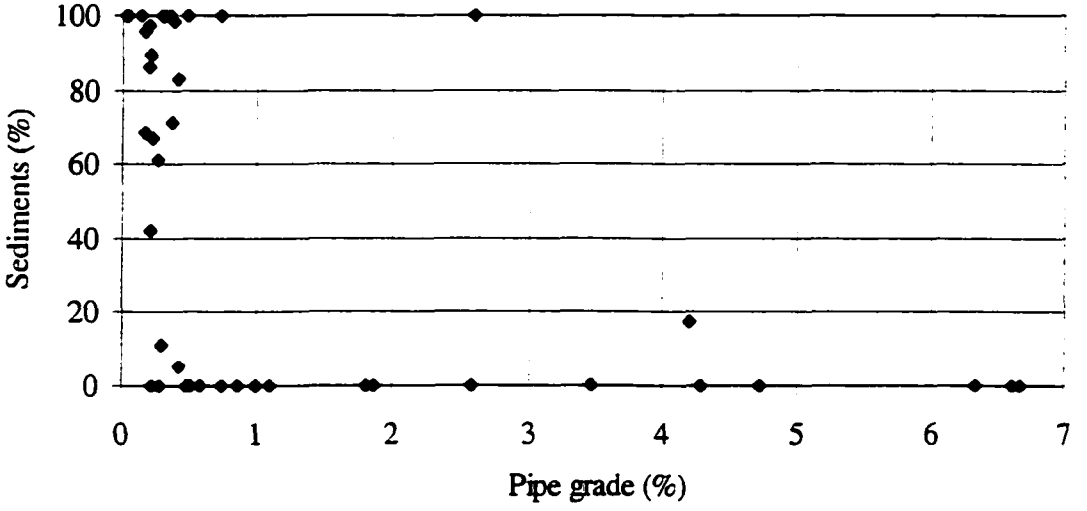

Figure 3.15. Change of percent of sediments with pipe grade.

4.CONCLUSIONS

In-service HDPE pipes were surveyed for structural problems. These problems were located along the pipe and then evaluated in this study. Ten projects with a total of 12,006 feet of pipe were studied and the following instances of structural problems were observed: 4 cases of dimpling or local buckling, 29 cross sectional deformations, 7 pipe sags, 27 wall cracks, and 25 joint separations.

Wall buckling affected 152 feet of the pipe length with a vertical deflection percent ranging from 3% to 7%. Wall buckling affected 1.3% of the total pipe length surveyed. At Gaylord, MN vertical deflections as high as 46% were observed in a 24 inch diameter pipe and could be included in the buckling category. Other vertical deflections ranged from 4% to 23%. Vertical deflections affected 266 feet of the pipe length or 2.2% of the total pipe length surveyed. In addition, 7 joints had vertical deflections from 4% to 12%. Most vertical deflection percentages were about 10%, and 17 of the 19 observed vertical deflections exceeded 5% (usually considered an allowable limit).

Horizontal deflections ranged from 3% to 13%, with the highest percent at Gaylord, MN. Horizontal deflections occurred at sites with shallow backfill and affected 354 feet of the pipe length or 3% of the total pipe length studied.

Pipe sags were observed at four sites, with a minimum of 3% and a maximum of 38%. The greatest sag was at the Gaylord site. Sag affected 145 feet of the pipe length or 1.2% of the total pipe length studied. Wall cracks were between 0.05 and 0.1 inch wide and extended between 10 to 20 inches around the pipe circumferences. Joint separations were usually an inch or less but at two projects in Maple Grove, MN there were 2 inches of vertical displacements at one joint.

The results of this survey lead to the conclusion that the frequency of structural problems increases as the pipe diameter increases. Pipes 48 inches in diameter experience cross sectional deformations regardless of the soil cover depth.

Our review of the ratio of the height of soil cover (H) to the inside pipe diameter (D) revealed no relationship between H/D and the frequency of structural problems. The highest H/D was associated with vertical shortening which resulted from the effects of geostatic loads. Pipes with low H/D ratios also had a high percent of structural problems in the form of horizontal shortening, likely resulting from side compaction during construction and insufficient surface loads to restore the pipe to 'round' configurations.

Dimpling, the precursor of general wall buckling, was observed at four different sites in pipes of 15, 24, 30, and 36 inches in diameter. Two of the four pipes that experienced dimpling were buried under two feet or less of soil cover and were subjected to traffic loads.

Pipes installed in 1999 showed a higher percentage of problems than pipes installed in 1995, 1996, and 1997. Pipes buried in a trench with vertical walls experienced a slightly higher percentage of structural problems (9%) than pipes buried in trenches with sloping walls (7%). One pipe had been pierced with two steel rods.

A 48 inch diameter pipe under 1.7 feet of soil cover heaved above the ground surface. The heave caused some joint separation and cracking. Buoyancy from a high water table and the shallow depth of soil cover probably caused the heave.

Pipes with diameters between 12 and 48 inches buried in regions where the native soil is glacial till or lake sediments showed cross sectional deformations, and some pipes showed longitudinal sag. Although no specific information was available on the foundation material,

this suggests that care should be exercised when using HDPE pipes in regions where till or lake sediments may be the foundation material.

It was reported that most of the sites investigated followed the MN. DOT specification. This may explain the few major structural problems noticed in this investigation due to the use of granular material as a backfill.

PART II. BURIED FLEXIBLE PIPE ANALYSIS USING FINITE ELEMENT ANALYSIS

5. INTRODUCTION

5.1 General Background

The theoretical study of flexible pipes was started by Spangler's work on metal pipes (1941). Since then, more flexible materials (i.e. Aluminum, Polyvinyl Chloride (PVC), and Polyethylene (PE)) have been used in the pipe industry. Part I of this thesis indicated the effect of the backfill material and soil structure interaction on HDPE pipe in-service behavior. In Part II, finite element analysis, a useful analytical tool in the study of soil structure interaction, will be used to study the flexible pipe behavior. One such analytical tool is *Culvert ANalysis and DEsign* (CANDE), a 2-D finite element program commonly used to analyze and design buried pipes that was developed by Katona (1976). The stated significant limitations of CANDE are 1) small deflection theory, 2) neglecting out-of-plane effects such as longitudinal bending, and 3) neglecting time dependence material response, Katona (1976).

A variety of other finite element analyses have been used to model the response of buried flexible pipes. Taleb and Moore (1999) performed a two dimensional finite element analysis for metal pipes under earth loading with an elastic-plastic soil model, where the modulus varied linearly with depth and the finite element procedure AFENA was used. Moore and Taleb (1999) studied the three dimensional response of metal culverts to live loading with a semi-analytic procedure based on the use of Fourier Integrals. The soil was modeled using a linear elastic response with the modulus varying linearly with depth. El Sawy et al. (1997) used the same approach to study the stability limit state of long span shallow and deeply buried metal culverts. All of the analytical studies cited above used a simplified soil constitutive law (elastic or elastic plastic) to model the soil.

Moser (1994) studied the structural performance of 1200 mm diameter buried PE pipes. In his work, PE pipes were loaded using the Utah State University loading pipe-soil cell shown in Figure 1.6 at different soil compaction levels in an SM soil and the pipe deflections were monitored.

Watkins and Anderson (1999) listed the differences between the analysis of soil-pipe interaction system and a simple linear elastic continuum. This list included the nonlinear stress-strain relationship of soil and large deflections that may be involved using very flexible pipes. The recent trend of using plastic pipes for deep applications increased the need for large deflections effect investigation. Although CANDE allows the use of non-linear soil models, it does not accommodate large deflections.

5.2 Objectives and Scope

The main advantage of CANDE relative to ANSYS is its capacity to use hyperbolic and power soil models, while ANSYS has the advantage of modeling large deflections. One objective of the theoretical analyses presented later in this part is to compare the results of CANDE with the small and large deflection theories of ANSYS for the case of elastic soil properties under geostatic loading conditions. The second objective is to write a code using the ANSYS programming language to model the soil behavior using hyperbolic tangent modulus with both power and hyperbolic bulk soil modulus models and to study the effect of large deflections on PE and PVC flexible pipes. The written code was also improved to accommodate the modeling of the construction process of buried pipes

5.3 Modeling

CANDE uses three types of elements in pipe-soil structure modeling. These elements are plane strain, beam column, and interface. The plane strain element is used to model the

soil and has two translational degrees of freedom in the X and Y directions. The pipe is modeled with beam-column elements. This element has three degrees of freedom at each node, two translations and one rotation. Plastic pipes are modeled as elastic materials.

The CANDE library has three solution levels, six soil constitutive models, and five pipe types. CANDE solution level 2,"homogenous model", generates the finite element mesh automatically, and is shown in Figure 5.1. This figure shows that the maximum soil cover above the pipe crown is 3R, where R is the pipe radius. If the soil cover exceeds this limit, the program automatically truncates the cover at the 3R level and applies the truncated soil load as a distributed load on the soil surface. Katona (1976) and Musser (1989) have a detailed description of the theory and use of CANDE.

ANSYS is a general finite element program used to solve different structural problems. It has a large library of element types, permits small and large deflection analyses, and eight types of material nonlinearities. ANSYS also allows the user to program using the ANSYS special programming language which is called "ANSYS Parametric Design Language (APDL)". This language allows the user to build the finite element model, repeat the commands, use macros, if-then-else branching, do loops, and vector and matrix operations. The file can be used to create the model, do the calculations, solve and generate the results for each load step. Problems with different load increments can also be solved, and the model parameters such as number of elements , can be updated for each load step.

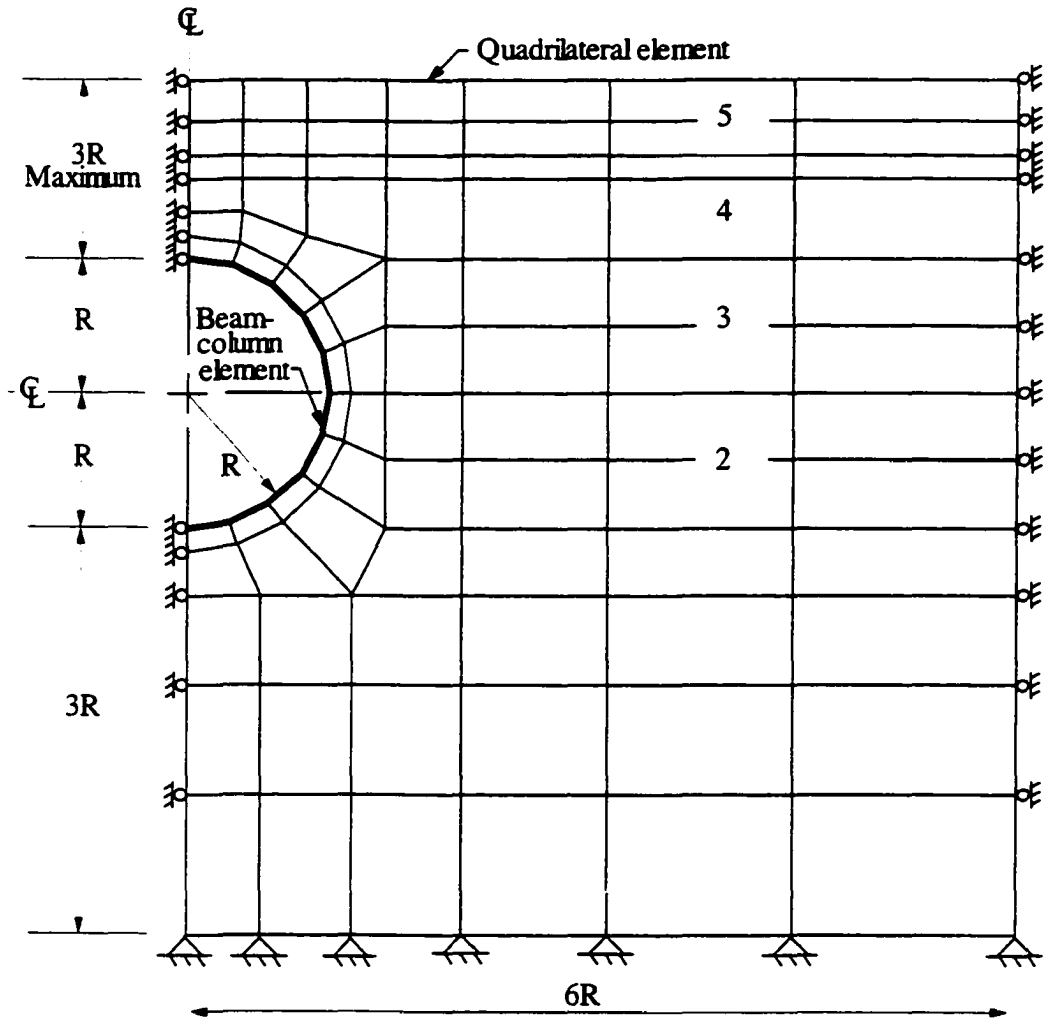

Figure 5.1. A schematic model for CANDE solution level 2.

6. ANSYS AND CANDE ANALYSES

6.1 Elastic Soil, Comparison of ANSYS and CANDE

A plastic pipe 610 mm in diameter with four different soil covers (1.5, 3.05, 4.6, and 6.1 m) above the pipe spring line was modeled using both CANDE and ANSYS as shown in Figure 5.1. In these models, the soil was assumed to be a linear elastic material, no interface elements were used between the soil and pipe elements, and the pipe was assumed to be elastic with a smooth "no corrugation" uniform thickness (T). The soil and pipe properties used are given in Table 6.1. Plastic pipe properties included in this table are CANDE default plastic pipe properties. PE, which also referred to as HDPE, pipe properties included in Table 6.1 are taken from Corrugated Polyethylene Pipe Association (CPPA) (1997) and meet ASSHTO M252 and M294.

Table 6.1. Pipe and elastic soil properties used in the analysis.

Property	CANDE plastic pipe	PE pipe	PVC pipe	Elastic soil
E (kPa)	11,024,000	757,900	2,756,000	6,890
μ	0.3	0.45	0.45	0.35
T (mm)	12.7*	29	18	--

* Assumed value
Soil γ = 1,920 kg/m^3

Figure 6.1 shows the computed vertical deflection of the plastic pipe crown with respect to soil cover above the pipe spring line using small and large deflection theories of ANSYS, and the small deflection theory of CANDE for the soil pipe system described above. This figure shows that the three solutions result in nearly identical pipe crown deflections. For the case of 1.5 m soil cover above spring line (1.22 m above pipe crown), the three

solutions give equal pipe crown deflections. This leads to the conclusion that for the systems modeled, small deflection theory modeling adequately describes the pipe behavior and so CANDE is adequate to be used for these cases.

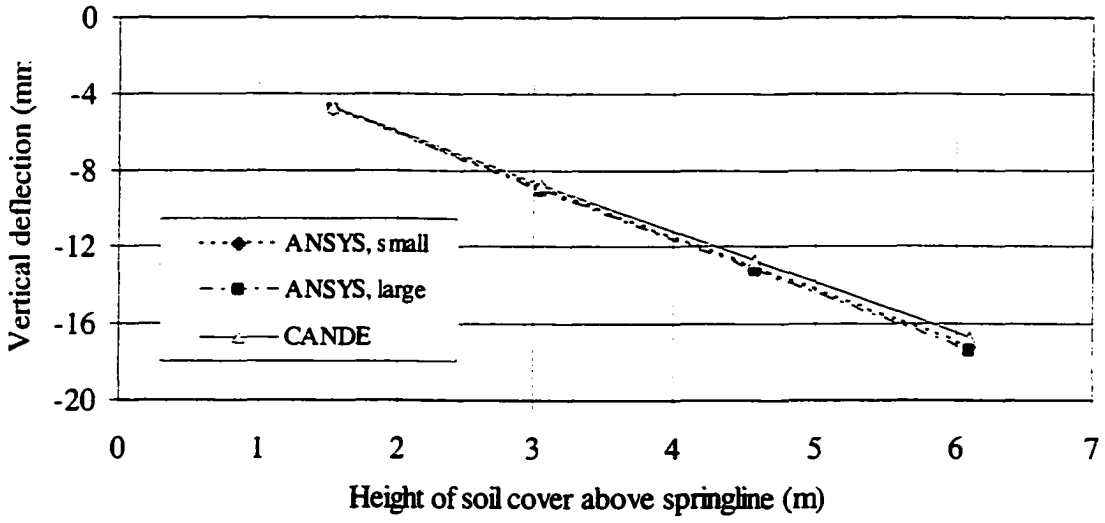

Figure 6.1. Plastic pipe crown deflection with respect to height of soil cover for elastic soil.

Figure 6.2 shows the vertical deflection for different points on the plastic pipe circumference for various depths of soil cover above the pipe spring line. This figure shows the same trend of a maximum deflection at the pipe crown and minimum deflection at pipe invert with virtually no difference in the results of all three methods for all cases of soil cover. As an overall comparison, the three different methods showed good agreement for this range of soil covers. The large deflection analysis using ANSYS has an insignificant effect on the plastic pipe behavior for the system studied here.

Figure 6.3 shows a comparison of the vertical stress above the plastic pipe for the case of 4.6 m of soil height. The three different methods used resulted in a similar trend with a maximum difference of 5% or less. The vertical stress above the pipe is equal to the geostatic vertical stresses to a depth of 50 cm above the pipe crown which is almost one pipe

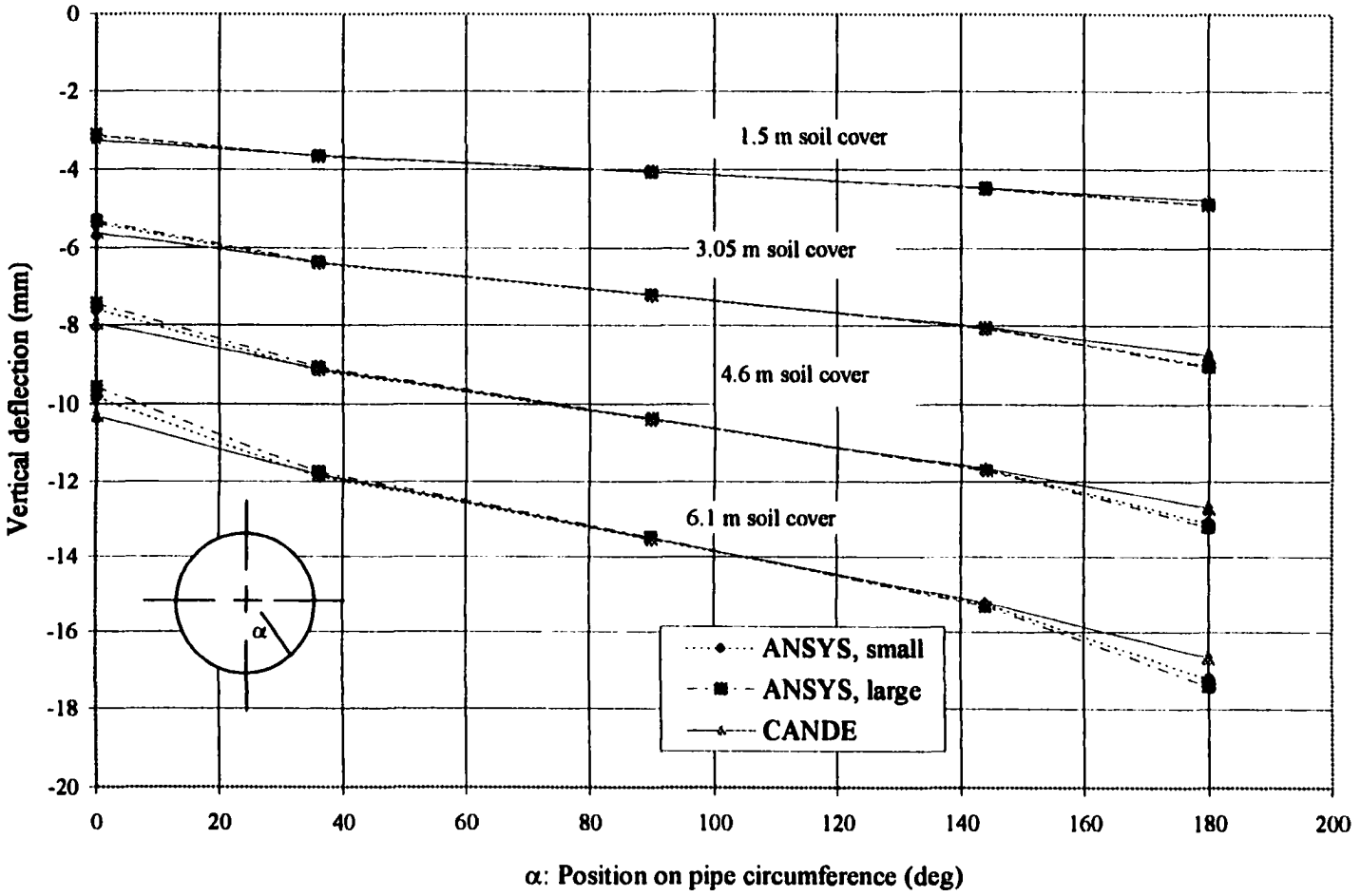

Figure 6.2. Plastic pipe crown vertial deflection with respect to position on pipe circumference for different height of soil covers for the case of elastic soil.

diameter. Sargand et al. (2001) measured the soil pressure above PVC and PE pipes and found that the soil pipe interaction zone was about one pipe diameter above the pipe for both PVC and PE pipes. Figure 6.4 shows the change in the horizontal stress with the change in the horizontal distance measured from the pipe center for the case of 4.6 m soil height. All three methods of solution resulted in the same trend and essentially the same values of horizontal stresses at different distances from the pipe center. The horizontal stress decreases as the distance from the pipe surface increases. The horizontal stress becomes constant at a distance slightly greater than one meter. This distance is about twice the pipe diameter which is an approximate value of the soil pipe interaction, Hoeg (1968).

Results of the same pipe-soil system described above, but using the properties of the PE pipe shown in Table 6.1, are shown in Figure 6.5. This figure shows that both CANDE and ANSYS, using both small and large deflection theories of ANSYS, give almost the same results for pipe invert and crown deflection with only slight differences for the case of 6.1 m soil height above the spring line. The change of vertical deflection percent, which is the change of the vertical pipe diameter divided by the inside pipe diameter, of PE pipe with soil cover is shown in Figure 6.6. This figure shows the same trend, with differences in the vertical deflection percent between the three methods increase as the soil height increases.

6.2 Soil Models

Figure 6.7 shows a typical soil stress-strain relationship and indicates the change of soil modulus with confining pressure (σ_3) according to Duncan et al. (1980). This response has been modeled using a hyperbolic stress strain relationship, Kondner (1963), discussed in chapter 1. Power bulk modulus and hyperbolic bulk modulus models were developed by Duncan et al. (1980) and Selig (1988) respectively. Figure 6.8 shows a flowchart of the code

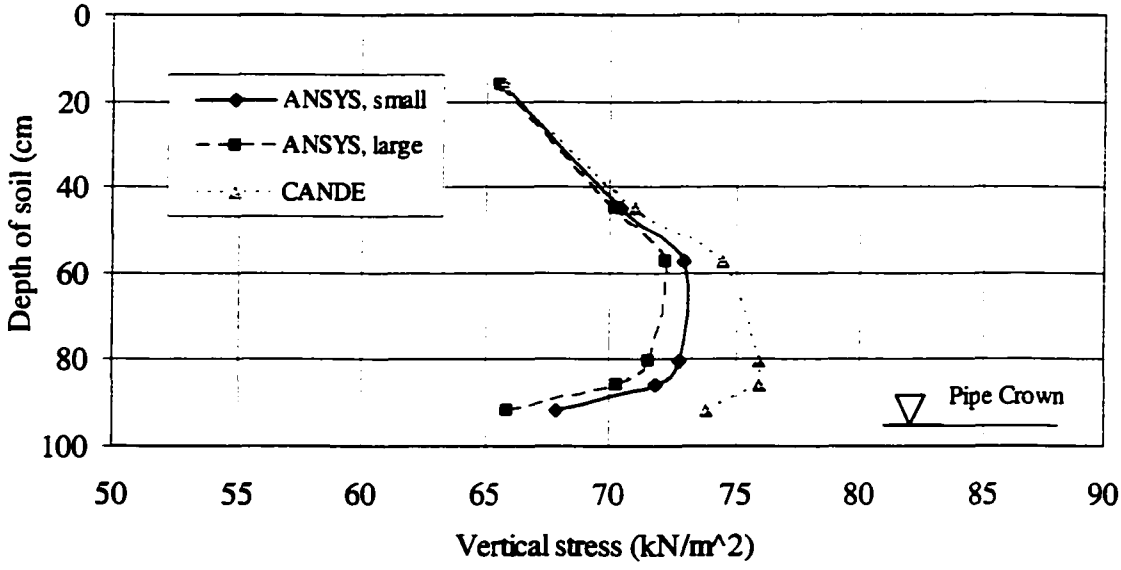

Figure 6.3. Vertical stress in a soil column above the pipe for 4.6 m soil height.

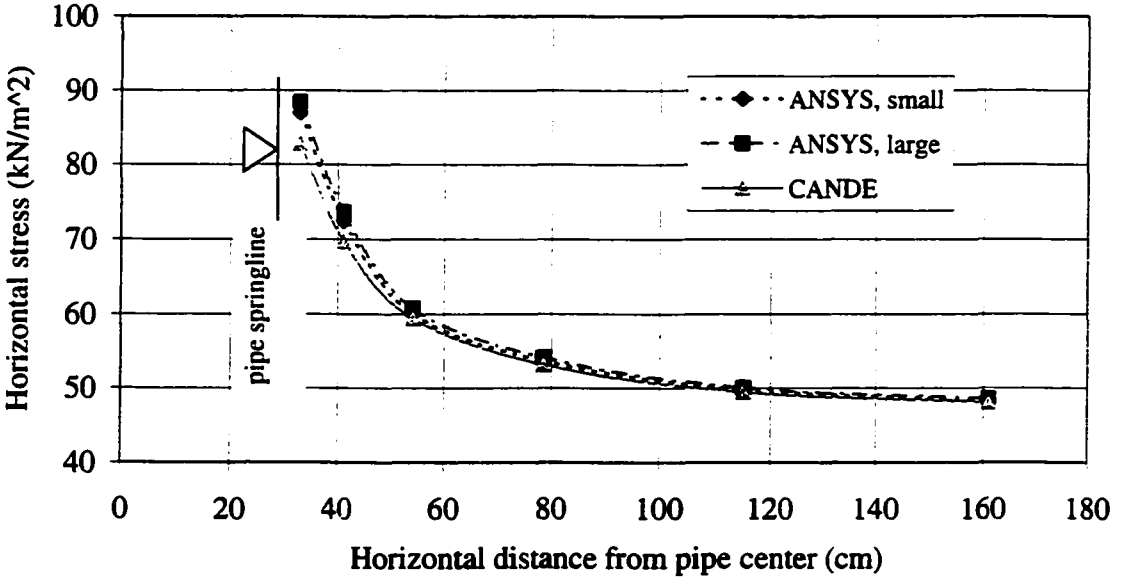

Figure 6.4. Horizontal stress vs. horizontal distance from pipe spring line for 4.6 m soil height.

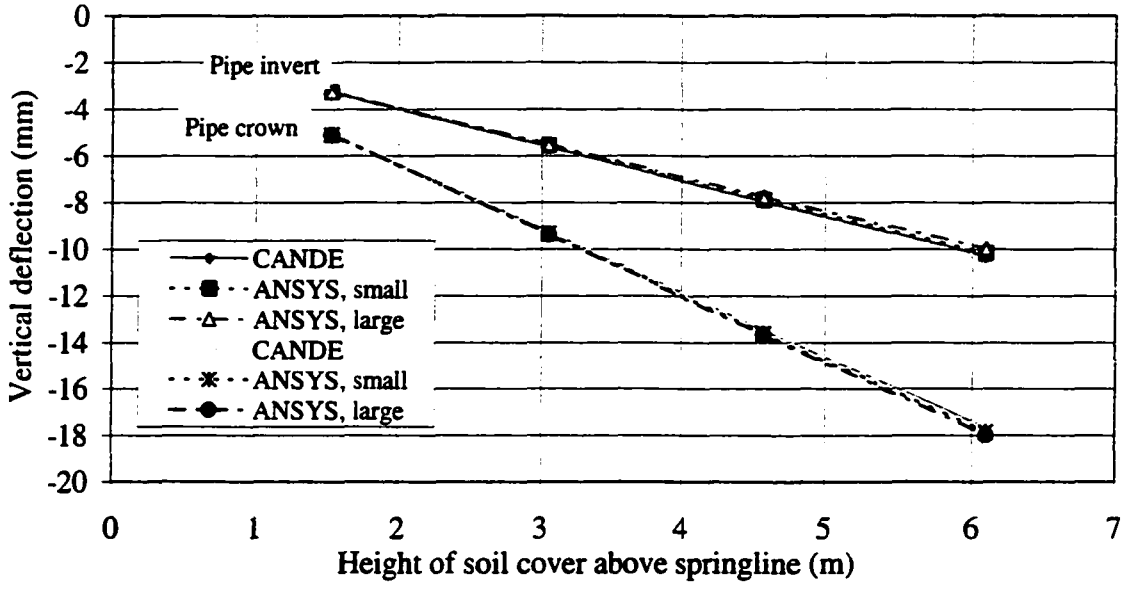

Figure 6.5. PE pipe vertical deflection vs. height of soil cover for elastic soil case.

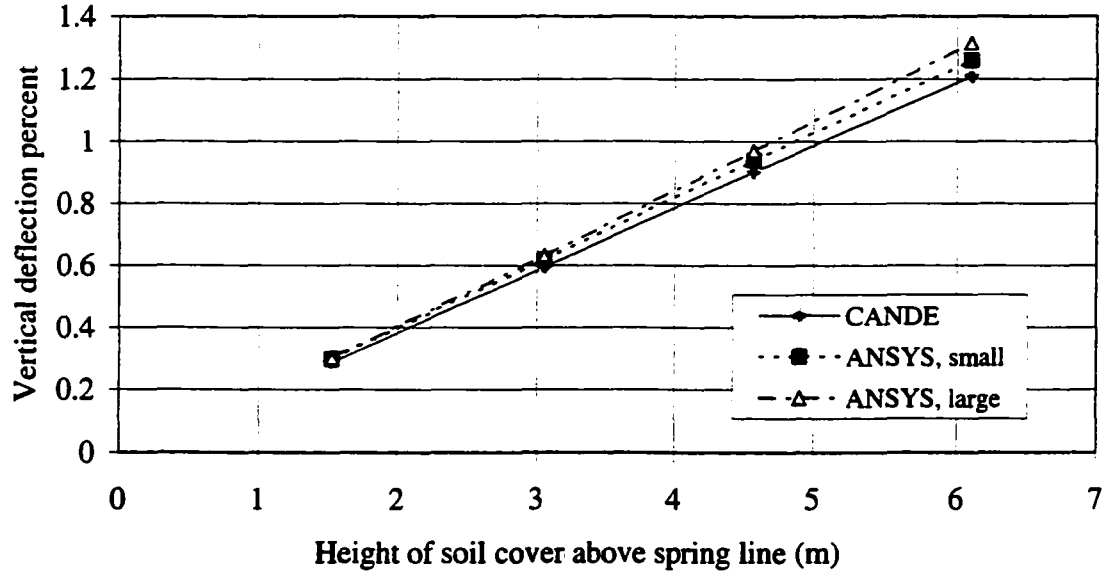

Figure 6.6. PE pipe vertical deflection percent vs. height of soil cover for elastic soil case.

for soil models, which was written in ANSYS using the APDL programming language. The improved code works as a load step program where the stresses induced at the beginning of the first load step used to calculate the soil modulus is based on the soil element depth. Soil elements are considered as blocks of soil masses with an average soil modulus for each soil block. These blocks will enable modeling different regions and different soil materials used in the backfill. Each load step is solved using "n" substeps by applying a stepped load incrementally within each load step. The results of each sub-step are used to calculate a new average modulus for each soil block and re-solved again until the end of the load step. The load step is solved using the average modulus calculated from all sub-steps for each soil block. This solution procedure was used

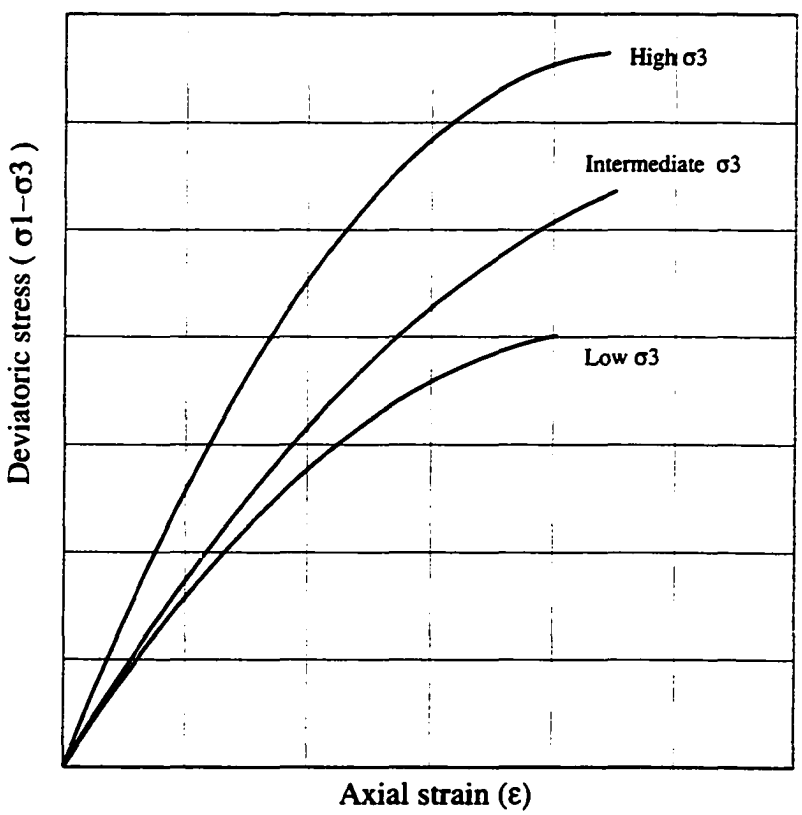

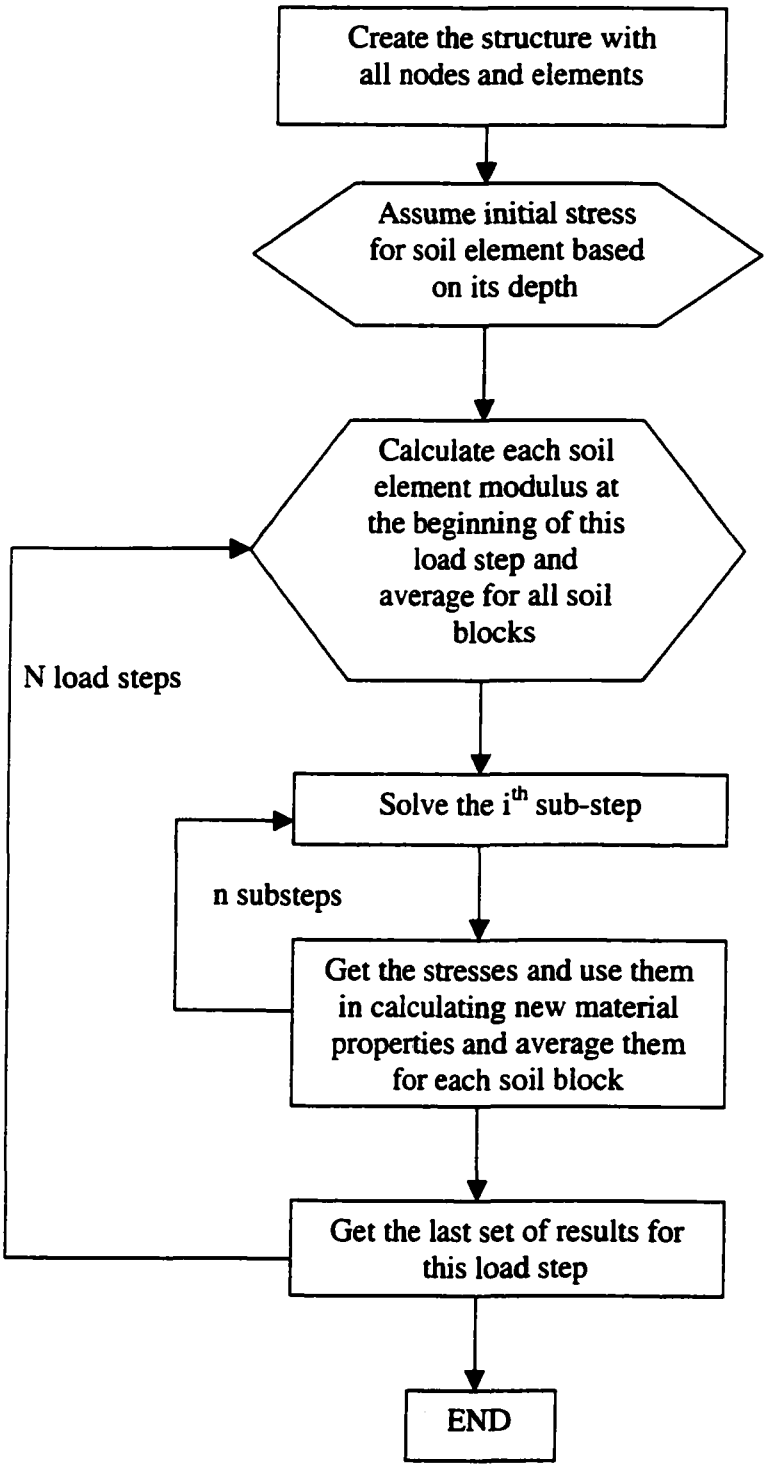

Figure 6.8. Flowchart of nonlinear soil models code written in ANSYS.

because solving the load step using the average calculated moduli at the beginning and at the end of each load step resulted in greater error when compared with CANDE results. The stresses calculated using the average modulus are then used to calculate the soil element modulus at the beginning of the next load step. This cycle will be repeated N times, where N is the number of load steps.

Figure 6.7 shows that as the shear stress applied on soil elements increases (i.e. $[(\sigma_1-\sigma_3)/2]$), the soil becomes weaker. Shear failure occurs when the tangent Young's modulus approaches zero. The improved code limits the parameter, $\{R_f((\sigma_1-\sigma_3)(i-\sin\varphi)/2(C.\cos\varphi+\sigma_3\sin\varphi)\}$, shown in Equation 1.18 to 0.95. If the value of this parameter is greater than 0.95, the value of the tangent modulus is assumed to be 0.05 of the initial tangent modulus. This avoids solving for the case of a zero modulus. The minimum and maximum soil bulk modulus values were set as the tangent modulus divided by 3 and tangent modulus multiplied by 8 ($E_t/3$ and $8E_t$) respectively. This limits the value of the Poisson's ratio within the range of zero and 0.48. A tension failure check was also included in the program. Tension failure occurs when the confining pressure becomes tensile. In this case, the stress ratio (σ_3/P_a) of the soil element is assumed to be equal to 0.1.

6.3 Comparison of ANSYS and CANDE

ANSYS utilizing the hyperbolic soil model with power bulk modulus was compared with CANDE for a pipe soil system of a 610 mm diameter pipe with the plastic pipe properties shown in Table 6.1. The buried pipe structure analyzed is shown in Figure 5.1. The soil model constants used in this analysis for an SM soil with 90% compaction (Moser (1990)) are shown in Table 6.2. Moser (1994) described the SM soil used in his work as "lesser quality than most soils specified as backfill and so it is a worst case test". Five cases

of different heights of the soil above the pipe spring line were used for comparison (1.5, 3.05, 3.8, 4.6, and 6.1 m).

Table 6.2. Soil parameters used in the analysis.

Soil Type	Density (kg/m^3)	Φ (deg.)	$\Delta\varphi$ (deg.)	C (kPa)	K	n	R_f	K_b	M	B_j/P_a	ε_u
SM	1,800	30	0	57	480	0.44	0.75	80	0.38	--	--
CL	2,300	34	0	28	440	0.4	0.95	--	--	120.8	0.043

Figure 6.9 shows the plastic pipe crown and invert deflections for all cases of soil cover using both CANDE and the small deflection theory of ANSYS. This figure shows that the results of ANSYS with the improved code show good agreement with the results of CANDE for both the pipe invert and the pipe crown. The vertical deflection percent of the pipe for the same plastic pipe-soil system is presented in Figure 6.10. This figure also shows a good agreement between both ANSYS and CANDE.

The same pipe-soil system was analyzed for the cases of PE pipe with 1.5, 3.05, 3.8, and 4.6 m of soil height above the pipe spring line. The soil was modeled using the hyperbolic bulk modulus model for an ML soil with parameters shown in Table 6.2 (Musser (1989)). The PE pipe invert and crown deflections using both ANSYS and CANDE are shown in Figure 6.11. The results of ANSYS with the improved tangent and bulk hyperbolic modulus code show a good agreement with the results of CANDE for both the pipe invert and the pipe crown. The vertical deflection percent of the PE pipe is presented in Figure 6.12. This figure also shows a good agreement between both ANSYS and CANDE. The comparison of the cases above validates the use of ANSYS with the improved code to model pipe soil systems.

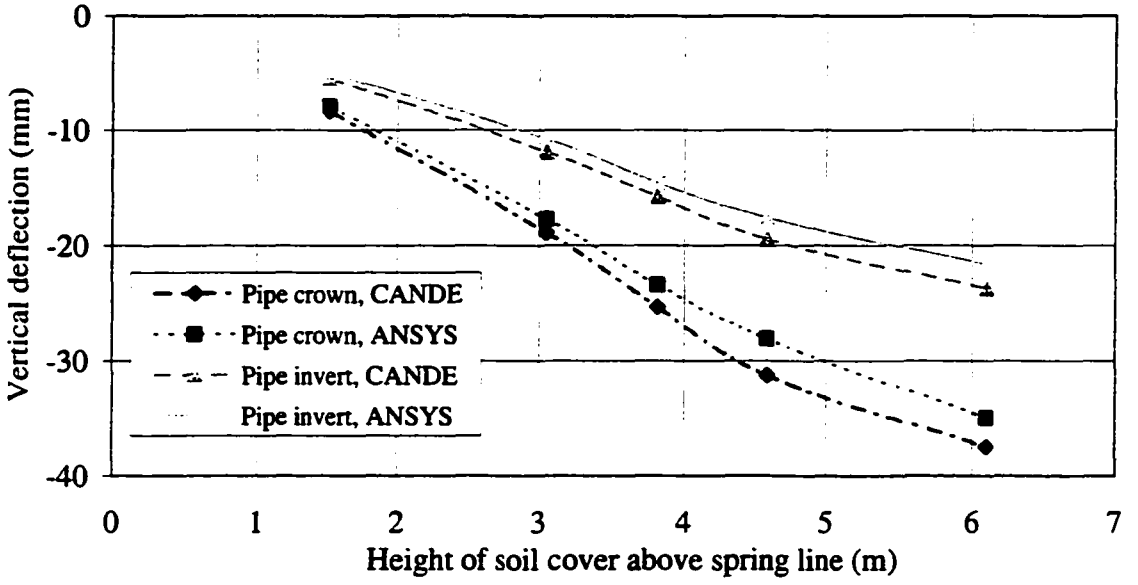

Figure 6.9. Plastic pipe vertical deflection using hyperbolic tangent soil modulus and power bulk soil modulus for both ANSYS and CANDE.

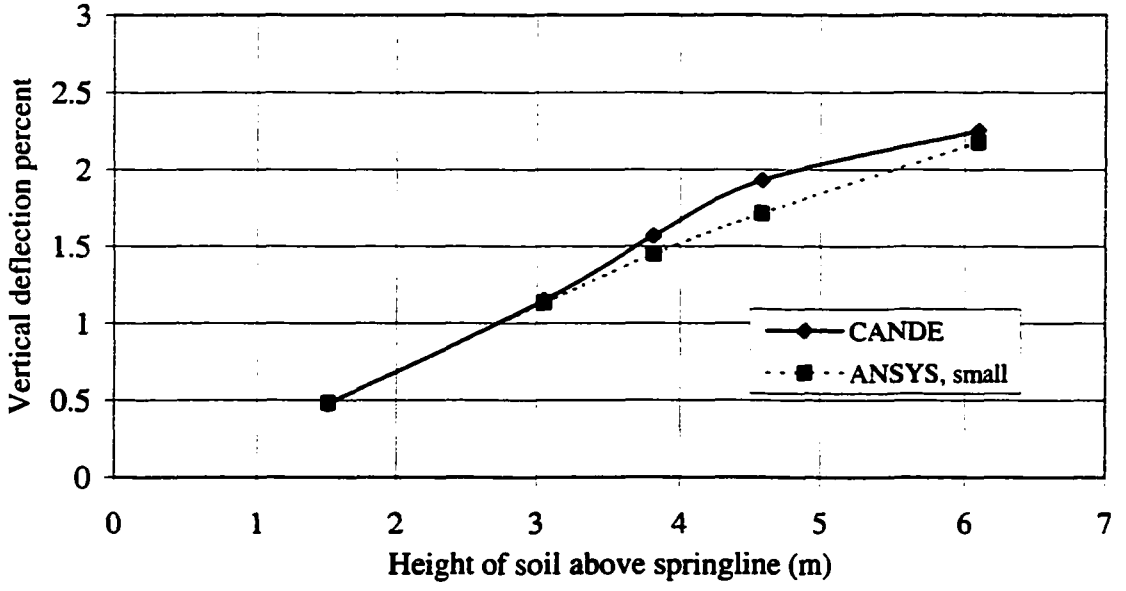

Figure 6.10. Plastic pipe vertical deflection percent using hyperbolic tangent soil modulus and power bulk modulus for both ANSYS and CANDE.

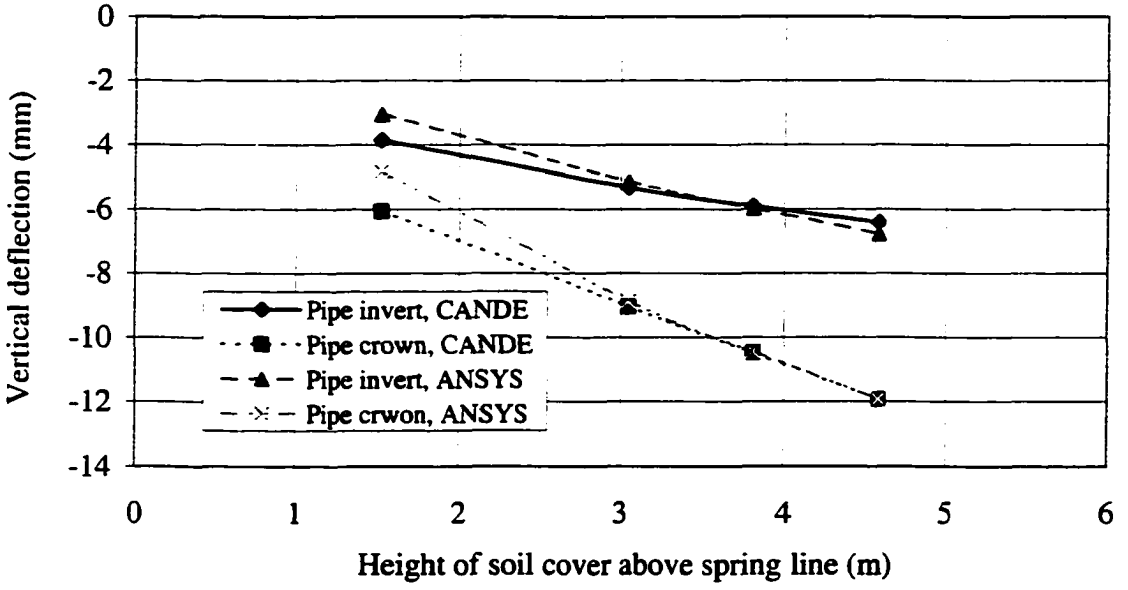

Figure 6.11. PE pipe vertical deflection using hyperbolic tangent and bulk soil moduli models for both ANSYS and CANDE.

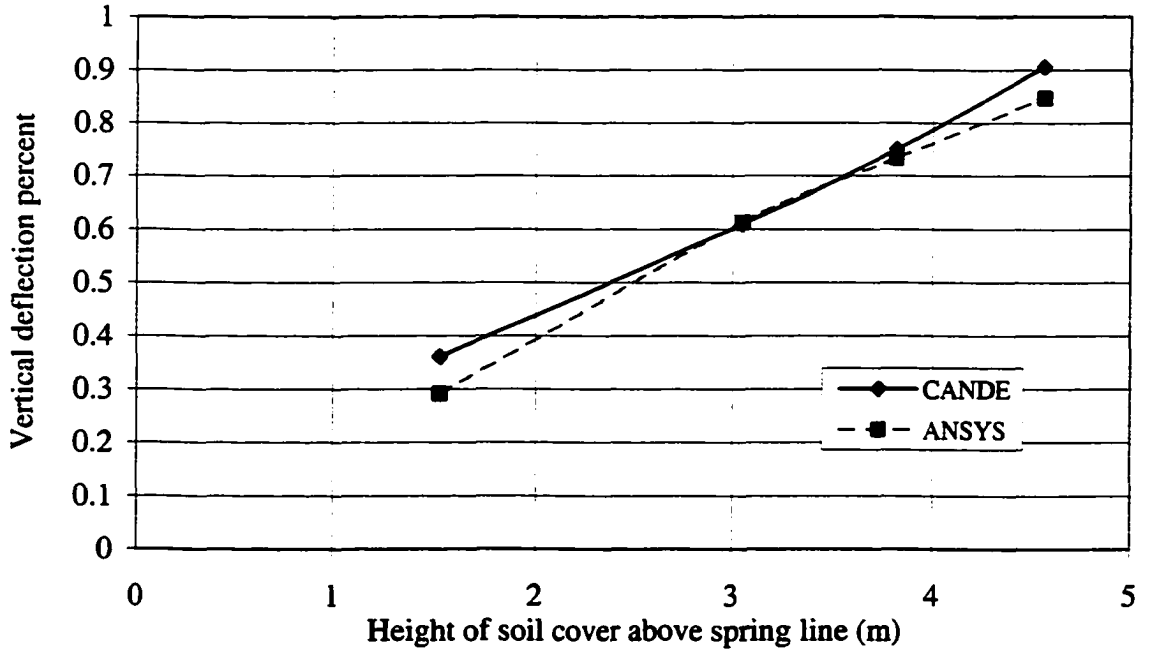

Figure 6.12. PE pipe deflection percent using hyperbolic tangent and bulk soil moduli for both ANSYS and CANDE.

Because PE pipes are flexible and the properties used are documented in CPPA (1997), the large deflection theory was used to compare the results of both CANDE and ANSYS. Figure 6.13 shows the vertical deflection percent of PE pipes using CANDE and the small and large deflection theories of ANSYS. The large deflection theory for PE pipes has little effect on the results for a soil cover of 3.05 m. Increasing the fill height from 4.6 to 6.1 m increases the effect of the large deflection theory. These figures show that both ANSYS with the small and large deflection theories and CANDE have a good agreement for soil covers up to 6.1 m.

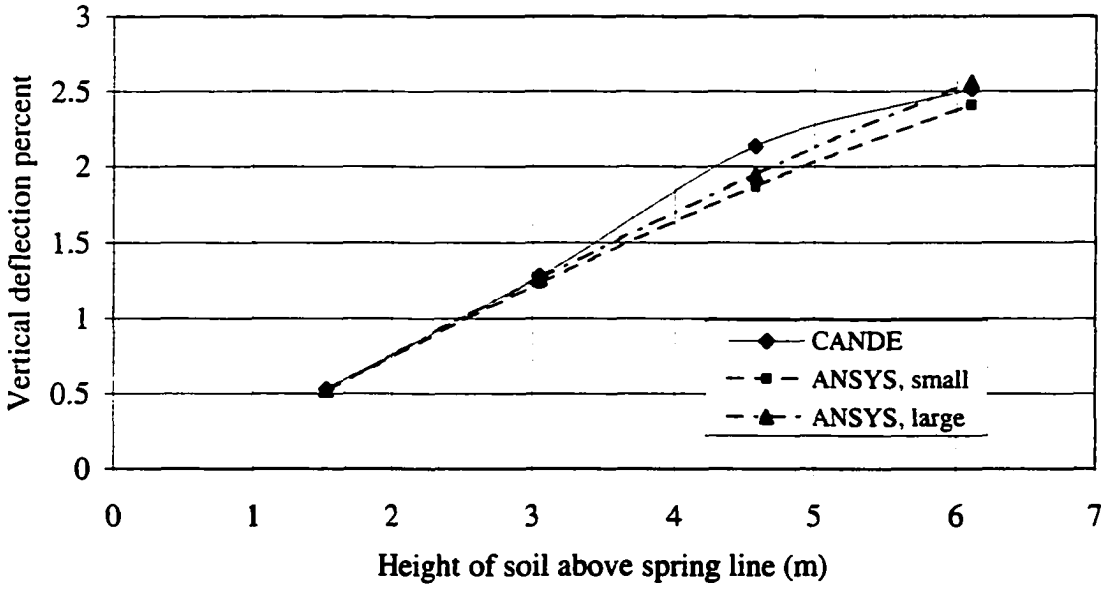

Figure 6.13. PE vertical deflection percent using hyperbolic tangent soil modulus with power bulk modulus for both ANSYS and CANDE.

Moser (1994) studied the behavior of 1200 mm diameter PE pipes using the Utah State University pipe-soil cell shown in Figure 1.6, with an SM soil at different compaction levels. The results of 90% compaction were reported in Moser (1994) and the associated soil model parameters in Moser (1990). Figure 6.14 shows the finite element model for soil-pipe system used in the Utah State University soil-pipe cell. This soil pipe system was analyzed

using ANSYS and CANDE level 3 analyses. Figure 6.15 shows the results of these analyses compared with Moser's (1994) experimental results. According to this figure, both ANSYS and CANDE results showed a good agreement with Moser's experimental results up to a soil depth of cover of 9.0 m. CANDE overestimated the pipe deflection as the applied load increased above 9.0 m. This is due to the fact that one soil element around the pipe reached the shear failure. The difference between CANDE and ANSYS in dealing with the soil element modulus may cause this difference. CANDE deals with a different modulus for each soil element, so any local soil failure will affect the pipe results more than that of ANSYS, where each soil block that consists of a number of elements has an average modulus. ANSYS results showed a good agreement with the results of Moser with a negligible large deflection theory effect up to 12.2 m of soil cover. The large deflection theory showed a better agreement with Moser's experimental results than the small deflection theory of ANSYS for the soil cover of more than 12.2 m, where the vertical deflection percent is between 3% and 4%. The maximum difference between ANSYS small and large deflection analyses was 12%.

6.4 Pipe Material Effect

ANSYS small and large deflection theories were used to compare the performance of both PE and PVC pipes for deeply buried pipes. A 610 mm diameter flexible pipe with different soil covers up to 18 m above the pipe spring line was modeled using ANSYS with both small and large deflection theories. The material and cross sectional properties for different pipe materials are shown in Table 6.1.

The PVC pipe properties used are specified in ASTM F-678-89, while the PE pipe properties used are taken from CPPA (1997) and meet ASSHTO M252 and M294. The soil is modeled using the hyperbolic tangent soil modulus with power bulk modulus model. The SM

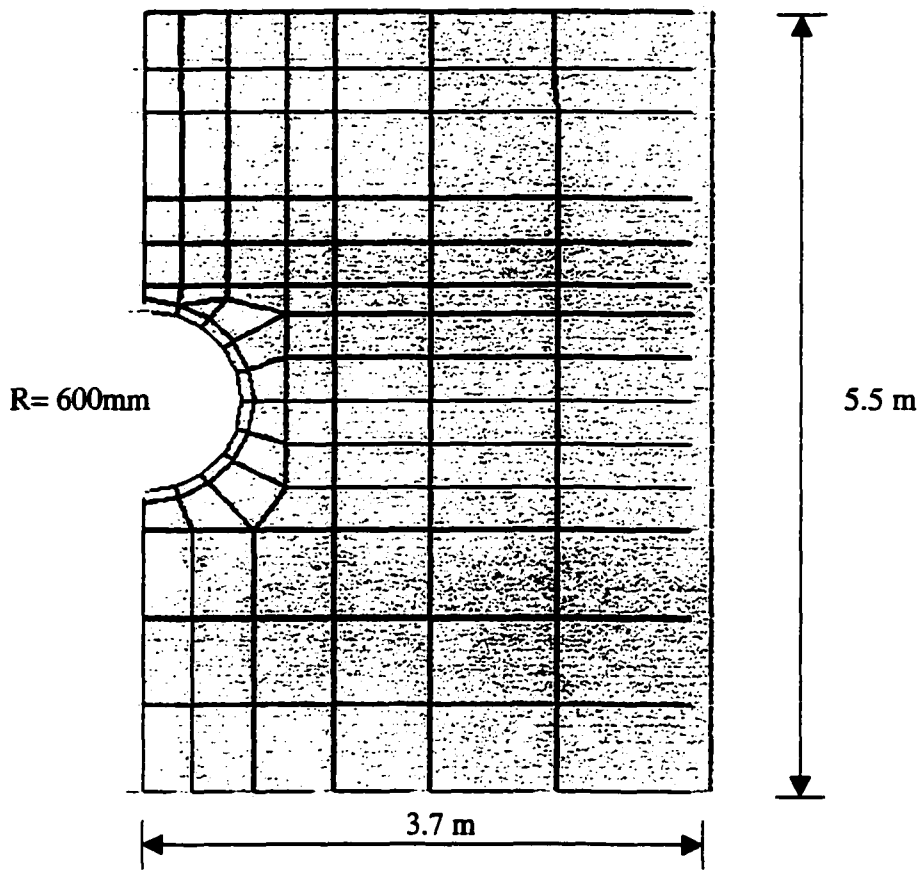

Figure 6.14. Finite element mesh used to model Utah State University soil-pipe cell.

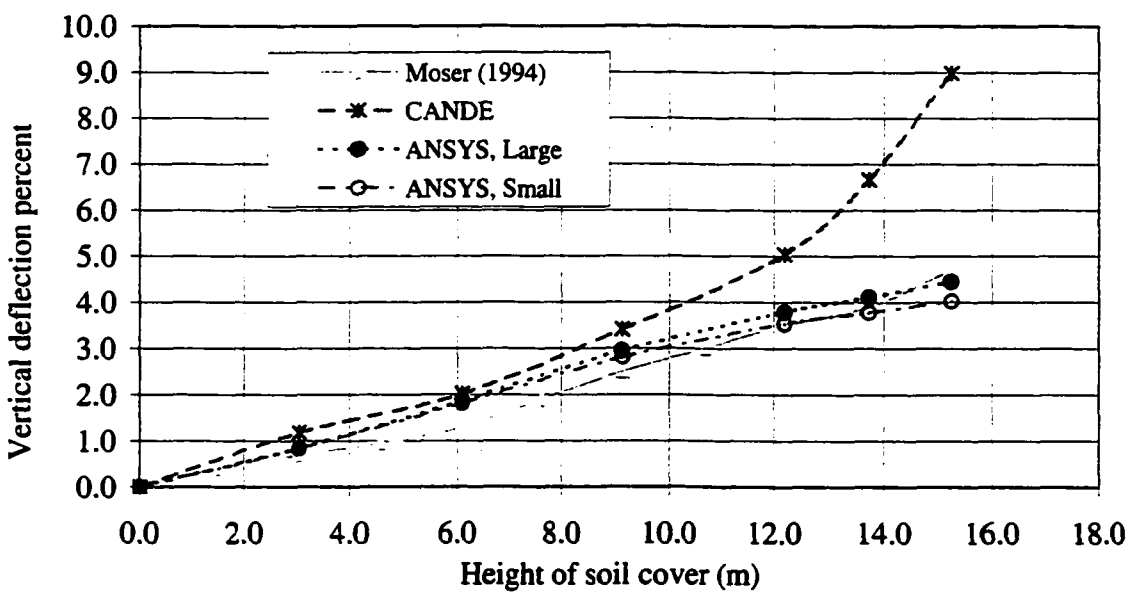

Figure 6.15. Vertical deflection percent with respect to soil cover for PE pipe compared with Moser (1994).

soil parameters for these models are shown in Table 6.2. The pipe-soil system shown in Figure 5.1 was used to investigate the effect of the large deflection theory as the height of soil cover increased for both PE and PVC pipes. The results of the pipe vertical deflection percent are presented in Figure 6.16. This figure shows that the PE pipe exhibited a greater deflection percent than the PVC pipes. The difference between the small and the large deflection theories is greater for PE pipes than for PVC pipes. PE pipes are more sensitive to the consideration of the large deflection theory than PVC pipes. Figure 6.16 also shows that the large deflection theory effect becomes significant, more than 10%, for vertical deflection percents of 4% or more.

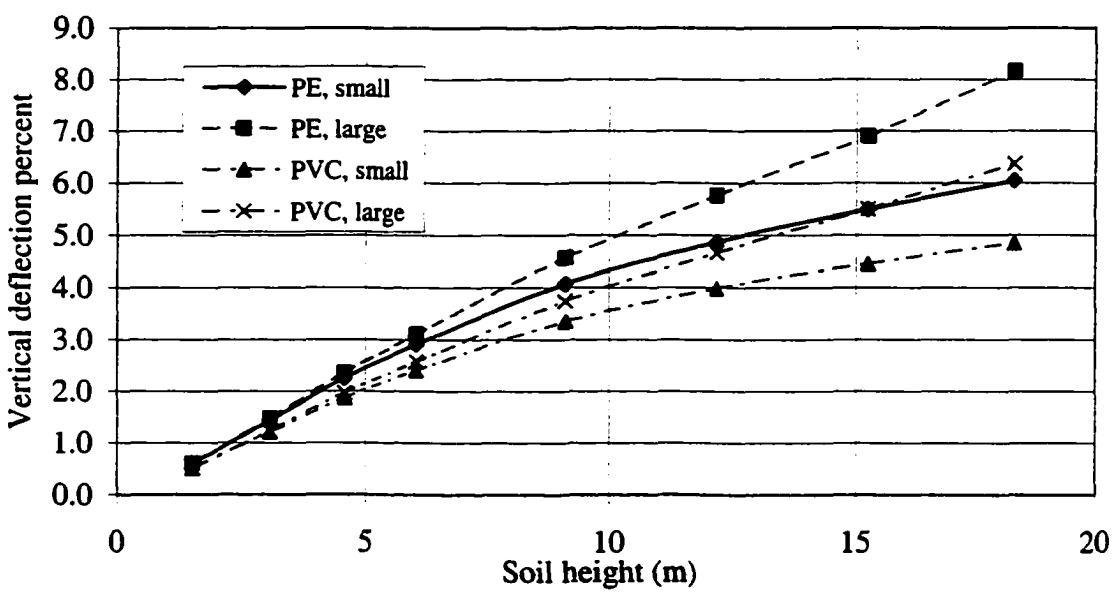

Figure 6.16. Vertical deflection percent with respect to soil cover above spring line.

6.5 Construction Process Modeling

The improved code in ANSYS was further developed to accommodate the construction process. If any material is added to the finite element model , ANSYS option of "element birth and death" can be used. The model with all elements and nodes was generated

and the elements which were added to the system in the subsequent load steps were set to the inactive mode. The status of an element in ANSYS, active or inactive, can be changed from one load step to another but not within a load step. The improved code reads the number of active elements for each load step and calculates the modulus for the active elements only. In this improved code, NN is the total number of construction lifts, nn is the soil lift under construction for the current load step, and nn-1 is the lift added to the system during the last load step. At the beginning of the construction of the nn soil lift, the CANDE construction technique assumes that displacements exist for the nn-1 lift but no displacement is considered for the nn lift. So lift nn does not experience any pre-existing settlement. This creates a displacement discontinuity between the soil lifts. To avoid this discontinuity, large deflection theory was used in ANSYS to consider the effect of the deflection of soil elements during the nn-1 lift construction. Therefore using the large deflection theory, the new soil elements (reactivated elements) added to the system as soil lift number nn will not be in their originally specified geometry but will be influenced by the deflection of the previous construction steps.

The initial soil stresses at the first sub-step are dependent upon whether the element is part of the initial pipe soil system (pre-existing soil) or part of the new construction increment. If the element belongs to a new construction, the initial σ_3/P_a is assumed to be equal to 0.1 for the first sub-step.

To validate the use of the improved program, an embankment construction of the pipe soil system shown in Figure 5.1 was modeled and solved using both ANSYS and CANDE. The numbers shown on soil elements in Figure 5.1 are the construction process steps. Five load steps of soil layers were added to the embankment as numbered in Figure 5.1. The soil

was modeled using the hyperbolic tangent modulus model with the power bulk modulus model for SM soil parameters shown in Table 6.2. Figure 6.17 shows the pipe invert and crown deflections as the soil is added to the embankment using both ANSYS and CANDE. This figure shows a good agreement between ANSYS and CANDE results. Figure 6.18 presents the vertical deflection percent for different load steps using both CANDE and ANSYS. This figure shows that both ANSYS and CANDE give the same trend and vertical deflection percent. This comparison further validates the improved soil models used in ANSYS and the procedure used in ANSYS to model the construction process. The effect of the displacement discontinuity in CANDE has a negligible effect on the pipe deflection during construction.

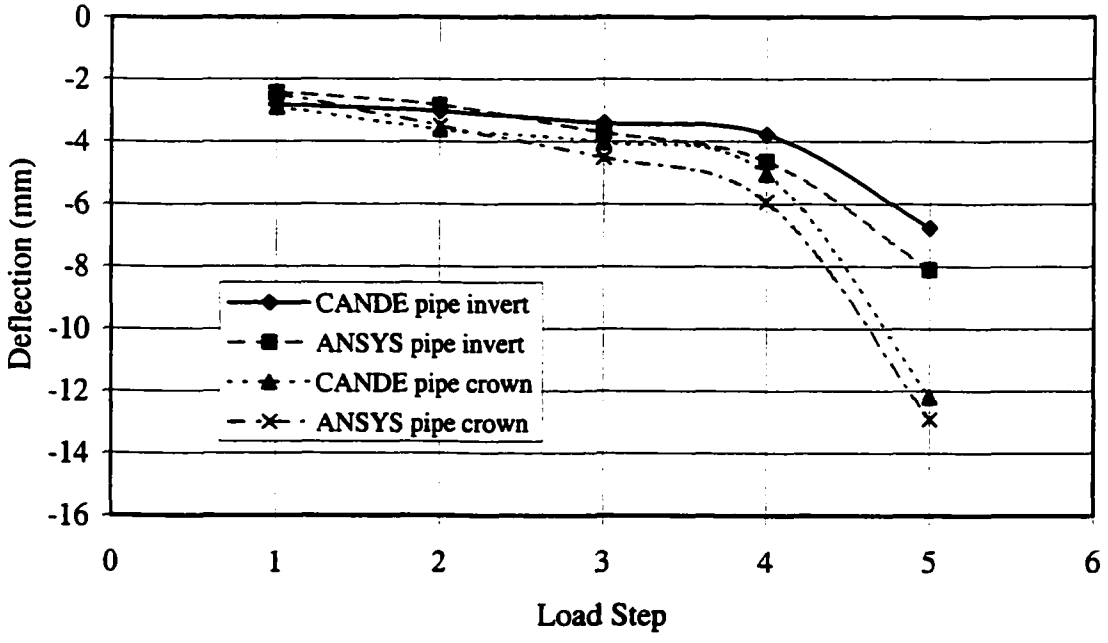

Figure 6.17. Deflection of 1200 mm diameter PE pipe vs. construction steps using both ANSYS and CANDE.

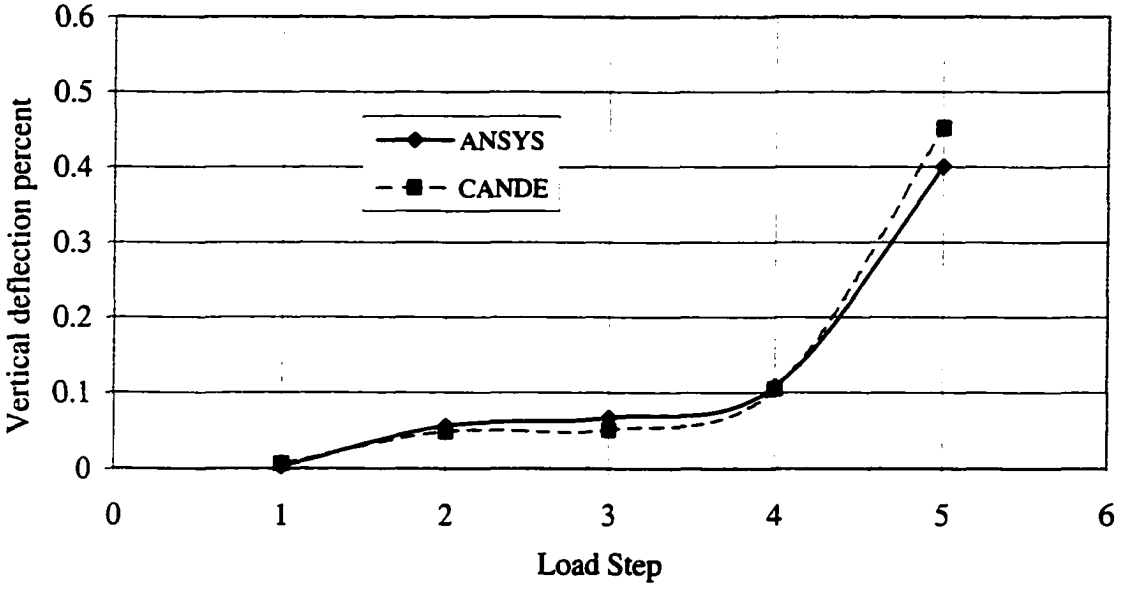

Figure 6.18. Vertical deflection percent for 1200 mm PE pipe vs. construction step for ANSYS and CANDE.

7. CONCLUSIONS

CANDE is one of the most commonly used programs for buried pipe analysis; however, the limitations of CANDE such as neglecting large deflections, leads to the consideration of an alternate analysis method. ANSYS, which is a general finite element program used in structural engineering, has been modified to provide a better analysis tool. There is little difference in the results calculated by both ANSYS and CANDE for the case of elastic soil with soil depth up to 6.1 m.

The improved code in ANSYS used to model the soil material behavior showed a good agreement with CANDE results for pipes with depth of burial up to 6.1 m. This, therefore, validates the use of improved soil models in ANSYS for buried pipe analyses.

For cases of 9 m or more of soil cover, using CANDE for deeply buried pipes, with SM soil which is described as having less quality than most soils used for pipe applications, did not show a good agreement with either ANSYS or the results provided by Moser (1994). As the soil elements approach shear failure, CANDE over-predict the pipe deflections.

ANSYS large deflection theory produces a better agreement with 1200 mm diameter PE pipes whose vertical deflection percent is around 4%. The maximum difference between ANSYS small and large deflection theories is 12%. The difference between ANSYS small and large deflection theories for PVC and PE pipes started to be significant at 4% vertical deflection. Both analyses shown in Figures 6.15 and 6.16 suggest that considering large deflection becomes significant for pipe deflections of 4% or more

The written code was further modified to accommodate the modeling of the construction process. This was accomplished by using the features of "element birth and death" in ANSYS and by reading the number of active elements for each load step within the

improved code to calculate the modulus for the active elements only. This also showed a good agreement with CANDE. The effect of displacement discontinuity of CANDE during the construction process on the pipe deflections was shown to be insignificant.

In general, CANDE is adequate for shallow buried pipes (up to 6 m for SM soil).

PART III. CONSTITUTIVE MODELS FOR HDPE MATERIAL

8. HDPE MATERIAL MODULUS MODELS

8.1 Introduction

As stated in the general introduction, objectives and scope, one objective is to improve the constitutive models for HDPE pipe to include strain rate and time effects. This part seeks to develop the appropriate constitutive models for HDPE material.

A structural element of steel responds to load in a manner that is essentially independent of loading rate and time duration of the applied load, provided that the load is sufficiently small to maintain a linear stress-strain response. For other than linear elastic time independent materials, a departure from this ideal behavior is to be expected. Thermoplastic materials respond to loads with a significant departure from that of linear elastic time independent materials. Thermoplastic pipes show creep and stress relaxation under constant load or constant strain conditions.

Stiffness is defined as the measure of force required to cause a unit displacement in the direction of the applied load. Stiffness may be considered to have two components: that due to the material and that due to the form of shape of the element. The material component of stiffness that acts to restrain deformation is the modulus. The geometric component of stiffness also acts to restrain deformation. This component can be moment of inertia, cross sectional area, and/or length. For time independent material, flexural compression and ring compression elastic moduli are close in value. It is inappropriate to assume that this applied to time dependent materials, Gabriel and Goddard (1999).

Since the parallel plate test deflection rate is not related to the practical loading rate, the time effect is not considered, and flexural compression dominates the pipe behavior in the

parallel plate test, compression tests conducted by Zhange and Moore (1997) were used to develop the nonlinear strain rate and time dependent HDPE tangent modulus models.

8.2 Objectives and Scope

The objective of this part is to develop mathematical models using the data available in Zhange and Moore (1997) discussed in chapter 1. The mathematical models describe the tangent modulus of HDPE material considering both strain rate and time effects. The mathematical models were programmed in ANSYS and used in a finite element analysis. A case study of the effect of decreasing HDPE modulus on pipe deflection was performed to validate the use of the ANSYS program with the HDPE moduli models and to investigate the effect of using both small and large deflection theories of ANSYS on HDPE pipe buried in SM soil.

8.3 HDPE Modulus Models

The hyperbolic mathematical model suggested by Kondner (1963) and Duncan and Chang (1970), used to model the time independent nonlinear soil response, is used in this chapter to develop mathematical models to describe the strain rate and time dependent response of the HDPE material. The stress strain curves and the creep curves reported by Zhange and Moore (1997) provided the raw data used to develop these mathematical models.

8.3.1 Loading rate effect

The stress strain relationship shown in Figure 1.16 was modeled as part of this research using the hyperbolic mathematical model given in Equation 8.1. The derivative of the stress-strain equation is the slope or the HDPE tangent modulus which is shown in Equation 8.2. Equation 8.1 can be linearized, as shown in Equation 8.3. This relationship represents a line with an intercept (a) related to the initial modulus and a slope (b) related to

the strain rate, as shown in Figure 8.1. The change of initial modulus (E_i) with strain rate was modeled using a power function, as shown in Figure 8.2 and Equation 8.4. The slope (b) of the normalized stress strain fits was mathematically modeled as shown in Equation 8.5 and Figure 8.3. By substituting the initial modulus (1/a) and the slope (b) shown in Equations 8.4 and 8.5 respectively into Equation 8.2, the tangent modulus model of HDPE pipes as a function of stress level and strain rate can be determined as shown in Equation 8.6. This model is called independent slope-intercept model.

$$\sigma = \frac{\varepsilon}{a + b\varepsilon} \tag{8.1}$$

$$\frac{\partial \sigma}{\partial \varepsilon} = E_t = \frac{a}{(a + b\varepsilon)^2} = \frac{(1 - b\sigma)^2}{a} \tag{8.2}$$

$$\frac{\varepsilon}{\sigma} = a + b\varepsilon \tag{8.3}$$

$$E_i = \frac{1}{a} = 29053 P_a \left(\frac{\Delta t}{\Delta \varepsilon}\right)^{-0.1207} \tag{8.4}$$

$$b = 0.0243 \left(\frac{\Delta \varepsilon}{\Delta t}\right)^{-0.0537} \tag{8.5}$$

$$E_t = 29053 P_a \left(\frac{\Delta \varepsilon}{\Delta t}\right)^{0.1207} \{1 - [0.0243 \left(\frac{\Delta \varepsilon}{\Delta t}\right)^{-0.0537} \sigma]\}^2 \tag{8.6}$$

where:

- a = the intercept of the normalized stress-strain line.
- b = the slope of the normalized stress strain line.
- ε =strain.
- σ = stress, MPa.
- Δ ε/ Δt = strain rate.
- E_t = tangent modulus at different stress levels, MPa.
- E_i = initial tangent modulus, MPa.
- P_a = reference atmospheric pressure.

Using a technique suggested by Coree (private discussion), the normalized stress strain relationship shown in Figure 8.1 can also be modeled using lines intersecting at a focus point. The focus point was found by determining the point of intersection of the normalized stress strain lines of 10^{-1}/sec and 10^{-2}/sec strain rates and assuming it as an initial guess for the focus point of all normalized stress-strain lines, as shown in Figure 8.4. Then, using the MS Excel solver to minimize the least square error between the measured data and the new intersected lines, the common focus point of all lines was found as shown in Figure 8.5. The statistical analysis of the focus point method showed a coefficient of correlation (R^2) of different lines in the range of 0.99. Equation 8.7 describes the linear relationship of stress to strain ratio versus strain for the case of strain rate of 0.1/sec using the focus point technique. The slope of the lines constructed using the focus point versus the strain rate was fit to a power mathematical model as shown in Figure 8.6. Equation 8.8 shows the mathematical model of the HDPE material tangent modulus using the focus point approach. It is

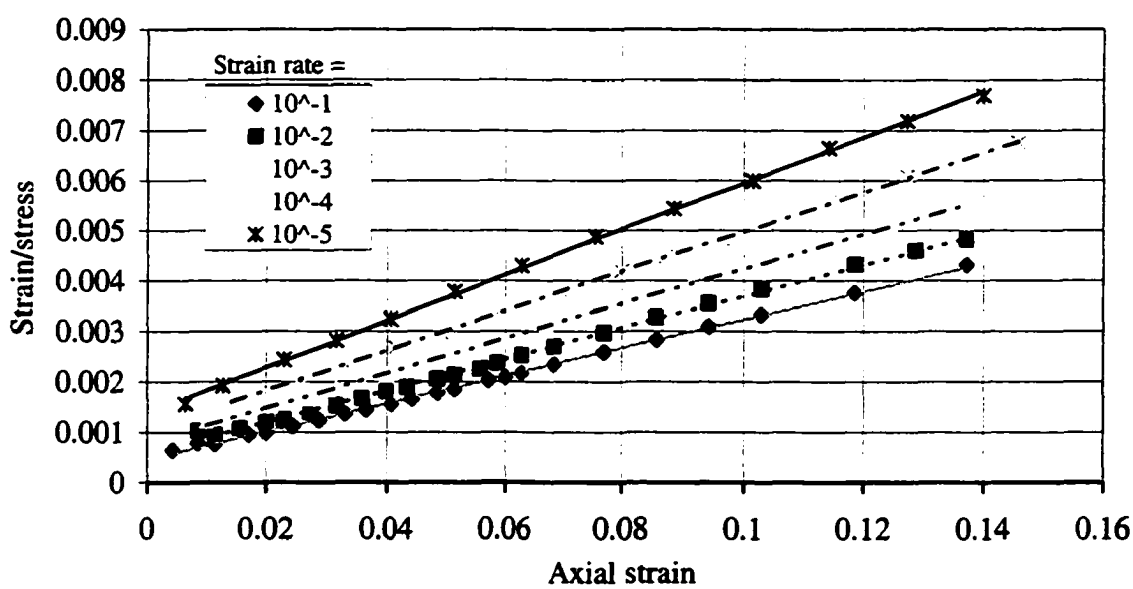

Figure 8.1. Normalized stress strain compression test results on HDPE material.

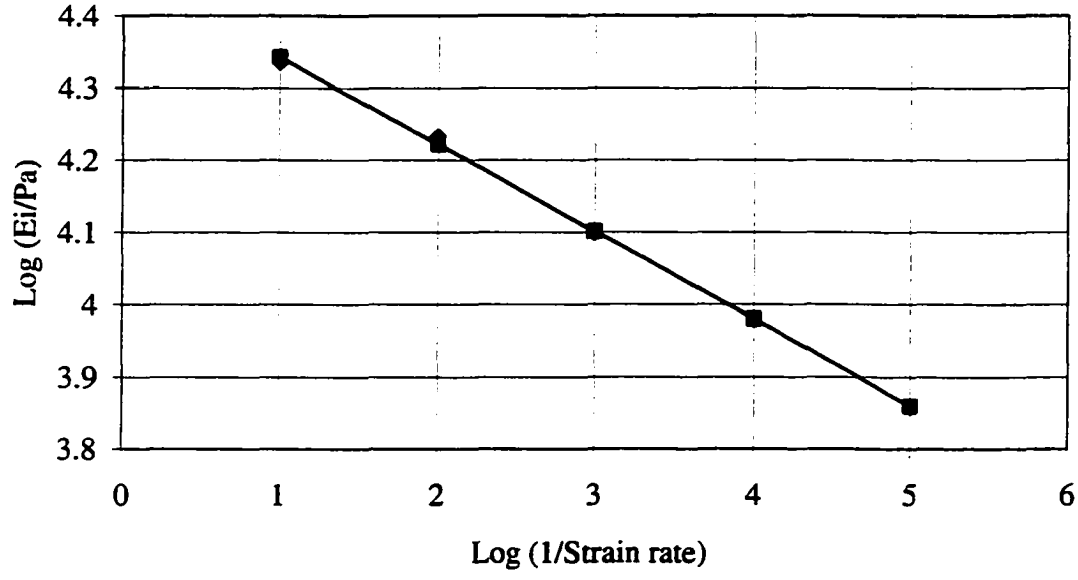

Figure 8.2. Change of initial tangent modulus for compression test.

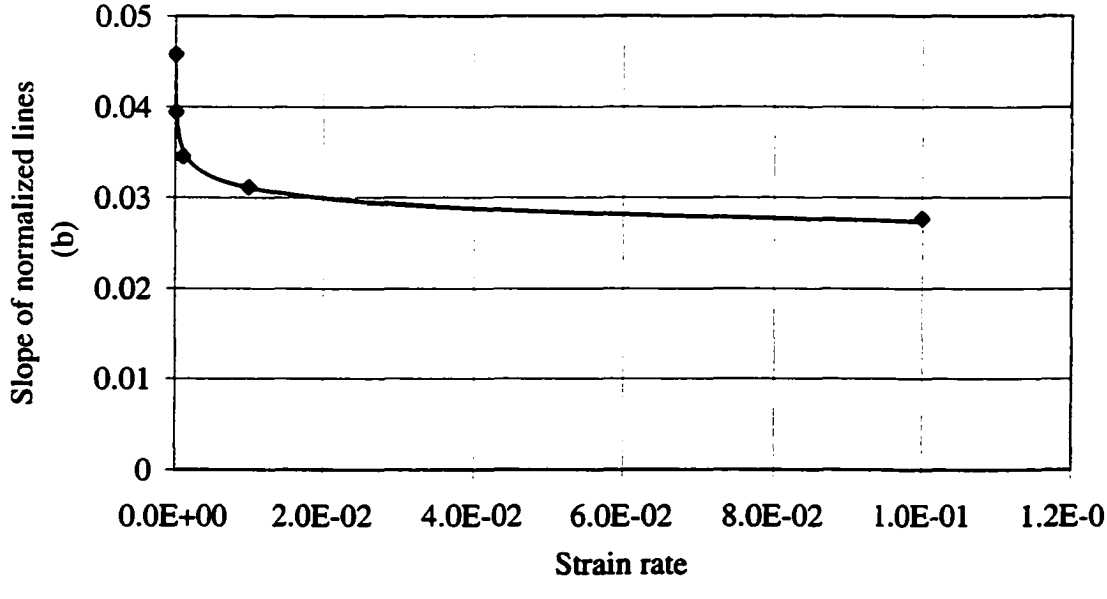

Figure 8.3. Change of normalized stress-strain lines slope with strain rate.

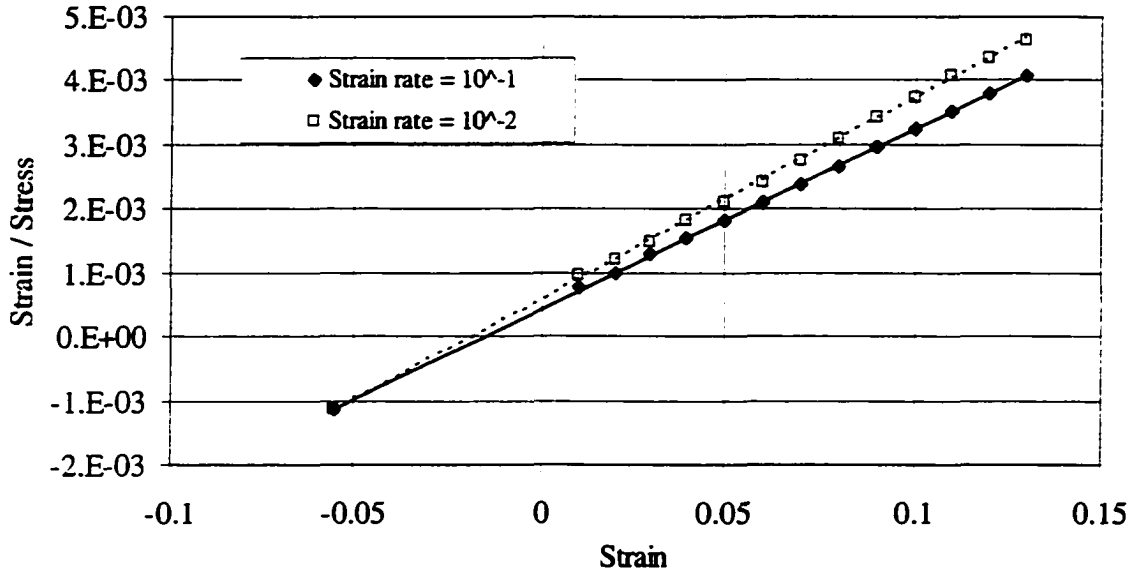

Figure 8.4. Intersection of normalized stress-strain lines for 10^{-1} and 10^{-2} / sec strain rates.

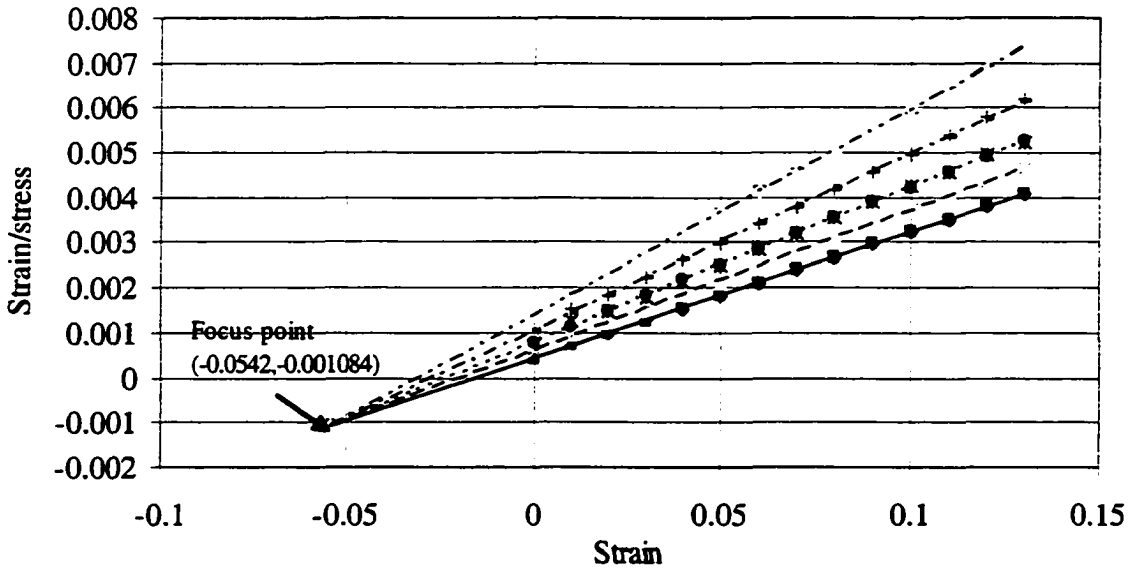

Figure 8.5. Normalized stress-strain relation using the focus point.

hypothesized that the focus point is related to the residual stresses and strains during the manufacturing process and sampling technique.

$$\frac{\varepsilon}{\sigma} = 0.02804\,\varepsilon + 0.00044 \tag{8.7}$$

$$E_t = \frac{\{1-[0.02447(\frac{\Delta\varepsilon}{\Delta t})^{-0.05256}\sigma]\}^2}{\{-0.001084 + 0.05418[0.02447(\frac{\Delta\varepsilon}{\Delta t})^{-0.05256}]\}} \tag{8.8}$$

Equation 8.8 was used to calculate the tangent modulus value for HDPE material under compression at different strain rates, as shown in Figure 8.7. This figure shows that the tangent modulus of HDPE at high strain rate is greater than that at less strain rates. This figure also shows that the tangent modulus is decreasing linearly but slowly and independent on the strain rate for strains greater than 5%.

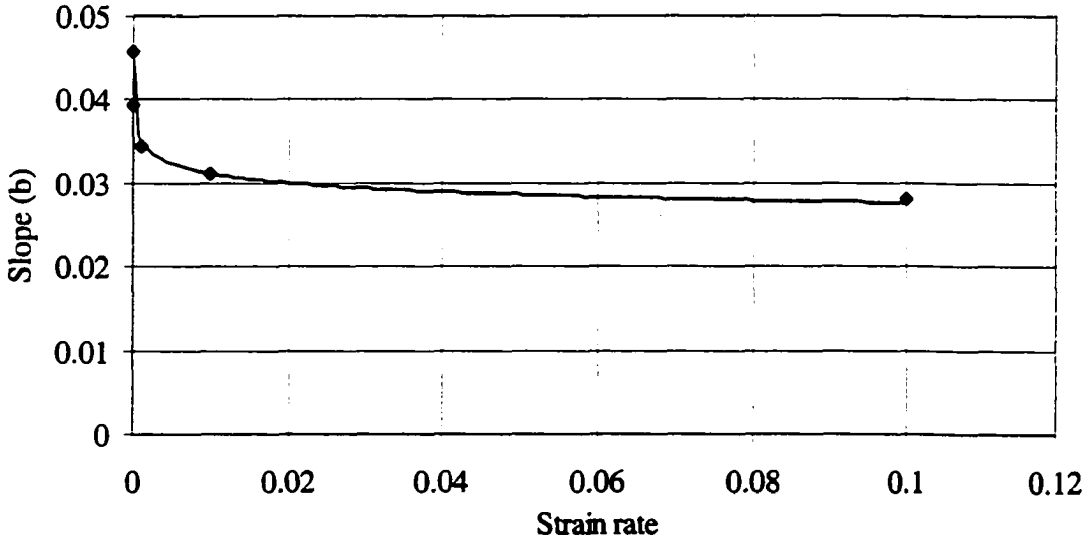

Figure 8.6. Change of slope of normalized stress-strain lines with strain rate using the focus point.

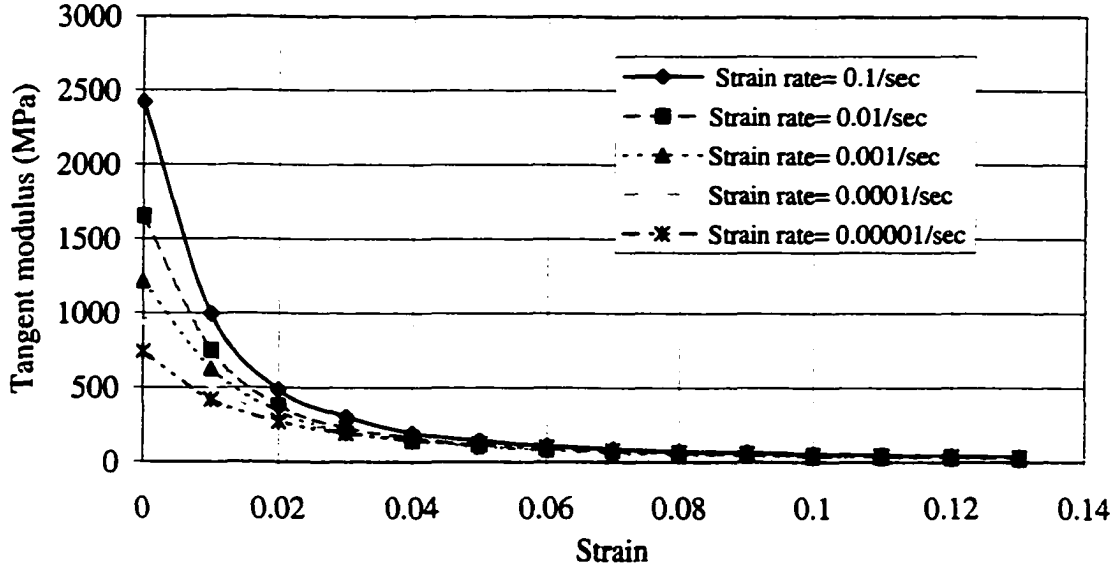

Figure 8.7. Change of HDPE tangent modulus with strain for five different strain rates.

The parallel plate test results shown in Figure 1.14 can also be used to fit a hyperbolic model. The normalized deflection load diagram of Figure 1.14 is shown in Figure 8.8. Since only two different rates were used, the change of slope and intercept with deflection rate change cannot be modeled mathematically. More tests need to be performed to determine pipe stiffness as a function of loading rate.

8.3.2 Effect of time

A hyperbolic model was also used to fit the creep strain curves shown in Figure 1.19. A linear function was used to fit the normalized creep strain data as shown in Figure 8.9. Figure 8.10 shows the results of using the focus point technique explained above which results in a coefficient of correlation (R^2) ranging between 0.97 and 0.99. The slope of the focus point lines versus the stress level was fit to a power mathematical model, as shown in Figure 8.11. The tangent modulus considering the time effect was derived using the same

technique described in section 8.3.1. The resulting tangent modulus considering time is given by Equation 8.9.

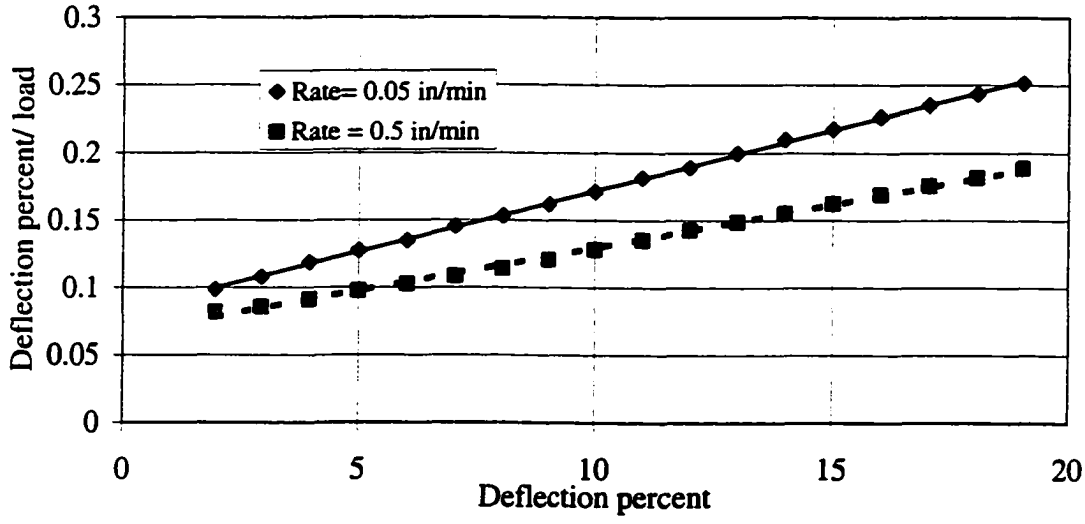

Figure 8.8. Normalized stress-strain results of parallel plate test.

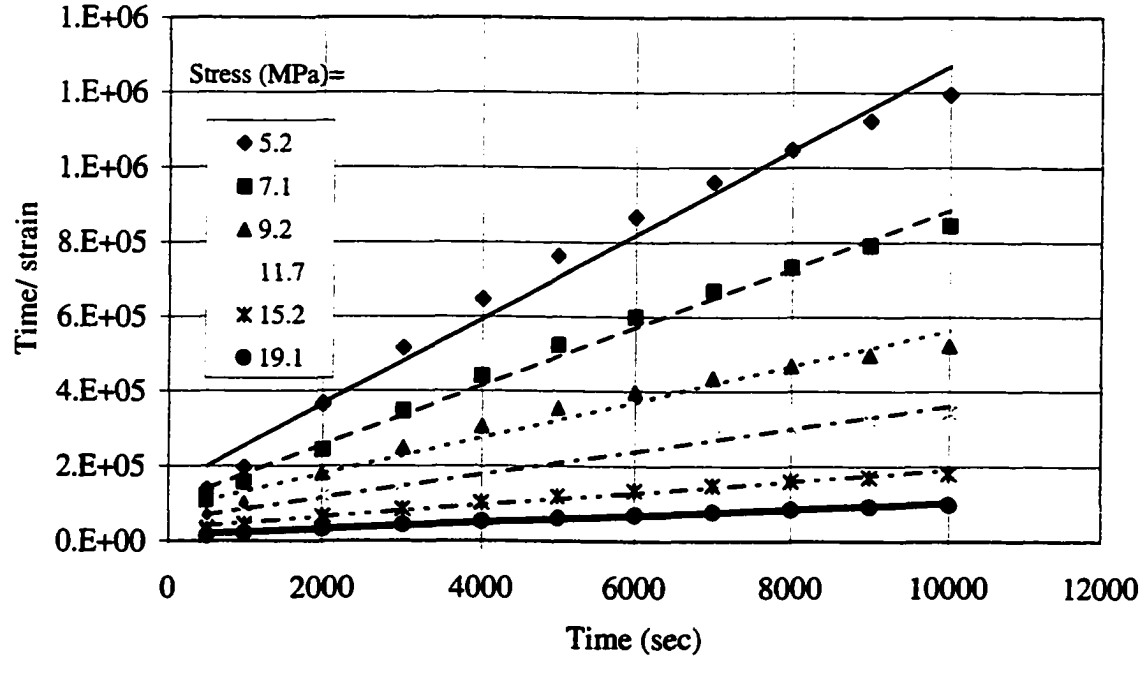

Figure 8.9. Normalized time vs. creep strain relationship for six different stress levels.

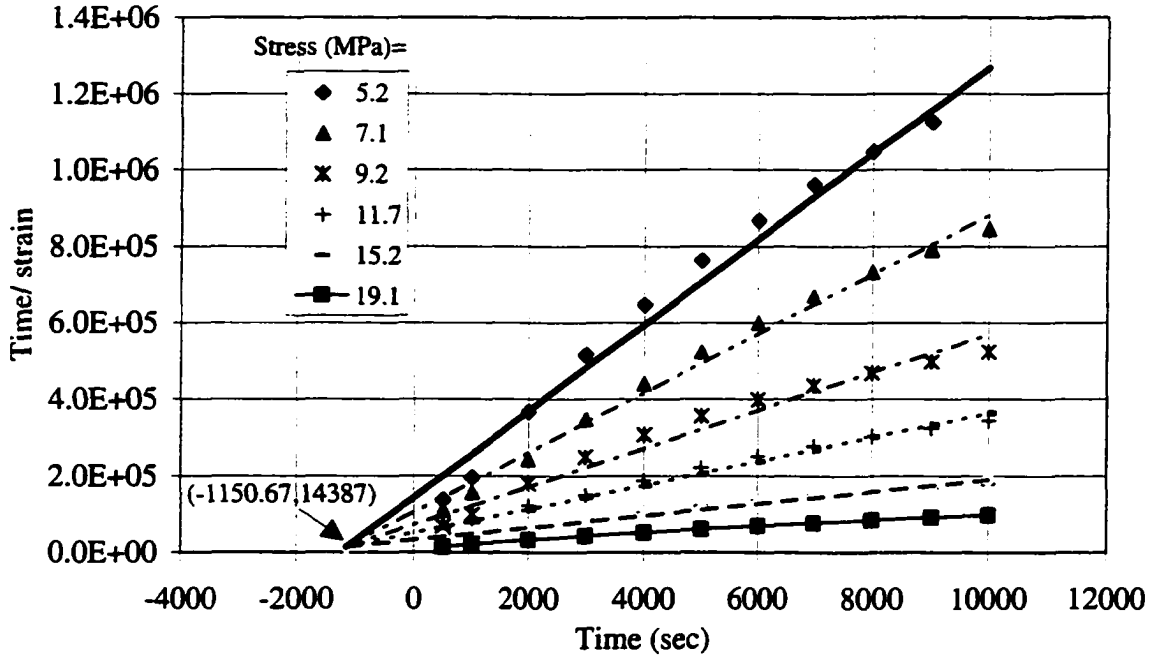

Figure 8.10. Normalized creep strain curves using the focus point.

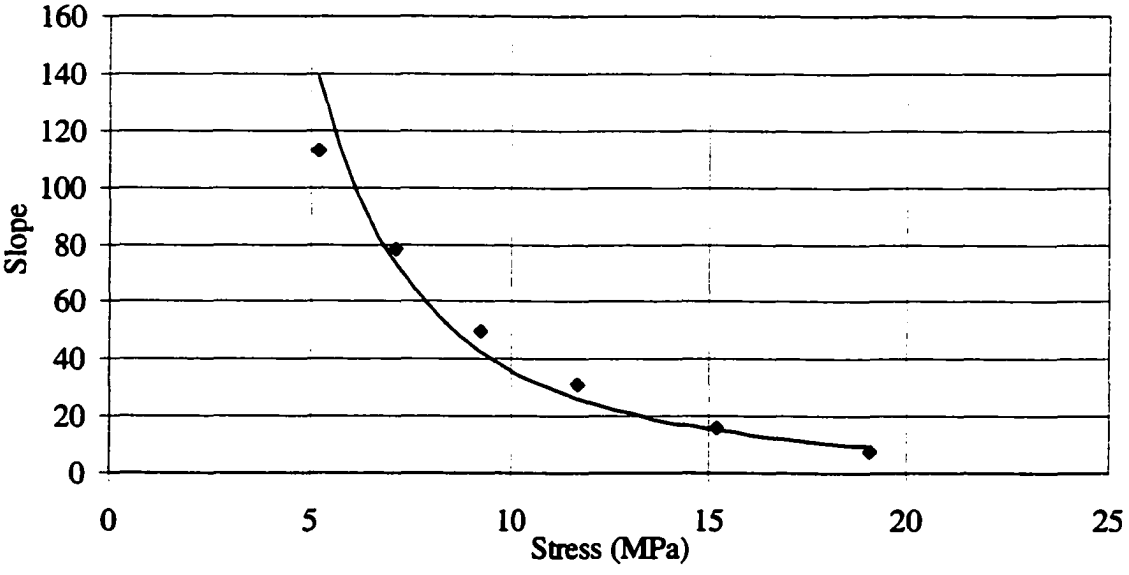

Figure 8.11. Change of the slope of focus point lines with stress level for creep tests.

$$E_t = \frac{[1-(0.02447(\frac{(1-B(\varepsilon-\varepsilon_{oi}))^2}{A})^{-0.05256}\sigma)]^2}{[-0.0010837+0.054179(0.02447(\frac{(1-B(\varepsilon-\varepsilon_{oi}))^2}{A})^{-0.05256})]} \qquad (8.9)$$

where:

A: Y coordinate of the focus point of the time creep strain curve.
B: X coordinate of the focus point of the time creep strain curve.
ε_{oi}: initial strain at the current stress level.

Sargand et al. (2001) and Lars Janson (1996) concluded, based on field tests, that the pipe deflection stabilizes in a period of six to eight weeks. Based on these results, in this research the HDPE modulus was extrapolated to a time of six weeks instead of 50 years. Table 8.1 shows the extrapolated values of the modulus considering the time effect and using Equation 8.9. This exploration showed an average decrease of the HDPE modulus of 77% at six weeks.

Table 8.1. HDPE modulus change with stress level and time.

Stress	**Modulus zero time**	**Modulus six weeks**	**Reduction %**	**Modulus 50 years**	**Reduction %**
MPa	**MPa**	**MPa**		**MPa**	
5.2	953.3	240.1	74.8	171.8	82.0
7.1	710.0	204.4	71.2	146.5	79.4
9.2	778.5	180.9	76.8	126.0	83.8
11.7	643.5	142.5	77.8	97.9	84.8
15.2	539.4	98.2	81.8	65.7	87.8
19.1	389.1	68.0	82.5	45.7	88.3
		Average =	77.5	**Average =**	84.3

8.4 Finite Element Modeling

The nonlinear strain rate and time dependent HDPE tangent moduli developed in section 8.3 were programmed in the ANSYS code which is used to model the nonlinear time independent soil properties and which was developed in Part II of this thesis. For each sub-

step, the HDPE modulus is calculated for each pipe element based on the element compression stresses and strains at the end of the previous sub-step. The sub-step is solved using the average modulus of all pipe elements. At the end of each load step an average value of the pipe modulus for all sub-steps is calculated and used to solve for the pipe response.

To validate the use of strain rate and time dependent HDPE tangent modului programmed in the ANSYS code, the pipe soil system shown in Figure 5.1, which was used to study the effect of pipe material shown in Figure 6.16, was used to compare the results of HDPE pipe deflection using a constant and variable HDPE pipe modulus. The soil used in this study is an SM soil with parameters given in Table 6.2. This soil is described as having lesser quality soil than most soils used for plastic pipe applications. The pipe modulus calculated using Equation 8.8 was employed in this analysis. The applied distributed load was increased linearly with time for each load step. The results of ANSYS small and large deflection theories using constant and strain rate dependent pipe moduli are shown in Figure 8.12. For both cases, this figure shows that considering the strain rate dependent HDPE modulus increased the pipe deflection. The difference between pipe vertical deflection percent using constant and strain rate dependent HDPE pipe modulus varies between 6% and 11%. Differences up to 32% were noticed between the small deflection theory solution using elastic pipe properties and the large deflection theory solution considering the strain rate dependent pipe properties. This shows that both large deflection theory and strain rate dependent pipe properties need to be considered for deeply buried HDPE pipes. The large deflection solution using the strain rate dependent HDPE modulus did not converge for the case of 18.25 m soil cover. This is due to the fact that increasing the load and decreasing the pipe modulus lead to pipe instability.

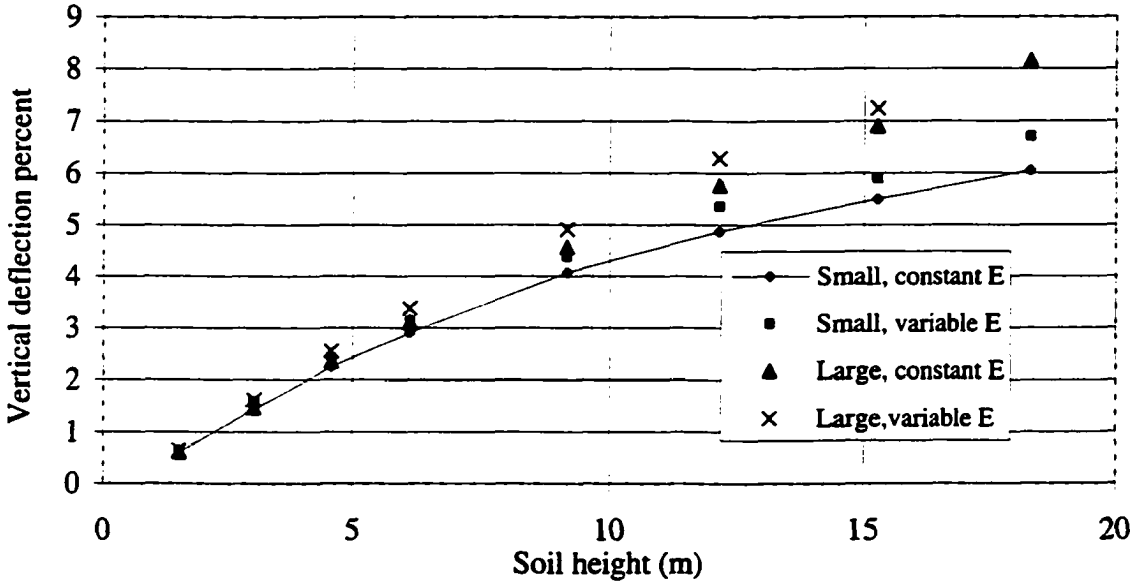

Figure 8.12.Vertical deflection percent with respect to soil cover using constant and strain rate dependent HDPE modulus.

The axial strains in the beam elements (i.e., the pipe walls) were also investigated to determine where they lie on the stress strain diagram for HDPE material. The maximum axial strains in the beam elements were observed at the pipe spring line. The calculated average percent strain, which is the average of strains at the end of each load step, varies between 0.07% at shallow depths and 1.1% for deeply buried pipes. These strains correspond to vertical deflection percents of 0.6% and 7% respectively. The calculated strains in the beam elements are below the 4% limit which defined region A in section 1.2.3.2.4 of this dissertation with reference to the compression test results of Zhange and Moore (1997) shown in Figure 1.16.

9. CONCLUSIONS

Since the parallel plate test deflection rate is not related to the practical loading rate and the time effect is not considered in parallel plate tests, compression tests conducted by Zhange and Moore (1997) were used to develop strain rate and time dependent HDPE tangent modulus models. Two different methods were used to model the dependency of the tangent modulus on the loading rate. These two methods were the independent slope-intercept method and the focus point method. The effect of modulus time dependency was also included in the focus point model. The pipe modulus as a function of time was extrapolated to six weeks instead of 50 years. This extrapolation showed a modulus reduction between 71% and 82%. The mathematical models were programmed in ANSYS and used in a finite element analysis. The effect of decreasing HDPE modulus on pipe deflection was studied using both small and large deflection theories of ANSYS. Comparing the results of both constant and variable HDPE pipe modulus for the case of SM soil, a maximum difference of 11% of the vertical deflection percent was noticed at soil cover of 15 m. Differences up to 32% were noticed between the small deflection theory solution considering elastic pipe properties and the large deflection theory solution considering the strain rate dependent pipe properties. This shows that both large deflection theory and strain rate dependent pipe properties need to be considered for deeply buried HDPE pipes.

10. GENERAL CONCLUSIONS

This research consists of the following tasks that were completed: a literature review, an investigation of in-service HDPE pipes at 10 different locations in Minnesota, an improvement of the capabilities of ANSYS, and an improvement of mathematical models for a nonlinear strain rate and time dependent tangent modulus of HDPE material using the results of compression test by Zhange and Moore (1997) which were programmed in ANSYS. The following conclusions can be formulated from the investigation of in-service HDPE pipes, finite element analysis of flexible pipes, and the development and study of the strain rate time dependent modulus models for HDPE material. It should be noted that some of these observations are based on limited number of investigations.

1. An investigation of in-service HDPE pipes was completed at 10 different locations, and 12,006 feet in length was completed; the structural problems observed were: 4 dimpling or local buckling, 29 cross sectional deformations, 7 pipe sags, 27 wall cracks, and 25 joint separations.
2. The frequency of the structural problems increases as the pipe diameter increases.
3. HDPE pipes buried in regions where the native soil is glacial till or lake sediments, regardless of pipe diameter, showed cross sectional deformations and some pipes showed longitudinal sag.
4. Significant structural problems were limited in the investigated pipes. The investigation showed that in most cases the MN. DOT specifications were followed. The limited significant structural problems are due to the use of the granular soils as a backfill material.

5. The small and large deflection theories of ANSYS were used to compare the pipe behavior in the elastic soil case with CANDE. The results of these analyses were well compared with CANDE. The large deflection theory did not show a significant effect on the response of flexible pipes for elastic soil with a maximum height of soil cover of 6.1 m.

6. ANSYS was improved to include the nonlinear time independent soil behavior using hyperbolic tangent modulus, bulk power modulus, and hyperbolic bulk modulus models. The small and large deflection theories of ANSYS showed good agreement with CANDE. Two different soils, two different pipe materials, and two different soil models were used in the comparison. This validates the use of ANSYS with the improved code to model pipe soil systems. Large deflection theory did not show a significant effect in case of nonlinear time independent soil modulus for soil heights up to 6.1 m. CANDE is adequate to model the cases discussed above.

7. CANDE and the small and large deflection theories of ANSYS were compared with Moser's results. This comparison showed that CANDE over-predicts the pipe deflections as the soil approaches a shear failure. CANDE can be used as long as the shear failure of the soil was not reached. The small and large deflection theories of ANSYS showed better agreement with Moser results for soil depth of 9 m or more. ANSYS large deflection theory showed better agreement than ANSYS small deflection theory with Moser results in cases where vertical deflection percent of 4%.

The maximum difference between ANSYS small and large deflection theories was 12%.

8. The response of PVC and HDPE pipes were compared using small and large deflection theories of ANSYS. PE pipes are more sensitive to the consideration of large deflection than the PVC pipes.

9. The cases discussed in conclusions 7 and 8 above lead to the conclusion that considering large deflection for flexible pipe analysis becomes significant for pipes deflections of 4% or more.

10. The written code in ANSYS was also improved to consider the construction process. The new code was compared with CANDE. The effect of displacement discontinuity of CANDE during construction was insignificant.

11. The mathematical models improved for the HDPE material were programmed in ANSYS. Comparing the finite element results of small deflection theory using constant and variable HDPE pipe modulus resulted in differences up to 11% in the vertical deflection percent calculated. The same differences were noticed when comparing the results of large deflection theory using constant and variable HDPE pipe modulus.

12. Differences up to 32% were noticed between the small deflection theory solution considering elastic pipe properties and the large deflection theory solution considering the nonlinear strain rate dependent pipe properties using SM soil as a backfill. This shows that both large deflection

theory and strain rate dependent pipe properties need to be considered for deeply buried HDPE pipes.

The global significance of the findings of this research are: 1) based on observations of in-place installations, the granular backfill materials around the HDPE pipes resulted in limited number of significant structural problems, 2) large deflections effect becomes significant for vertical deflection percent of 4% or more, 3) CANDE is adequate for shallow buried pipes and over predicts the pipe deflections if soil elements approached the shear failure, 4) linear elastic pipe material properties and small deflections are not adequate to model deeply buried HDPE pipe in SM soil.

APPENDIX A.

PIPE PERFORMANCE EVALUATION FORMS

Project Pipe Performance Evaluation

Site No._____ Survey date_____ Page 1 of ___

Project Information:

County_____ Street Name_____ Alignment_____

Project length _____from MH/CB_____ to MH/CB_____

No. of segments_____

Site Characteristics:

Native soil _____

Backfill material_____

Backfill density _____Water table depth_____

Pipe characteristics:

Type _____ Material_____ Manufacturer_____

Unit Length_____ Diameters_____

Installation:

Average depth to top of pipe _____Trench width _____

Surface loads _____

Pipe Grade:

Design grades_____

Beginning elevation_____ Final elevation_____

Other observations:

_____

Figure A-1. Project data sheet.

Segment Pipe Performance Evaluation

Site No._____**Segment no.**_____**Survey date**_____ **Page** ____ **of** ___

Segment length _____ from MH/CB_____ to MH/CB_____

Diameter _____ Grade _____Depth_____

Segment Grade:

Design grade_____ Beginning elevation _____ Final elevation _____

Other observations:

_____

_____

Location from the start of this segment (feet)	0 - 10	10 - 20	20 - 30	30 - 40	40 – 50	50 - 60	60 - 70	70 - 80	80 - 90	90 - 100	100 - 110	110 - 120
Criteria	**Magnitude of the problem**											
Cross-section Deformation												
Wall buckling												
Wall crushing												
Wall cracking												
Joint separation												
Sediments												

Figure A-2. Segment pipe performance evaluation data sheet.

APPENDIX B.

OBSERVATIONS AT ALL SITES SURVEYED

B.1 Woodland Avenue; Mankato, MN

This project which has a 24 inch diameter dual wall ADS HDPE pipe, 329 feet in length with a slope of 0.23%, is buried at an average depth of 11.3 feet. The native soil is a limestone rock. This pipe was installed in 1999 and surveyed July 24, 2000 from MH 37-3 to MH 37-6. Figure B-1 shows a schematic diagram of this project. Slightly elliptical cross section deformations with vertical shortening were observed over 125 feet that started 170 feet from MH 37-3. Water infiltration was observed at two joints 36 and 132 feet from MH 37-3 respectively, as shown in Figure B-2. The arrow in Figure B-2 is pointing to the infiltration location. Sediments and water were observed over 49% of the pipe length.

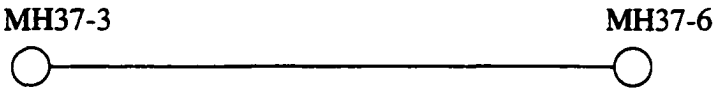

Length: 329 feet

Diameter: 24 inch

Slope: 0.23%

Figure B-1. Schematic diagram of the pipe surveyed at Woodland Avenue, Mankato.

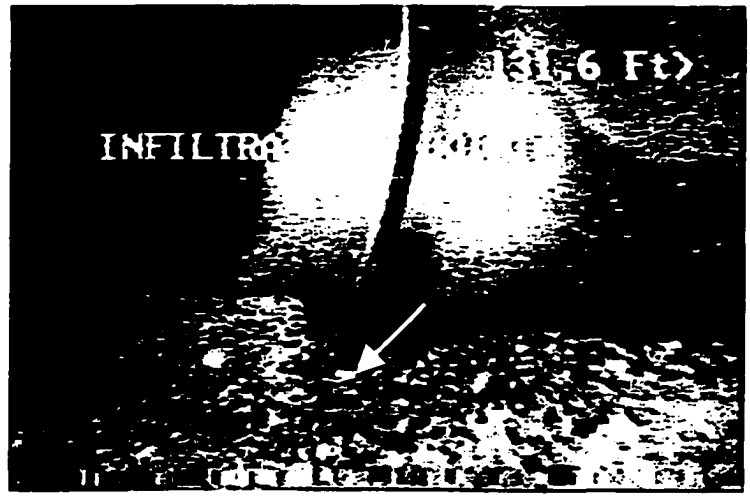

Figure B-2. Water infiltration at a joint.

B.2 Thompson Street; Mankato, MN

This project which has a 24 inch diameter dual wall ADS HDPE pipe, 295 feet in length with a slope of 0.42%, is buried at a depth of 3.1 feet. The native soil in this region is peat. The pipe was installed in 1996 and surveyed July 24, 2000 from MH B-30 to MH A-9. Figure B-3 shows a schematic diagram of this project. Figure 3.11 shows one of the two 12 inch cracks (about 0.04 inch (1 mm) wide) between "9 and 12 o'clock" that were observed at 180 and 190 feet from MH B 30. Three joints (at 63, 103, and 207 feet from MH B 30) of the 14 joints have root penetration. Sediments and water were observed over 83% of the pipe length.

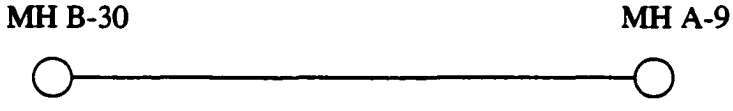

Length: 295 feet

Diameter: 24 inch

Slope: 0.42%

Figure B-3. Schematic diagram of the pipe surveyed at Thompson Street, Mankato.

B.3 Bronson Drive & Belle Lane; Moundsview, MN

This project which has 24, 42, and 48 inch diameter ADS HDPE pipes, 1,886 feet in length with slopes ranging from 0.2% to 0.44%, is buried at depths ranging from 1.2 feet to 11.5 feet. The native soil is fine sand of glacial outwash origin. These pipes were installed in 1997 and surveyed July 26, 2000 from MH 119 to MH 202. In addition, observations were made at the ground surface between MH 201 and MH 202. Figure B-4 shows a schematic diagram of the pipe surveyed at Bronson drive and Belle lane. The video survey revealed significant elliptical deformation with horizontal shortening of about 2 inches in the

48 inch diameter pipe 28 feet from MH 109 to 360 feet toward MH 202. Other problems noted are about 0.4 inch (10 mm) joint separation at 170 feet from MH 201 toward MH 202 as pointed by the arrows in Figure B-5, and two steel rods penetrating the pipe wall at 133 feet from MH 201 toward MH 202 as shown in Figure B-6. Water and sediments were observed over 86% of the 48 inch diameter pipe. No significant problems were noted in the 24 or 42 inch diameter pipes.

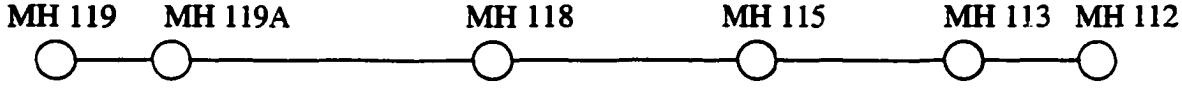

Length:	23	450	342	280	21	feet
Diameter:	24	24	42	48	48	inch
Slope:	0.44%	0.44%	0.3%	0.2%	0.2%	

a. MH 119 to MH 112.

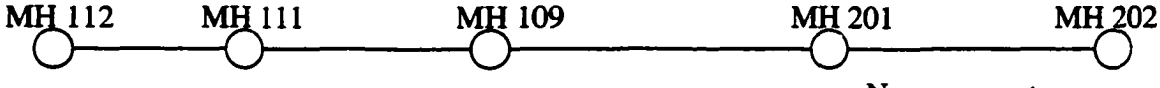

Length:	43	100	360	267	feet
Diameter:	48	48	48	48	inch
Slope	0.2%	0.218%	0.218%	0.218%	

b. MH 112 to MH 202.

Figure B-4. Schematic diagram of the pipe surveyed at Bronson Drive, Moundsview.

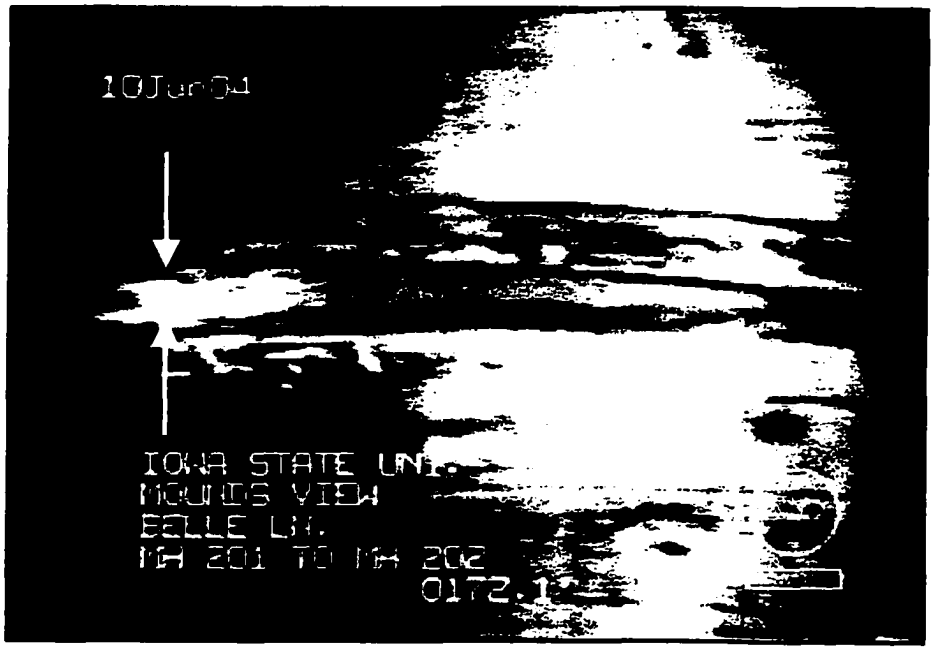

Figure B-5. Joint separation of 0.4 inch at 170 feet from MH 201.

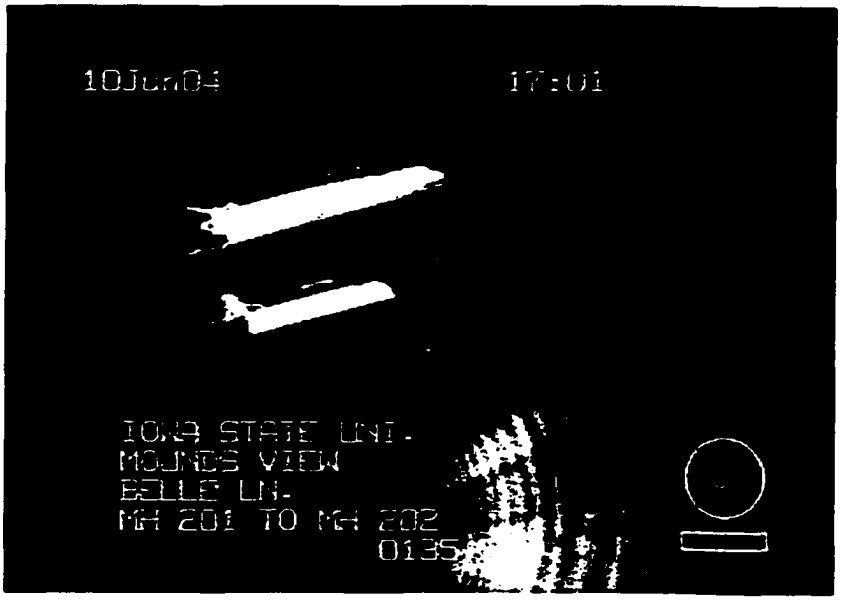

Figure B-6. Two rods penetrating the pipe wall at 133 feet from MH 201.

Surface observation of the 48 inch diameter pipe between MH 201 and MH 202 with 1.7 feet of soil cover revealed a pipe heaved above the ground surface. Associated with the heave was a joint separation and outside circumferential crack 75 inch long and about

0.04 inch (1 mm) wide as shown in Figures 3.9, 3.10, and 3.11. The location of the heave, about 30 feet from the outlet into a marsh, suggests that buoyancy from a high water table combined with shallow depth of cover most likely caused the heave.

B.4 Xylite Street; Blaine, MN

This project which has 24 and 30 inch diameter ADS HDPE pipes, 1,354 feet in length with slopes varying between 0.15% and 0.27%, is buried at depths ranging from 3.6 feet to 5.6 feet. This pipe was installed in 1995 and surveyed on July 26, 2000 from MH 7 to MH 1. Figure B-7 shows a schematic diagram of the surveyed pipe. The native soil is fine sand with the water table 3 to 4 feet deep. According to Blaine City specifications, this soil can be used as a foundation for the pipe after dewatering. Localized wall buckling of less than 1 inch at the pipe crown was noted over 118 feet of 460 feet of the 30 inch diameter pipe. These deformations were between 110 to 160 feet and 200 to 218 feet measured from CB 3 toward CB 2 and between 20 to 70 feet from CB 2 toward MH 1. These deformations occurred as a dimpling pattern similar to that shown in Figures 1.7 and 3.5. Sediments were observed over 88% of the pipe length.

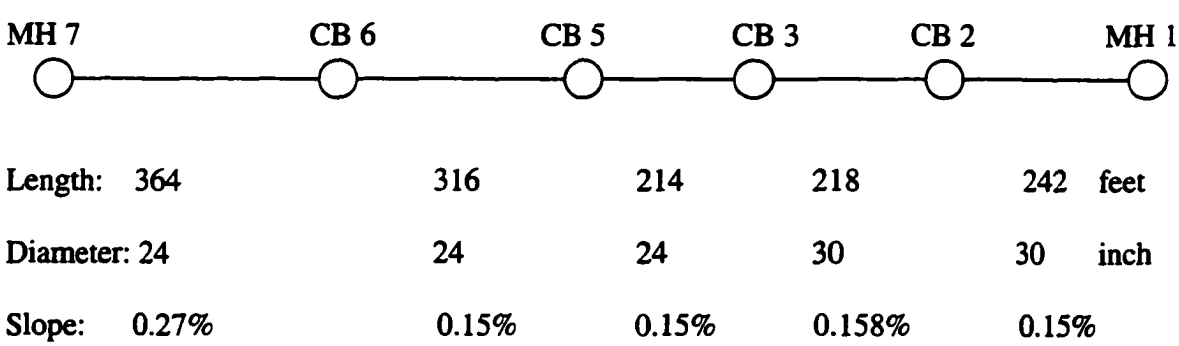

Figure B-7. Schematic diagram of the pipe surveyed at Xylite Street, Blaine.

B.5 Ottawa street; Le-Center, MN

This project which has 30 and 36 inch diameter HDPE pipe, 1,528 feet in length was surveyed December 27, 2000 from MH 1 to MH 6 and 251 feet beyond toward the outlet of a lake. No plans were available for this site. Figure B-8 shows a schematic diagram of the Ottawa Street pipe. The survey was stopped at 251 feet from MH 6 toward the lake outlet because of ice ("No access") as shown in Figure B-8. Joint separations of 1 inch wide and 7 inch long at "7 o'clock" were observed 7 feet from MH 1 and also at 256 feet from MH 2. Pipe sag of 1 to 2 inch in the 30 inch diameter pipe was observed over a 2 feet length starting at 54 feet from MH 3. Figure B-9 shows elliptical cross sectional deformations with vertical shortening at a joint 227 feet from MH 3 toward MH 4 which has a 30 inch diameter pipe. Another elliptical cross sectional deformation with vertical shortening of 3 to 4 inches over 105 feet in length was observed in the 36 inch diameter pipe; this deformation started 50 feet from MH 5. Horizontal diameter shortenings were noticed at two locations: at a joint 277 feet from MH 2 toward MH 3 that has 30 inch diameter pipe and also in the 36 inch diameter pipe (1 inch horizontal shortening over 22 feet) starting at 312 feet from MH 5. Heart shape pipe deformations with 1 to 2 inch crown deformation in the 36 inch diameter pipe was noted at a joint 23 feet from MH 5. Deformations of the plastic connection between two pipe segments were observed at 10 locations. An example of this connection deformation is shown in Figure B-10. All of these connections were between MH 5 and the end of the survey toward the lake outlet. In this region, an average of 2 to 3 inches of water above 1 inch of sediments was noticed. A layer of ice was also observed in the region between MH 6 and the end of survey toward the lake outlet. The ice started at 214 feet from MH 6 and

extended for 37 feet toward the lake outlet. Sediments and water were observed over a length of 1,314 feet, which is 86% of the total pipe length surveyed at this site.

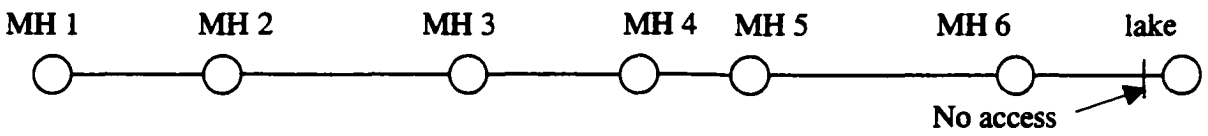

Length:	108	311	290	30	538	251	feet
Diameter:	30	30	30	36	36	36	inch
Slope:	NA	NA	NA	NA	NA	NA	

Figure B-8. Schematic diagram of the pipe surveyed at Ottawa Street, Le-Center.

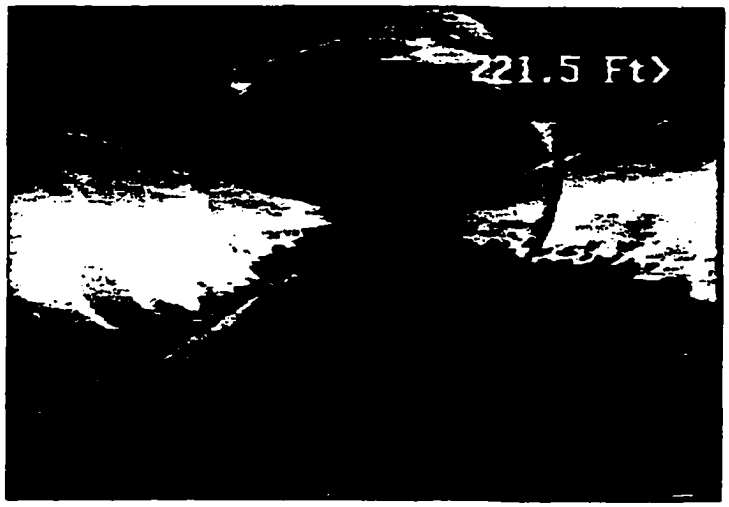

Figure B-9. Deflection in 30 inch diameter pipe at a joint 227 feet from MH 3.

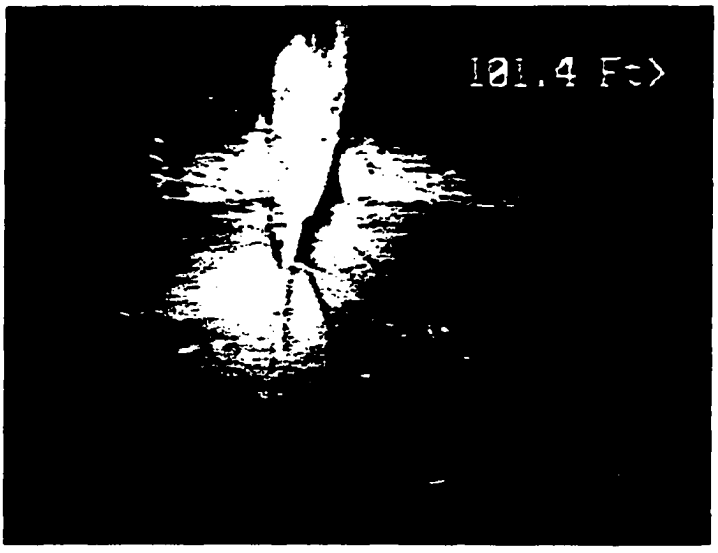

Figure B-10. Joint separation and water infiltration due to deformation of the piece connecting two pipes.

B.6 Highland Avenue and Shoreacres Drive; Fairmont, MN

This project which has 12, 24, 27, 30 and 36 inch diameter HDPE pipe, 2,231 feet in length with a slope ranging from 0.32% to 6.6%, buried at depth ranging from 1.65 feet to 8.36 feet was surveyed December 21, 2000 from MH OR 215 to MH 7. This project consists of four different installations. Schematic diagrams of these installations are shown in Figures B-11, B-12, B-13, and B-14. Cross sectional deformation with horizontal shortening of 1 inch in the 36 inch diameter pipe was noticed at a joint 132 feet from MH OR 211 toward MH OR 210. Dimpling (localized wall buckling pattern) of less than 1 inch at "1 o'clock" was noticed over 20 feet of 1,143 feet of the 36 inch diameter pipe. These deformations were located between 425 and 445 feet measured from MH OR 210 toward MH OR 208. Pipe sag of 1 to 2 inch in the 36 inch diameter pipe was noticed between 12 and 22 feet measured from MH OR 215 toward MH OR 214. Two dents and two joint separations were also observed. The two dents were 1 inch deep at 33 feet from MH OR 215 toward MH OR 214

Length:	163 feet
Diameter:	24 inch
Slope:	0.32%

Figure B-11. Schematic diagram of the pipe surveyed at Shoreacres Drive, Fairmont.

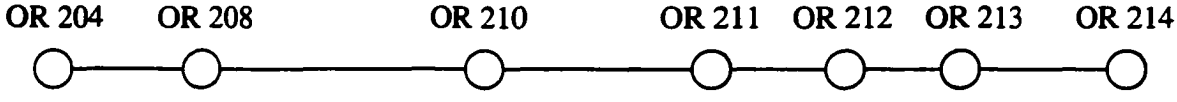

Length:	100	537	200	28	49.5	187.5	feet
Diameter:	36	36	36	36	36	36	inch
Slope:	0.76%	0.76%	1.8%	0.52%	0.52%	0.52%	

a. MH OR 204 to MH OR 214.

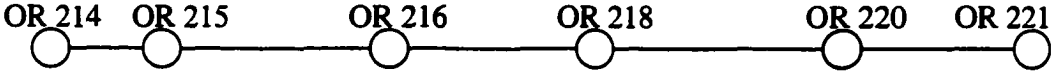

Length:	41	122	95	142	61	feet
Diameter:	36	30	30	30	27	inch
Slope:	6.6%	1.1%	2.58%	1.0%	0.88%	

b. MH OR 214 to MH OR 221.

Figure B-12. Schematic diagram of the pipe surveyed at Highland Avenue, Fairmont.

while the two 1 inch joint separations were at 266 feet from MH OR 210 and 88 feet from MH OR 208 toward MH OR 204. Elliptical cross sectional deformations with vertical shortening of 2 inches in the 12 inch diameter pipe were observed over 10 feet between 30 and 40 feet from MH 5 toward MH 6 as shown in Figure B-15. An average of a half inch of water was observed over 80% of the total pipe length of this site, while 11% of the length covered by water has sediments.

No pavement

Length:	158 feet
Diameter:	24 inch
Slope:	0.38%

Note: *MH 2 in this figure is not the same MH 2 in Figure B-11.

Figure B-13. Schematic diagram of the pipe surveyed near Interlaken Road, Fairmont.

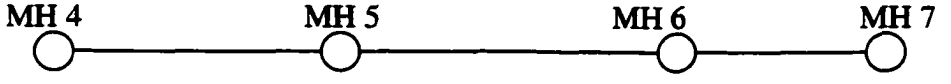

Length:	120	152	75	feet
Diameter:	12	12	12	inch
Wlope:	NA	NA	NA	

Figure B-14. Schematic diagram of the pipe surveyed at Fairmont.

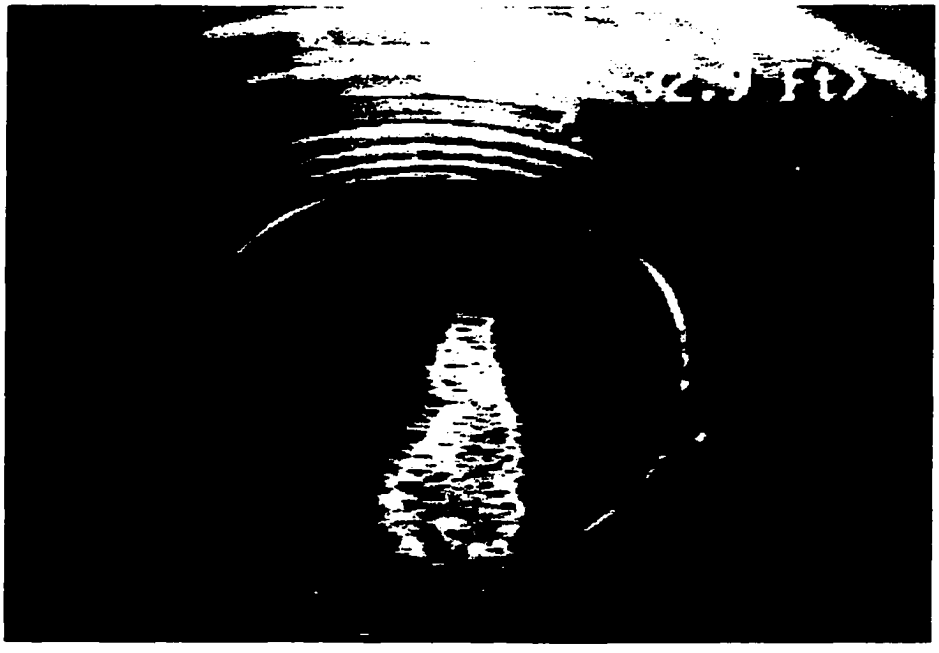

Figure B-15. Two inch deflection in 12 inch pipe.

B.7 Railroad Avenue; Gaylord, MN

These installations which have 24, 30, and 48 inch diameter HDPE pipes, 1,941 feet in length with a slope ranging from 0.03% to 0.39%, buried at depths ranging from 1.6 feet to 6.5 feet were surveyed January 17, 2001 from MH A to MH 29 and continued to a lake outlet. This project consists of four different installations. Schematic diagrams of these installations are shown in Figures B-16, B-17, B-18, and B-19. The survey was stopped as shown in Figure B-16 for unknown reasons and no plans were available. A 15 inch circumferential crack, 1 inch wide, extended between "9 and 3 o'clock" at 30 feet measured from MH A. Elliptical cross sectional deformations with vertical shortening of 10 to 12 inches in the 24 inch diameter pipe, which represents an average of 46% deformation of pipe diameter, were observed over 10 feet length that started 30 feet from MH A as shown in Figure 3.3. Associated with the deformations, were 1 to 2 inch dimples and pipe wall cracks at "2 o'clock" as shown in Figures 3.5 and 3.6. Pipe sag of 8 to 10 inches in the 24 inch

diameter pipe starting at 34 feet measured from MH A extended for 6 feet. Elliptical cross sectional deformation with horizontal shortening of 1 inch in the 48 inch diameter pipe was noticed over 22 feet starting 190 feet from CB 22 toward CB 20. A 4 inch pipe sag in the 48 inch diameter pipe extended over 104 feet between CB 23 and CB 24 and also a 2 inch sag over 5 feet starting 440 feet from CB 20 toward CB 19 were noticed. Sediments, water, and snow were observed over 1,750 feet, which is 90% of the total pipe length.

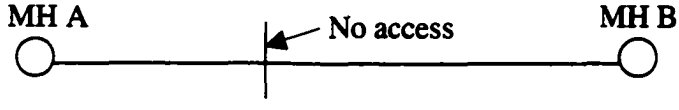

Length: 40 feet

Diameter: 24 inch

Slope: 0.29%

Figure B-16. Schematic diagram of pipe 1 surveyed at Gaylord.

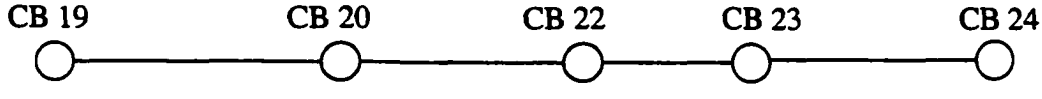

Length:	510	258	58	104	feet
Diameter:	48	48	48	48	inch
Slope:	0.031%	0.39%	0.05%	NA	

Figure B-17. Schematic diagram of the pipe surveyed at Railroad Avenue, Gaylord.

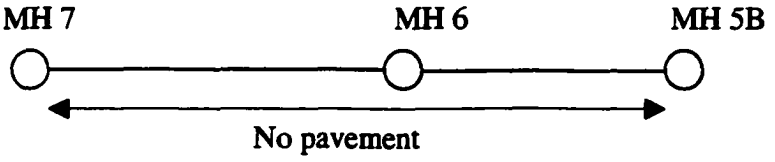

Length:	351	148	feet
Diameter:	30	30	inch
Slope:	0.36%	0.3%	

Figure B-18. Schematic diagram of pipe 2 surveyed at Gaylord.

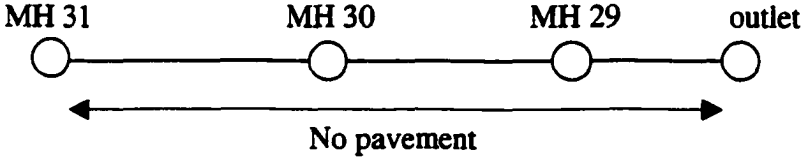

Length:	286	96	90	feet
Diameter:	48	48	48	inch
Slope:	0.17%	0.24%	0.24%	

Figure B-19. Schematic diagram of pipe 3 surveyed near Gaylord.

B.8 Jonquil Lane; Maple Grove, MN

This project which has 15 and 18 inch diameter HDPE pipe, 346 feet in length with a slope ranging from 0.76% to 4.73%, is buried at an average depth of 4.0 feet. This pipe was surveyed March, 2001 from MH 170A to MH 167. Figure B-20 shows a schematic diagram of the pipe surveyed at this project. The survey was stopped twice in this survey because of

ice ("No access") as shown in Figure B-20. Elliptical cross section deformations with horizontal shortening of 1 inch were observed over 129 feet of the 18 inch diameter pipe from MH 169 to MH 168. Elliptical cross sectional deformations with horizontal shortening were also observed at two joints, one in the 15 inch diameter pipe and one in the 18 inch diameter pipe. These joint deformations were located 21 feet from MH 169 toward MH 170, and 35 feet from MH 168 toward MH 167, respectively. Pipe wall deflections of 1 to 2 inches between "9 and 11 o'clock" were also observed over 1 foot at 104 feet from MH 169 toward MH 168, and at a joint 14 feet from MH 170A toward MH 170B. Sediments and/or water were observed over 100% of the pipe length.

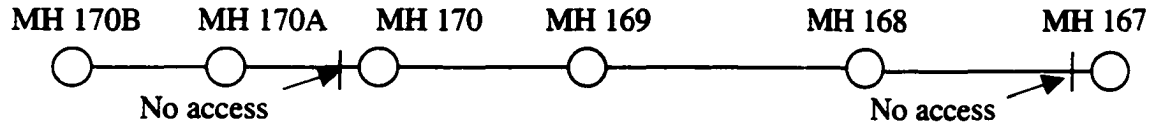

Length:	33	23	40	129	121	feet
Diameter:	15	15	15	18	18	inch
Slope:	0.76%	2.59%	4.21%	4.73%	1.86%	

Figure B-20. Schematic diagram of the pipe surveyed at Jonquil Lane, Maple Grove.

B.9 77th Place North; Maple Grove, MN

This project which has 15 and 18 inch diameter HDPE pipe, 687 feet in length with a slope ranging from 0.5% to 6.66%, is buried at average depth of 4.5 feet. This project was surveyed March, 2001 from MH 106 to an exit manhole. A schematic diagram of the pipe surveyed at this site is presented in Figures B-21 and B-22. The survey was stopped because of ice ("No access") at the location shown in Figure B-21. Elliptical cross sectional deformations with vertical shortening of 1 to 2 inches were noticed at two joints in the 15

inch diameter pipe, 101 feet from MH 104 toward MH 105 and 116 feet from MH 104 toward MH 103. Pipe wall deflections of 3 to 4 inches between "1 and 3 o'clock" and 1 to 2 inches at the pipe crown were observed in the 15 inch diameter pipe. These deflections were over 2 feet, each starting at 84 and 159 feet from MH 102 toward MH 101, respectively. Figure 3.7 shows a pipe wall deflection in the 15 inch diameter pipe. As shown in Figure 3.8, wall crushing (tearing) associated with a hole and two cracks (both 0.08 inch (2 mm) wide and 10 inch long) were noticed between "9 and 12 o'clock" in the 2 foot region starting 112 feet from MH 102 toward MH 101. A vertical offset of 2 inches in the 18 inch diameter pipe was observed in a joint 40 feet from MH 101 toward the exit manhole. Water 1 to 2 inches deep was noticed over 100% of the pipe length.

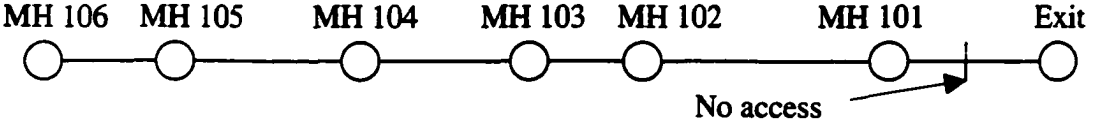

Length:	30	138	140	27	205	50 feet
Diameter:	15	15	15	15	15	18 inch
Slope:	0.5%	3.47%	4.89%	0.6%	6.66%	6.33%

Figure B-21. Schematic diagram of pipe 1 surveyed at 77th Place Lane, Maple Grove.

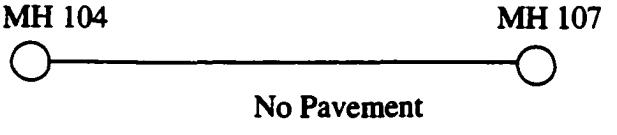

Length:	97 feet
Diameter:	15 inch
Slope:	0.5%

Figure B-22. Schematic diagram of pipe 2 surveyed at 77th Place Lane, Maple Grove.

B.10 96th Place North; Maple Grove, MN

This project which has 15, 18, and 24 inch diameter HDPE pipes, 1,409 feet in length, is buried at an average depth of 4.5 feet. No plans are available for this project. This project was surveyed March, 2001 from MH 7 to MH 1. Figure B-23 shows a schematic diagram of the pipe surveyed at this site. The survey was stopped because of large amount of sediments ("No access") shown in Figure B-23. Elliptical cross sectional deformations with horizontal shortening of 2 inches were observed at three locations. Deformation number 1 (over a region 10 feet long) was 27 feet from MH 7 toward MH 6 in the 15 inch diameter pipe as shown in Figure 3.2; associated with this deformation, were a 2 inch joint vertical offset and 2 inch of accumulated sediments. Deformations number 2 and 3 were observed at a joint 76 feet from MH 4 toward MH 3 in the 18 inch diameter pipe and at a joint 31 feet from MH 2 toward MH 1 in the 24 inch diameter pipe. Elliptical cross sectional deformations with vertical shortening of 2 inches were observed at two joints (54 and 92 feet from MH 2 toward MH 1) in the 24 inch diameter pipe. Deflections at the pipe crown of 1 to 2 inches over 4 feet followed by 1 inch dimpling over 4 feet at the pipe crown were observed starting 280 feet from MH 6 toward MH 5 in the 15 inch diameter pipe. Pipe wall deflections were observed between "9 and 11 o'clock" at three different locations. These deflections were over 4 feet of 2 to 3 inch deflection in the 15 inch diameter pipe as the arrow points in Figure B-24, over 1 foot of 1 inch deflection in the 18 inch diameter pipe associated with a 0.08 inch (2 mm) wide and 10 inch long crack, and over 2 feet of 1 inch deflection in the 24 inch diameter pipe associated with two cracks; each crack was 1 inch wide and 10 inches long. These deformations were located at 266 feet from MH 6 toward MH 5, 121 feet from MH 4 toward MH 3, and 21 feet from MH 2 toward MH 1, respectively. Pipe sags of 2 to 3 inches were

noticed at three locations. These sags in the 24 inch diameter pipe were over 3 feet starting 76 feet from MH 3 toward MH 2, over 3 feet starting 15 feet from MH 2 toward MH 1, and over 12 feet starting 166 feet from MH 2 toward MH 1. Associated with the pipe sag at 166 feet, were a hole and two cracks 0.12 inches (3 mm) wide and 15 inches long, between "9 and 12 o'clock". Joint separation of 1 inch was observed at 146 feet from MH 5 toward MH 4 associated with a hole at the pipe crown. Two vertical joint offsets of 2 inches were observed at 30 feet from MH 7 toward MH 6 and at 100 feet from MH 3 toward MH 2. One of these vertical joint offsets is shown in Figure B-25. A utility line penetrating through the pipe wall was observed between "10 and 1 o'clock" at 202 feet from MH 5 toward MH 4. Water and/or sediments were observed over 100% of the pipe length.

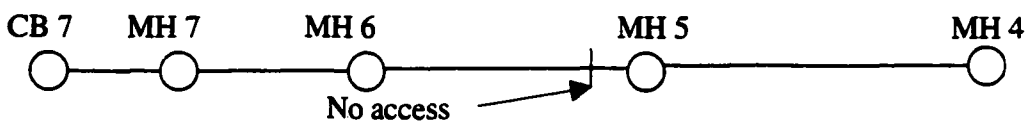

Length:	51	94	288	424	feet
Diameter:	15	15	15	15	inch
Slope:	N/A	N/A	N/A	N/A	

a. CB 7 to MH 4.

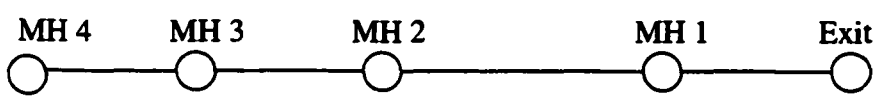

Length:	97	164	235	56	feet
Diameter:	18	24	24	18	inch
Slope:	N/A	N/A	N/A	N/A	

b. MH 4 to exit.

Figure B-23. Schematic diagram of the pipe surveyed at 96th Place North, Maple Grove.

Figure B-24. Pipe wall deflection in the 15 inch diameter pipe.

Figure B-25. Vertical joint offset in the 24 inch diameter pipe.

B.11 Summary

Data from all the sites surveyed are summarized in Tables B-1, B-2, and B-3. In these tables the site properties of pipe diameter, pipe length, pipe depth, design grade, structural problems, and sediments observed for all projects surveyed are presented. The structural problems noted in these tables are also summarized in Table 3.2. Sediments are mentioned in more detail in these tables. The manholes numbers in these tables correspond to the manholes numbers shown in the various site schematic diagrams presented in this appendix.

Table B.1. Performance evaluation for the sites surveyed in July, 2000.

Project	MH-MH	Diameter (inch)	Length (feet)	Ave. depth (feet)	Design grade (%)	Cross -section deformation	Pipe sag	Joint seperated	Wall cracking	Wall buckling	Sediments and/or Water in pipe
Mankato Thompson street	MH B30A-MH A9	24	295	3.1	0.42			3 roots going through	Two 12 in. cracks less or equal 1 mm		60ft, 0-1in. sed, below 1.5 water 160ft,1-2 sed., below 0.5 water 25ft,0-1sed,below 0.5 water
Mankato Woodland Av.	MH 37-3-MH 37-6	24	329	11.3	0.23	*1", 125 ft		2 water infiltration			60ft, 0-1in. Sed 80ft, 0-1in. sed, below 1in. water 80ft, 1-2in. sed, below 1in. water
Moundsview Belle lane and Bronson drive	MH 119-MH 118	24	473	8	0.44						24ft,0-1 sed.
	MH 118-MH 115	42	342	11.5	0.3						38ft ,1-2 in. sed.
	MH 115-MH 113	48	280	6.8	0.2						273 ft, 1-2 in.sed.
	MH 113-MH 111	48	64	2.8	0.2						20ft, 0-1 sed.below 1in water 35ft, 0-1 sed.
	MH 111-MH 109	48	100	1.7	0.218						22ft,0-1sed 20ft,1-2 sed
	MH 109-MH 202	48	627	1.2	0.218	**2", 332 ft		2			90ft,0-1 sed below 1 in water 90ft,2-3 sed 100ft,1-2 sed 140ft,2-3 sed below 1 in water 45ft,1-2 sed 95ft,2-3 sed, below 1-2 in water
Blaine Xylite Street	MH 7-CB 6	24	364	5	0.27						87ft, 1-2 in sed, 115ft, 2-3 in sed, 20ft, 0-1 in sed.
	CB 6-CB 5	24	316	4.06	0.15						86ft, 0-1 in sed, 160ft, 2-3 in sed, 70ft, 1-2 in sed.
	CB 5-CB 3	24	214	5.6	0.15						214ft 1-2 in sed.
	CB 3-MH 1	30	460	3.6	0.17					***1", 118 ft	220 ft,0-1 in sed 220ft,0-1 sed, below 1-2 in water

* elliptical deformation with vertical shortening.

** 2 in. eliptical deformation with horizontal shortening.

*** Dimpling local buckling.

Table B.2. Performance evaluation for the sites surveyed in December, 2000 and January, 2001.

Project	MH-MH	Diameter (inch)	Length (feet)	Ave depth (feet)	Design grade (%)	Cross -section deformation	Pipe sag	Joint seperated	Wall cracking	Wall buckling	Sediments and/or Water in pipe
Le Center Otaawa street	MH1-MH2	30	108	N/A	N/A			1			8 ft,0-1" sed 100 ft 0-1" sed. below 0-1" water
	MH2-MH4	30	601	N/A	N/A	* 3-4" at joint **1" at a joint	1-2",2ft	1			110 ft,0-1"water 20 ft, 1"sed ,below 1" water 90 ft,0-0.5" water 137 ft, 0-1" sed. below 0-1" water 64 ft,1"sed below 2" water
	MH4-MH6	36	568	N/A	N/A	* 3-4",105 ft ** 1" ,22 ft 1-2" at joint (3)		5 (1)			180 ft,1" sed. below 1-2" water 300 ft,0-1"sed 88 ft,1"sed. below 1" water
	MH6-outlet	36	251	N/A	N/A			5 (1)			180 ft,1" sed below 2-3"water 37 ft,4"water below 1" ice
Fairmont	OR215-OR214	36	41	8.36	6.6		1-2",10ft		2 dents		10 ft,1" water
Highland Avenue	OR214-OR212	36	237	6.78	0.52						236 ft, 0-1" water
	OR215-OR216	30	122	7.24	1.1						122 ft,0-0.5" water
	OR216-OR218	30	95	4.25	2.58						95 ft,0-0.5" water
	OR218-OR220	30	142	3.94	1						142 ft, 0-0.5" water
	OR220-OR221	27	61	5.1	0.88						55 ft, 0-1" water
	OR211-OR212	36	28	5.05	0.52						28 ft, 0-0.5" water
	OR211-OR210	36	200	3.35	1.8	** 1" at a joint					200 ft, 0-0.5" water
	OR210-OR204	36	637	3.43	0.76			2		1", 20ft ***	625 ft, 0-0.5" water
Shoreacres drive	MH2-MH3	24	163	3.2	0.32						163 ft,0-1.0" sed. and water
	(2) MH2-lakeoutlet	24	158	1.65	0.38						85 ft,0-0.5" water 28 ft,1" sed. below 1" water
	MH4-MH7	12	347	N/A	N/A	*1-2",10 ft					
Gaylord	MH A-MH B	24	40	N/A	0.29	10-12 ",10 ft	8-10",6 ft		1-2",18 cracks 1"-15" length	1-2 ", 10 ft ***	33 ft, 1 in sed 6 ft, 8-10 in. sed.
	MH7-MH6	30	351	5.45	0.36						351 ft,0-1" sed. and water
	MH6-MH5B	30	148	4.6	0.3						50 ft, 1" sed 98 ft,0.5" sed and water
Railroad Avenue	CB23-CB24	48	104	N/A	N/A		4",104 ft				104 ft, 1"sed. below 0.5" water
	CB23-CB22	48	58	1.6	0.05						58 ft, 1"sed below1"water
	CB22-CB20	48	258	2.5	0.39	** 1",22 ft					127 ft, 1" sed below 1" water 127 ft,0.5" sed below 0.5" water
	CB20-CB19	48	510	6.5	0.031		1-2",5 ft				445 ft, 1" sed below 1" water 65 ft,0.5" sed and water
	MH30-MH31	48	286	N/A	0.17						35 ft,0.5" sed and water 95 ft, 1" sed below 1" water 66 ft,1" sed below 2" water
	MH30-outlet	48	186	N/A	0.24						90 ft, 1-2" snow

* Eliptical deformation with vertical shortening
** Elliptical deformation with horizontal shortening
*** Dimling local buckling

(1) Deformation of the connection piece between two pipes
(2) MH2 different than the one above
(3) heart shaped pipe

Table B.3. Performance evaluation for the sites surveyed March, 2001.

Project	MH-MH	Diameter (inch)	Length (feet)	Ave.depth (feet)	Design grade (%)	Cross -section deformation	Pipe Sag	Joint seperated	Wall cracking	Wall buckling	Wall crushing	Sediments and/or Water in pipe
Maple Grove Jonquil Lane	MH170A-MH 170B	15	33	4	0.74	*1-2" at joint						33 ft,3-4" sed.
	MH170A-MH 170	15	23	3.5	2.59							23 ft,3-4" sed.
	MH169-MH170	15	40	4	4.21	** 1" at joint						33 ft, 0 5" water 7 ft, 2-3"sed below 0 5" water
	MH169-MH168	18	129	4	4.73	** 1",129 ft 1-2", 1 ft						129 ft,1" running water
	MH168-MH167	18	121	4.7	1.86	** 1" at joint						121 ft,1-2" running water
Maple Grove 77th Place North	MH104-MH105	15	138	4.89	3.47	*1-2" at joint						138 ft,0.5" runnig water
	MH105-MH106	15	30	4.84	0.5							30 ft,1"sed below 1" water
	MH104-MH107	15	97	2.98	0.5							97 ft, 2-3" water
	MH104-MH103	15	140	3.98	4.29	*1-2" at joint						140 ft, 1" runnig water
	MH103-MH102	15	27	4.7	0.6							27 ft, 1" running water
	MH102-MH101	15	205	4.98	6.66	*3-4", 2 ft *1-2", 2 ft			2mm,20" long 2 holes		2 ft	205 ft, 1" running water
	MH101-Exit	18	50	5.41	6.33			1, 2" vertical disp.				50 ft, 1" runnig water
Maple Grove 96th Avenue	MH7-CB7	15	51	4	N/A							51 ft,1" sed. Below 1-2" water
	MH7-MH6	15	94	4	N/A	**2", 10 ft		1,2" vertical disp.				70 ft,1" running water 24 ft,1-2" sed. Below 1" water
	MH6-MH5	15	288	4	N/A	2-3", 4 ft *1-2, 4 ft				***1", 4 ft		288 ft, 1-2" water.
	MH5-MH4	15	424	3	N/A			1, 1"				401 ft, 1"sed. below 2" water 23 ft, 1" water.
	MH4-MH3	18	97	4	N/A	1", 1 ft **1" at joint			2mm,10" long			97 ft, 1"sed below 2-3" water
	MH3-MH2	24	164	4	N/A		2-3",3 ft	1,2" vertical disp				144 ft, 1" runnig water 20 ft,1-2" sed below 1" water
	MH2-MH1	24	235	6	N/A	1-2",2ft **2-3",1ft *2", 2 joints	2", 15 ft		4 cracks 2, 1",10" long 2, 3mm,15" long hole			204 ft, 1" water 12 ft, 2" water 19ft,1" sed below 1-2" water
	MH1-SSMH1	24	56	7	N/A							56 ft,1" water

* Eliptical deformation with vertical shortening

** Elliptical deformation with horizontal shortening

*** Dimling local buckling

REFERENCES

American Society of Testing Material, 1992. "Standard Method for Determination of External Loading Characteristic of Plastic Pipe by Parallel Plate Loading". ASTM D2412.

American Society of Testing Material, 1992. "Standard Practice for Underground Installation of Thermplastic Pipe for Sewers and other Grsvity Flow Applications". ASTM D2321.

American Association of State and Highway Transportation Officials, 1992. " Standard Specifications for Highway Bridges". American Association of State and Highway Transportation Officials, Washington D.C.

Burns, J. O., and Richard, R. M., 1964. "Attenuation of Stresses for Stresses for Buried Cylinders". Proceedings, Symposium on Soil-Structure Interaction, pp. 378-392. University of Arizona, Tucson, Ariz.

Chambers, R. F., McGrath, T. J., and Heger, F. J., 1980. "Plastic Pipe for Subsurface Drainage of Transportation Facilities". NCHRP. Report 225, Transportation Research Board, pp. 122-140. Washington, D.C.

Corrugated Polyethylene Pipe Association,1997. "Structural Integrity of Non-Pressure Corrugated Polyethylene Pipe".

Corrugated Polyethylene Pipe Association, 1997. "Structural Design Method for Corrugated Polyethylene Pipe".

Duncan, J. M. and Chang, C. Y., 1970. " Nonlinear Analysis of Stress and Strain In Soils". Journal of the Soil Mechanics and Foundations Division. Proceedings of the American Society of Civil Engineers, Vol. 96, No. SM5, pp. 1629-1654.

Duncan, J.M., Byrne, P., Wong, K.S., and P. Mabry, 1980. "Strength, Stress-Strain and Bulk Modulus Parameters for Finite Element Analysis of Stresses and Movement in Soil Masses". *Report No. UCB/GT/80-01. University of California, Berkeley.*

El-Sawy, K., Moore, I.D., and B. Taleb, 1997. "Analysis of Stability Limit States for Long Span Culverts". *50th Canadian Geotechnical Conference of the Canadian Geotechnical Society*, pp. 178-184.

Gabriel, L.H, Ster, J. F., and Anthony, B. 2001. "A Test apparatus for Time Independent Stiffness of Thermoplastic Pipe". PREPRINT, *Transportation Research Board.* Washington D.C.

Gabriel, L.H. and Goddard, J. R., 1999. "Curved Beam Stiffness for Thermoplastic Gravity Flow Drainage Pipes". *Transportation Research Record 1656*, pp 51-57. Washington D.C.

Goddard, J. 1999. "Curved Beam Stiffness Test and Profile wall stability". PREPRINT, *Transportation Research Board.* Washington D.C.

Greenwood, Mark E. and Lang, Dennis C., 1990. "Vertical Deflection of Buried Flexible Pipes". *Buried Plastic Pipe Technology.* Philadelphia, PA: ASTM.

Hartley, James D. and Duncan, James M.1988 "E' and Its Variation with Depth," *ASCE Journal of Transportation Engineering*, pp. 538-533, Vol. 113, No 5.

Hashash, N., and E. T. Selig, 1990. "Analysis of the Performance of a Buried High Density Polyethylene Pipe". *The First National Conference on Flexible Pipes*, Columbus, Ohio, pp 95-109.

Hoeg, K. 1968. "Stress Against Underground Structural Cylinders", *Journal of Soil Mechanics and Foundations Division*, ASCE, Vol. 94, No. SM4.

Howard, Amster K. 1977. "Modulus of Soil Reaction Values for Buried Flexible Pipe". *Journal of the Geotechnical Engineering Division.* pp 33-43.

Janbu, N. 1963."Soil Compressibility as Determined by Odometer and triaxial tests, Proceeding European Conference SM,FE,Weisbaden, vol 1.

Katona, M. G., 1976." CANDE: A Modern Approach for the Structural Design and Analysis of Buried Culverts". *Report FHWA-RD-77-5. FHWA, U.S. Department of Transportation.*

Katona M.G., 1990. "Minimum Cover Height for Corrugated Plastic Pipe Under Vehicle Loading". *Transportation Research Record 1288*, pp127-135. Washington D.C.

Klaiber, F.W.,Lohnes, R.A., Wipf, T.J., and Phares, B.M., 1996. "Investigation of High Density Polyethylene Pipe for Highway Applications: Phase I", Iowa Department of Transportation Project HR-373, Ames, Iowa.

Kondner, R. L. 1963. "Hyperbolic Stress-Strain Response: Cohesive Soils". *Journal of the Soil Mechanics and Foundations Division*, ASCE, Vol. 89, No. SM1, Proc. Paper 3429, pp. 115-143.

Krizek, R. J., et al. 1971. "Structural Analysis and Design of pipe Culverts," *Report No. 116, National Cooperative Highway Research Program, Highway Research Board*, Washington, D.C., 155 pp.

Lohnes, R.A.,Wipf, T.J.,Klaiber,F.W., Conard, B.E., and Ng, K.W 1997. "Investigation of Plastic Pipes for Highway Applications: Phase II", *Iowa Department of Transportation Project HR-373A*, Ames, Iowa.

Marston, Anson, and A. O. Anderson, 1913. " The Theory of Loads on Pipes in Ditches and Tests of Cement and Clay Drain Tile and Sewer Pipe," *Bulletin 31, Iowa Engineering Experiment Station*, Ames, Iowa.

Marston, A. and A. Anderson 1930. "The Theory of External Loads on Closed Conduits in the Light of the Latest Experiments," The Iowa State College bulletin, No. 96, vol.XXVIII, Iowa Engineering Experiment Station, Iowa State College.

McGrath, Timothy J. and Selig, Ernest T. 1994, "Backfill Placement Methods Lead to Flexible Pipe Distortion." PREPRINT, *Transportation Research Board*, Washington, D. C.

Meyerhof, G. G. and Baike, L. D. 1963. "Strength of Steel Culvert Sheets Bearing against Compacted Sand Backfill". Highway Research Board Proceedings, vol. 30.

Moore, I.D, 1995. "Three Dimensional Response of deeply Buried Profiled Polyethylene Pipe". *Transportation Research Record 1514*, pp 49-58. Washington D.C.

Moore, I.D., and B. Taleb, 1999. " Metal Culvert Response to Live Loading Performance of Three Dimensional Analysis". *Transportation Research Record 1656*, pp. 37-44. Washington D.C.

Moser, A. P,1990. "Buried Pipe Designs". McGraw Hill, Inc., New York.

Moser, A.P, 1994. "The Structural Performance of Buried 48 inch diameter N-12 HC Polyethylene Pipes". Buried Structural Laboratory, Utah State University, Logan, Utah.

Moser, A.P, 1997. "Analytical Methods for Predicting Performance of Buried Flexible Pipes". PREPRINT, *Transportation Research Board*, Washington D.C.

Moser, A.P., 1998. "The Structural Performance of Buried Profile-Wall HDPE Pipe and The Influence of Pipe Wall Geometry". *Transportation Research Record 1624*, pp 206-213. Washington D.C.

Morgan, B.C., Lohnes, R.A., Klaiber F.W., and B. H. Kjartanson, 1996. " Design Method for Preventing Longitudinal Uplift of Corrugated Metal Pipe". *Transportation Research Record 1541*, pp. 107-111. Washington D.C.

Musser, S.C, 1989. "CANDE-89 User Manual". *Report FHWA-RD-89-169. FHWA, U.S. Department of Transportation.*

Rankine, W. M. J. 1857. "On Stability on Loose Earth," *Philosophic Transactions of Royal Society*, London, Part I, 9-27.

Rogers, C.D.F., Fleming, P.T., and Talby R.. 1996. "Use of Visual Methods to Investigate The Influence of Installation Procedure on Pipe-Soil Interaction". *Transportation Research Record 1541*, pp 76-85. Washington D.C.
Sargand, S.M., Hazen, G.A., and Masadda, T. 1998. "Structural Evaluation and Performance of Plastic Pipe". *Report FHWA-OH-98-011. FHWA, U.S. Department of Transportation.*

Sargand, S.M., Hazen, G., White, k., Moran, A., 2001. "Time-dependent deflection ofthermoplastic pipes under deep buried burial". *Transportation Research Record 1770*, pp. 236-242. Washington D.C.

Sargand, S.M., Masada, T., and Schehl, D, 2001. "Soil pressure measured at various fill heights above deeply buried thermoplastic pipes". *Transportation Research Record 1770*, pp. 227-235. Washington D.C.

Schluter C. J. and Shade J.W, 1999, " Flexibility Factor or Pipe Stiffness, Significant Stiffness Considerations. *Transportation Research Record 1656*, pp 45-50. Washington D.C.

Selig, E.T., 1988. "Soil Parameters for design of buried pipelines". *Pipeline infrastructure, proceeding of pipeline infrastructure conference of ASCE, ASCE, NY.*

Selig, E. T. 1990. "Soil Properties for Plastic Pipe Installations," *Buried Plastic Pipe Technology, ASTM STP 109.* American Society for Testing and Materials, Philadelphia.

Spangler, M.G, 1941."The Structural Design of Flexible Pipe Culverts". *Iowa Engineering Experiment Station. Bulletin 153.* Ames, Iowa.

Spangler M. G., and Handy R. L. 1982. Soil Engineering. Harper and Row, New York, NY, 4th Edition.

Taleb, B., and I.D. Moore, 1999. "Metal Culvert Response to Earth Loading- Performance of Two Dimensional Analysis". *Transportation Research Record 1656*, pp. 25-36. Washington, D.C.

Trantina, G. and Nimmer, R., 1994. "Structural analysis of Thermoplastic Components". Mcgraw-Hill, Inc.

Watkins, Reynold K. and Spangler, M.G. 1958. "Some Characteristics of the Modulus of Passive Resistance of Soil: A Study in Similitude," *Highway Research Board Proceedings*,Vol. 37, pp. 576-583.

Watkins, R. K., Anderson, L.R, 1999. "Structural Mechanics of Buried Pipes". CRC Press, New York.

Watkins, R. K., 1999. "Performance Limits of Buried Profile Wall Pipe" PREPRINT, Transportation Research Board, January, 2001. Washington D.C.

Webb, M.C., Sussmann, J., and Selig, E.T., 1998. "Large Span Culvert Field Test Results". NCHRP Project 12-45. Department of Civil and Environmental Engineering, University of Massachusetts, Amherst.

Zhange C and Moore, I.D, 1997. "Nonlinear Mechanical Response of High Density Polyehtylene. Part I.: Experimental Investigation and Model Evaluation". *Polymer Engineering and Science*, Vol. 37, No.2 pp 404, 413. Washington D.C.

ACKNOWLEDGMENTS

I would like also to thank my major professors, Robert Lohnes and Terry Wipf for their guidance and input during the course of this project. Thanks to Professor Wayne Klaiber for his help. I also would like to thank Professor Brian Coree for his continuous help, understanding, and encouragement (SHUKRAN). Thanks to Professor Thomas J. Rudolphi for serving on my program of study and teaching me "Theory of Elasticity" where I got an *A*!.

This research was funded by the Minnesota Concrete Pipe Association (MCPA). I would like to thank MCPA for funding this project and providing the opportunity to investigate the performance of in-service HDPE pipes. I would also like to thank the city officials in Mankato, Moundsview, Blaine, Le-Center, Fairmont, Gaylord, and Maple Grove (all in Minnesota) for allowing us to video-tape the in-service pipes and providing the design drawing of the surveyed projects.

Thanks to all of my friends specially, Haider Qleibo and IL-Seok Oh.